
Characterization of the Atmosphere of Extrasolar Planets

A thesis submitted for the degree of

Doctor of Philosophy

in

**The Department of Physics,
Pondicherry University,
Puducherry - 605 014, India**



by

**Soumya Sengupta
Indian Institute of Astrophysics
Bangalore - 560034**



May, 2022

Characterization of the Atmosphere of Extrasolar Planets

Soumya Sengupta
Indian Institute of Astrophysics



Indian Institute of Astrophysics
Bangalore-560034, India

Title of the Thesis : **Characterization of the Atmosphere of Extrasolar Planets**
Name of the author : **Soumya Sengupta**
Address : Indian Institute of Astrophysics
II Block, Koramangala
Bangalore-560 034, India
Email : soumya.s@iiap.res.in
Name of the supervisor : **Prof. Sujan Sengupta**
Address : Indian Institute of Astrophysics
II Block, Koramangala
Bangalore-560 034, India
Email : sujan@iiap.res.in

Declaration of Authorship

I hereby declare that the matter contained in this thesis is the result of the investigations carried out by me at the Indian Institute of Astrophysics, Bangalore, under the supervision of Prof. Sujan Sen-gupta. This work has not been submitted for the award of any other degree, diploma, associateship, fellowship etc. of any other univer-sity or institute.

Signed:

Date:

Certificate

This is to certify that the thesis entitled '**Characterization of the Atmosphere of Extrasolar Planets**' submitted to the Pondicherry University by Mr. Soumya Sengupta for the award of the degree of Doctor of Philosophy, is based on the results of the investigation carried out by him under my supervision and guidance, at the Indian Institute of Astrophysics. This thesis has not been submitted for the award of any other degree, diploma, associateship, fellowship, etc. of any other university or institute.

Signed:

Date:

List of Publications

1. Referenced:

- (a) **Effect of thermal emission on Chandrasekhar's semi-infinite diffuse reflection problem**

Soumya Sengupta, 2021, The Astrophysical Journal (ApJ), Volume 911, pp.126

DOI: 10.3847/1538-4357/abeb72

2. Under Preparation:

- (a) **Effect of atmospheric heat redistribution on Emission spectra of Hot-Jupiters**

Soumya Sengupta & Sujan Sengupta, Submitted in New Astronomy

Conference Participation

1. National Conference:

- (a) *Meeting:* 40th Annual Meeting of the Astronomical Society of India (ASI)
March 25 - 29, 2022, IIT, Roorkee,
Nature of Participation: **Poster Presentation**
Title: **Thermal emission effect on Chandrasekhar's diffuse reflection problem**
Author: Soumya Sengupta
- (b) *Meeting:* 38th Annual Meeting of the Astronomical Society of India (ASI)
February 13 - 17, 2020, IISER, Tirupati,
Nature of Participation: **Poster Presentation**
Title: **Modelling and Characterization of Exoplanet Atmosphere**
Author: Soumya Sengupta

2. International Conference:

- (a) *Meeting:* The 6th UK Exoplanet community Meeting, April 22, 2021, Birmingham (in Virtual mode)
Nature of Participation: **Contributory Talk**
Title: **Effects of thermal Emission on Chandrasekhara's Semi-infinite Diffuse Reflection Problem**
Author: Soumya Sengupta
- (b) *Meeting:* 2021 Sagan Exoplanet Summer Virtual Workshop Circumstellar Disks and Young Planets, July 19-23, 2021, NASA Exoplanet Science Institute, California Institute of Technology, PASADENA, CA
Nature of Participation: **Poster Presentation**
Title: **Thermal emission Effect on Chandrasekhar's Semi-infinite Diffuse Reflection Problem**
Author: Soumya Sengupta

Dedicated to

**My beloved brother late *Koustabh Sengupta*
and my uncle late *Asit Sengupta*.**

**Both of them made me what I am and left me
behind..**

Acknowledgements

"One best book is equal to hundred good friends but one good friend is equal to a library."

- Dr. Avul Pakir Jainulabdeen Abdul Kalam

During my Ph.D. period, I was blessed with both a best book and a good friend. The book **Radiative Transfer** by S. Chandrasekhar gave me the immense pleasure of research on a particular subject and showed how the solutions can be obtained by following your own path however difficult it is. For me it was the Candle in the darkest nights of this period.

In this journey called Ph.D., I was blessed by a good friend Ms. Manika Singla. She has made this journey possible by her continuous support and belief on me even when I lose my self-confidence totally. It is beyond my capability to repay what she has done in my difficult period. Her simple rule of success (fig 1) made me courageous to struggle over and over again.

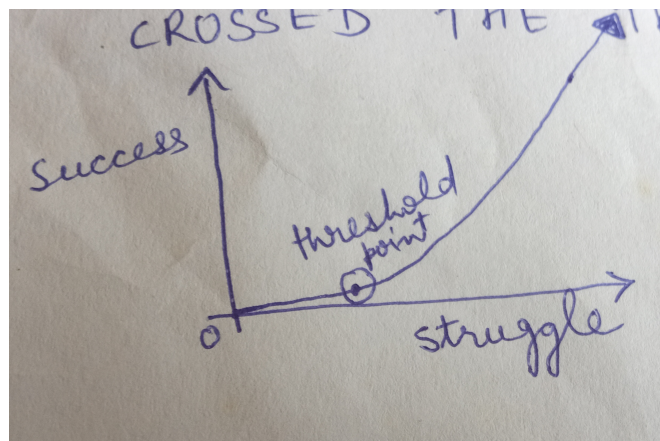


Figure 1: Success vs. struggle graph. We all are at the threshold point.

The other person who played a crucial role in this whole journey is my supervisor Prof. Sujan Sengupta. He has never done any spoon-feeding and taught me to be an independent researcher of my own. Though the approach seemed difficult for me at first but the fruit of it came at the end. Although Dr. Richard

Dawkins said, “..there are influential scientists in the habit of putting their names to publications in whose composition they have played no part.”, I have found a contrasting character in my supervisor, when he suggested me to withdraw his name from my own work and publication. I found myself lucky in this regard and will try to follow this attitude in my whole career.

Now I want to thank the following persons from my whole heart due to their direct or indirect contribution to my work. Dr. Rakesh Mazumdar has shown me the way to proceed through the difficult situations when no one believes in you. My friend Mr. Vishnu Madhu who has discussed with me even with my wildest ideas and try to find a way out of it. My senior Dr. Prerna Rana helped me in writing the Abstract for my first paper and guided me wisely through the whole process of the manuscript submission. My other seniors Dr. Priya Goyal, Dr. Chayan Mandal, Dr. Sandeep Kataria, Dr. Raghubar Singh and Dr. Aritra Chakrabarty has helped me at different stages of my Ph.D. work as well as a work life balance. My Doctoral Committee members Prof. Maheswar, Prof. S.V.M. Satyanarayana provide questions and suggestions at my each and every presentation which helps me to progress in the work.

I want to thank three people particularly who always stand just beside me and encouraged me with their everlasting love and care. Prof. Amarendranath Chatterjee, Mr. Partha Sarathi Dey and Ms. Devaparna Bhattacharya played the role of Friend, Philosopher and Guide in this Journey. I am thankful to Dr. Debiprosad Duari to ignite my mind towards the astrophysical research during my Graduation days.

I also want to thank them who have doubted, criticized and even thought that the thesis will not be possible ever. The darkness created by them helped me to find the light inside.

I would like to express my immense gratitude to my parents for relieving me from all the responsibilities and giving me a chance to make my dream come true. It is inexpressible what they have done for me to make the person I am today.

Finally, I would like to thank the person I see in the mirror who, sometimes fighting, sometimes supporting, but always stay with me. I trust the person that whatever be the situation he will always be with me.

Thank you all.

Bengaluru,
May, 2022

Soumya Sengupta

Abstract

Context: Starting from the first discovery of extrasolar planet or exoplanet around a sun-like star, more than 5,000 confirmed exoplanets have been detected till now. But still we have very less information and interpretations about the atmosphere of such outside worlds.

Aim: In this project we mainly focus on gas-giant exoplanets, commonly known as hot-jupiters due to their jupiter-like shape and structure but a huge temperature. We studied the atmosphere in two different aspects. At first we modeled the day-side emission spectra and studied their variation with respect to different amount of atmospheric flow and heat-redistribution using the existing radiative transfer theory. Then we modified the current theory of diffuse reflection problem according to the context of Hot-Jupiter atmospheric temperature structure to provide more accurate interpretations of present and future data.

Methodology: For the first part of the work we used numerical simulation and analytical approach to study the atmospheric redistribution effect. In the numerical context the discrete space theory formalism is used for the first time to solve the line-by-line radiative transfer equation and generates the planetary emission spectra. In the second part of the project, a purely analytical approach is taken to modify the existing theory of diffuse reflection problem by adding the atmospheric thermal emission contribution to it. The Invariance principle method is used for this modification treatment.

Results: In the first part of this work we have showed that the atmospheric heat redistribution plays a major role in changing the vertical atmospheric temperature-pressure structure as well as the day-side emission spectra. Depending on the amount of (full, semi and no) heat redistribution the magnitude of the day-side emission flux changes substantially. We also considered a particular case of hot-jupiter XO-1b and showed that this planet has efficient day-night heat redistribution and holds the same temperature structure all over the planet. In the second project we showed that the modified results of diffuse reflection problem incorporates both the effects of thermal emission and diffuse reflection in the final radiation from the planetary atmosphere. Also our results in this context is more general and consistent with the previous results as obtained by Chandrasekhar in

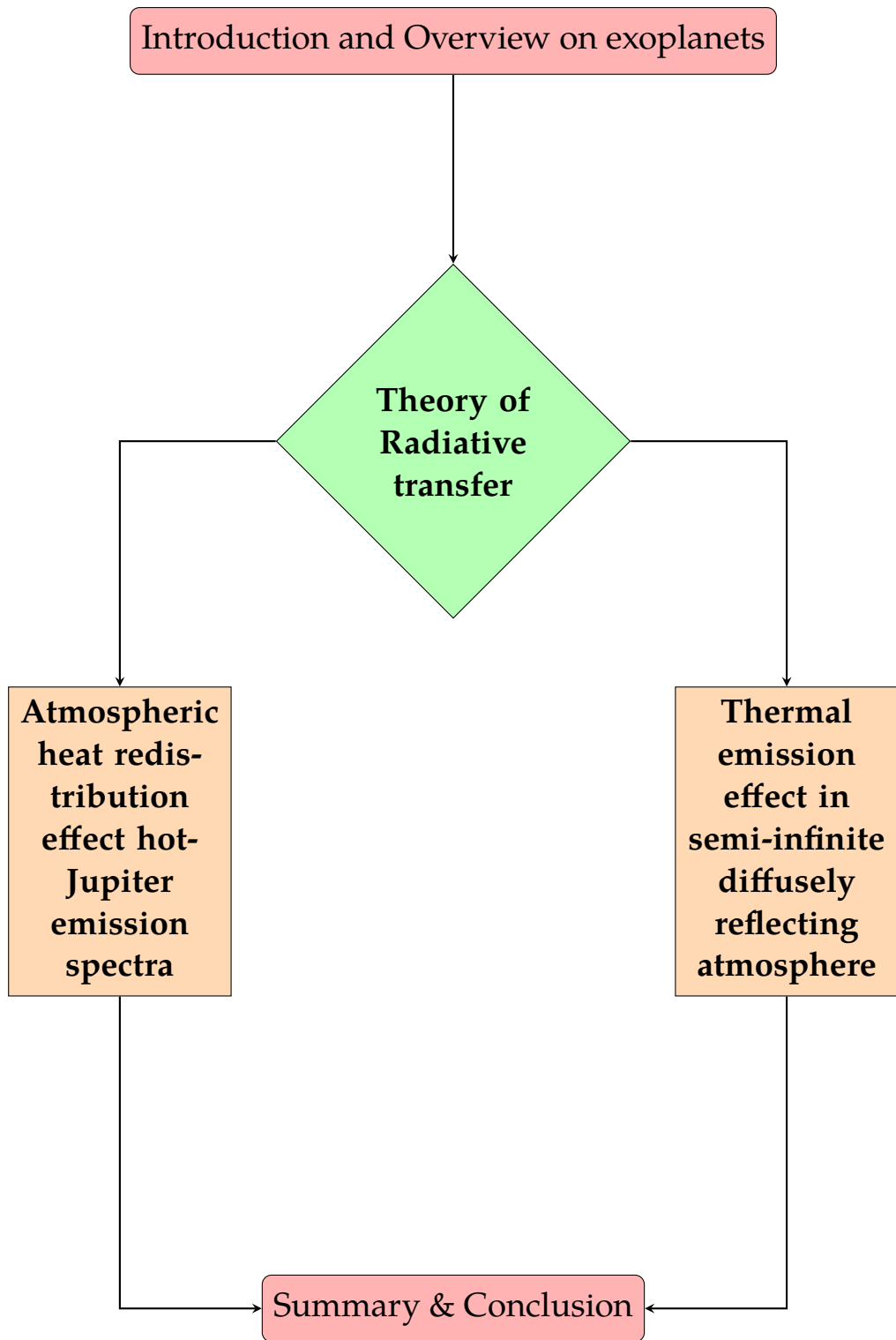
case of only scattering. Hence we conclude that our approach will provide more accurate and reliable interpretations of the data observed in exoplanetary science.

Contents

1	Introduction and overview of exoplanetary study	1
1.1	Types of Exoplanets:	1
1.2	Detection Techniques:	2
1.3	Types of atmospheric spectra:	5
1.4	Our Target:	5
1.5	Goal of the Thesis:	7
1.6	Plan of the Thesis:	8
2	Radiative Transfer Theory	10
2.1	Introduction	10
2.2	Basic definitions	10
2.2.1	Specific Intensity I :	10
2.2.2	Absorption co-efficient:	11
2.2.3	Emission co-efficient:	12
2.2.4	The Source Function	13
2.2.5	Optical Depth	13
2.3	General equation of transfer	14
2.4	The Plane Parallel Approximation	14
2.4.1	Moments of specific intensity	15
2.5	The Local Thermodynamic Equilibrium Condition	16
2.6	The condition of Radiative Equilibrium	17
2.7	The Hydrostatic Equilibrium Condition	18
2.8	The Transfer equation with scattering	18
2.9	Scattering phase functions:	20
2.10	The Scattering and Transmission Function:	22
2.11	Different types of plane-parallel atmosphere:	23
2.12	The principle of Invariance:	24
2.12.1	Semi-infinite Atmosphere:	24
2.12.2	Finite Atmosphere case:	25
2.13	Integral form of Scattering function in semi-infinite atmosphere:	27

2.14	Explicit form of the scattering integral equation for different phase functions	28
2.14.1	Isotropic Phase Function:	28
2.14.2	Asymmetric scattering:	29
2.14.3	Rayleigh scattering phase function:	31
2.14.4	Scattering function for the general phase function:	34
3	Effect of atmospheric heat redistribution on Emission spectra of Hot-Jupiters	37
3.1	Introduction	37
3.2	Theoretical Models	39
3.2.1	Values of the redistribution parameter for isotropic approximation	42
3.3	Numerical methodology	43
3.3.1	Atmospheric temperature-pressure profiles	43
3.3.2	Co-efficients of absorption and scattering	44
3.3.3	Numerical method to generate the emission spectra:	44
3.3.4	Validation of our model	45
3.4	Results	48
3.4.1	Effect of redistribution parameter on T-P profiles and on emission spectra	48
3.4.2	Case study: Emission Spectra of exoplanet XO-1b:	51
3.5	Discussions & Conclusion	51
4	Effects of thermal emission on Chandrasekhar's semi-infinite diffuse reflection problem	55
4.1	Introduction	55
4.2	Derivation of Diffusion Transfer equation in presence of Thermal Emission	56
4.3	General Integral equation of scattering Function	58
4.4	Explicit form of the scattering integral equation with different phase functions	59
4.4.1	Isotropic scattering:	60
4.4.2	Asymmetric scattering:	61
4.4.3	Rayleigh scattering:	62
4.4.4	Scattering function for the general phase function:	64
4.5	Comparison of our general model with Chandrasekhar's diffusion scattering model	66
4.6	Contribution of thermal emission:	70

4.7	Discussion:	71
5	Summary and Conclusions	75
5.1	Highlights:	75
5.2	Limitations:	77
5.3	Future Aspects:	78



Chapter 1

Introduction and overview of exoplanetary study

"Innumerable suns exist. Innumerable earths revolve around these. Living beings inhabit these worlds."

- **Giordano Bruno** (1548-1600)

Searching for an earth-like planet and human-like civilization is the long lasting quest of humankind. After discovering the details of our solar system planets, scientists are now interested to know about extra-solar system planets which are commonly known as Exoplanets. After the confirmed detection of a Jupiter like Exoplanet orbiting around one sun like star (Mayor and Queloz 1995), it seems we are at the verge to answer this long lasting question. According to [NASA exoplanet archive](#) more than 5,000 exoplanets have been detected till the year 2022. In this zoo of detected exoplanets, there exist much more different kind of exoplanets which are way too different than the solar system planets both by composition and size. In this chapter we will discuss briefly about these new extrasolar worlds.

1.1 Types of Exoplanets:

A planet is defined as an astrophysical object where the gravitational collapse is balanced by pressures generated due to Electrostatic (Coulomb) or electron degeneracy but do not sustain any nuclear fusion in the entire history of its life (Seager 2010a). However in case of solar system planets it was believed that a planet should have its host star but the idea is changed after the discovery of freely floating exoplanets. In solar system there are two major categories of the planets : Terrestrial with rocky core which are smaller in size and resides inner solar system (e.g. Mercury, Venus, Earth, Mars) and Giants with no core which are bigger and in outer solar system (Jupiter, Saturn, Uranus, Neptune). But in case of exoplanets no such discrimination can be done as there are surprisingly different kind of exoplanets discovered which totally different compared to our solar sys-

tem planets. So in case of exoplanets the currently accepted definition is that the planetary size should be $< 13M_J$, where M_J is the solar system Jupiter mass.

According to the currently accepted specifications the exoplanets are divided in different types as follows,

1. Terrestrial: They have a rocky surface, solid core and very thin atmospheric layer.
2. Giant planet: These planets are bigger than terrestrial planets but smaller than brown dwarfs ($0.03M_J < M_p < 13M_J$) and the interiors contain metallic hydrogen of a considerable fraction surrounding a rocky core.
3. Earth-like: They are described as similar to the Earth by mass, radius and surface temperature.
4. Super-Earth: These are rocky planets bigger than earth of mass $1\text{--}10 M_{\oplus}$, where M_{\oplus} is the mass of the earth.
5. Hot-Jupiter: They are Jupiter sized planets very near to their host stars but the temperature is too high (1000-2000K). Their distance from the host star is so small that they are gravitationally locked to the star and have permanent day at one side and permanent night on the other.

Here we mentioned some of the many different types of exoplanets which has been discovered till date. Our work will be mainly focused on Hot-Jupiter type of planets.

1.2 Detection Techniques:

Although detecting an exoplanet is a big challenge, there are different techniques such as radial velocity, Transit method, Direct imaging technique, Microlensing, Astrometric detection etc for detecting exoplanets. We will discuss only the first two methods here as follows. For a detailed discussion on different detection methods we refer the standard texts, by Seager [2010b](#) and Perryman [2011](#).

1. Radial Velocity Method: When two celestial objects of equal mass orbit each other, they don't rotate around the center of any of the two objects but around a common center called barycenter which situated at the bisecting point of the line connecting the centers of the planet and star. In such a scenario, if object **A** is heavier than object **B**, then the barycenter shifts towards the heavier object **A**. In a star-planet system, the star (object A) is so heavy as compared to

the planet (object B) that the barycenter is located inside the star. This causes a wobble to the star that hosts a planet. If the planet is orbiting at edge on view to the observer, then the motion of the star appears to and fro. This is called radial velocity of the star. Astronomers collect the starlight under such condition through a spectrograph and detect the periodic Doppler shift in starlight by monitoring the shift in the dark vertical lines caused by the absorption of starlight by the material present at the outer layer of the star. From the periodic Doppler shift towards red and blue of a particular absorption line, the radial velocity of the star is measured and the presence of the planet is confirmed. From the observation of the doppler shift in radial velocity method, the planetary upper mass limit $M \sin i$ can be obtained (Seager 2010b), where i is the orbital inclination along the observer's line of sight.

The radial velocity method is used to detect the binary stars for more than half a century, but the idea to use this method for detecting Jupiter-like exoplanets was started by the proposal given by Struve 1952. It is worth noting that the detection of the hot-Jupiter planet 51 Peg-b was done by Radial velocity method (Mayor and Queloz 1995).

2. Transit Method: The radial velocity method can give us the information about the upper limit of the planetary mass depending on the inclination of the orbit. But to get the information about the size, radius and atmosphere of the planet the observation should be done using planetary transit method.

From the edge on view of a planet hosting star, the observer can observe periodic brightness dip of the star light. First one is at transit point when the planet is in front of the star and the second when the planet is just behind the star (see fig. 1.1). For continuous observation of such a system, there will be a periodicity of this brightness dip conforming the planetary rotation around the star.

Besides the detection of exoplanet, this technique is also useful to observe the planetary atmosphere. At the Transit or primary eclipse point (fig.1.1) the starlight passes through the planetary atmosphere whereas, at the secondary eclipse point the reflection of the starlight from planetary atmosphere reaches to the observer. While passing through a spectrograph, this light gives the absorption and emission lines depending on the composition of the planetary atmosphere.

Now using this observation the following parameters can be estimated. From the periodicity of transit the orbital distance can be derived using Kepler's law (it is assumed that the planets are in keplerian orbit). From the brightness dip at transit point (fig. 1.1) the size of the planet is found. Moreover

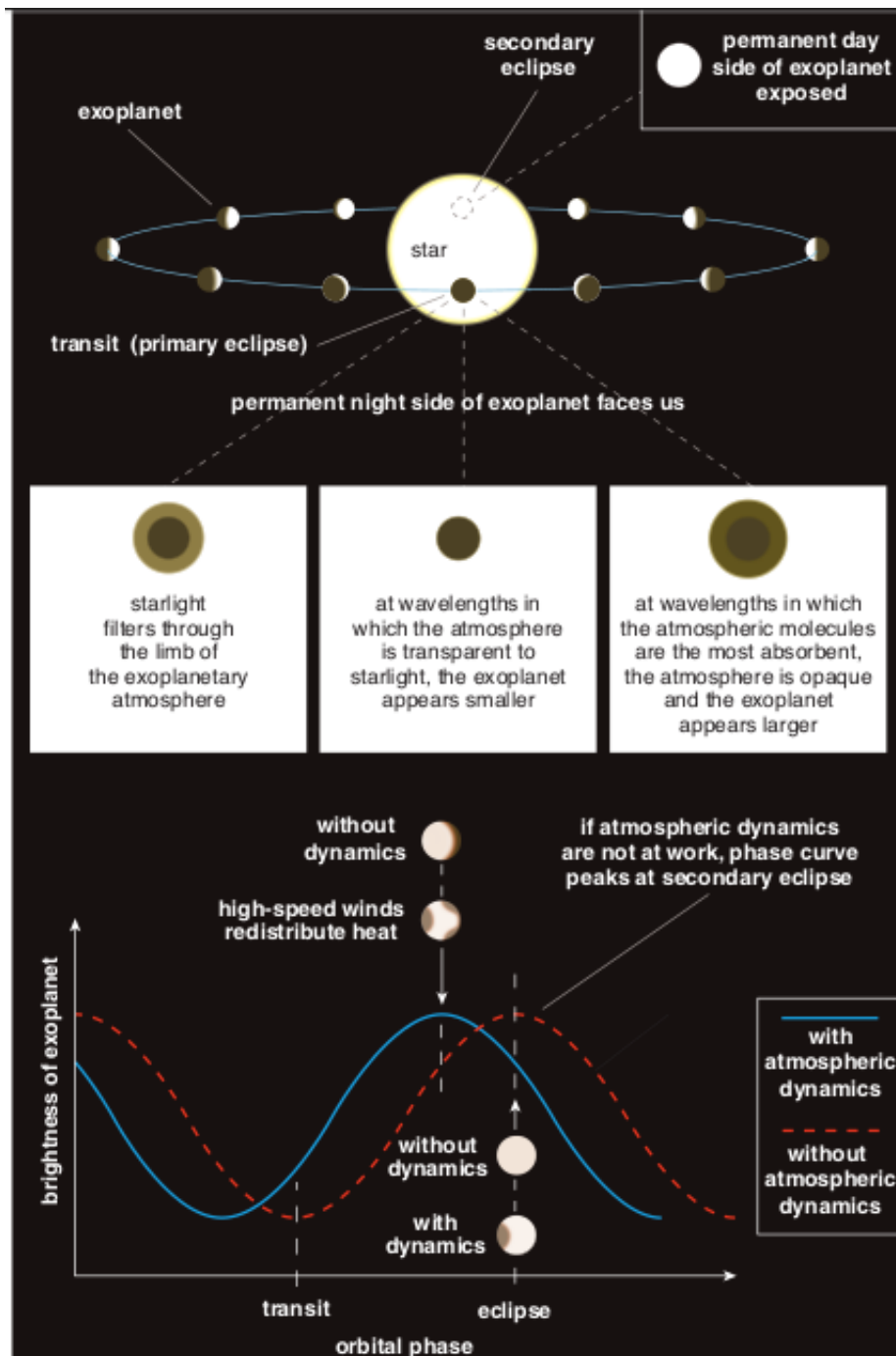


Figure 1.1: This picture depicts an observer's edge on view to a gravitationally locked planet orbiting its host star. There are primary and secondary eclipse points where the night and day side of the planetary atmosphere can be observed respectively. Even by detecting the brightness peaks at different orbital phases, the atmospheric dynamics can be interpreted. This image is taken from Heng 2012

observing the transit at different wavebands, the dayside and nightside atmospheric spectra can also be obtained. For an extensive discussion on it we refer (Tinetti, Encrenaz, and Coustenis 2013) and (Seager 2010a).

1.3 Types of atmospheric spectra:

As we have discussed in the previous section, the planetary atmospheric spectra can be observed by the transit method. While analysing the atmospheric temperature, composition etc. of different kind of exoplanets, it is customary to observe them in terms of the observed spectra. There are fundamentally three different kind of spectra which can be observed and modeled in case of exoplanetary atmosphere.

1. **Transmission Spectra:** When the planet is at primary eclipse or transit point, then the starlight comes to the observer by transmitting through the planetary atmosphere. Hence it is known as the Transmission spectra of the planet. This spectra contains mainly the atmospheric information of the Hot-Jupiter's day-night terminator region. The spectra can be observed in optical as well as infrared region.
2. **Reflection Spectra:** This is the star flux reflected from planetary surface which can be observed before and after the secondary eclipse point. The spectra is also depends on the orbital phase and carries the information about the day-side atmosphere. The waveband to observe the flux is entirely depends on the blackbody wavelength peak of the corresponding host star. For example, if an exoplanet orbit a sun-like (G-type) star then the reflection spectroscopy is in optical wavelength region.
3. **Emission Spectra:** This is the planet's own emission coming from the day-side of the atmosphere. It is also observed before and after the secondary eclipse point but at different waveband depending on the blackbody wavelength peak of the planetary day-side atmosphere. For instance in case of Hot-Jupiter it is mainly emitting in infrared. Also by studying the variation of this spectra the atmospheric dynamics can be predicted. In our work we will discuss about it in detail.

1.4 Our Target:

Although there are more than 5,000 exoplanets detected till now (Year 2022), we have very little information about the atmosphere of a small handful of exoplanets. The observation and modeling of exoplanetary atmosphere goes hand in hand. In this thesis we concentrate on **the modeling part of Hot-Jupiter's day-side emission spectra**.

The observations provide the emitted and/or reflected planetary flux the stellar flux units (Deming et al. 2005; Charbonneau et al. 2005), whereas the ratio

of planet and star flux can be estimated theoretically as (Tinetti, Encrenaz, and Coustenis 2013),

$$\eta(\lambda) = \left(\frac{R_p}{R_*}\right)^2 \frac{F_p(\lambda)}{F_*(\lambda)} \quad (1.1)$$

where $R_p; R_*$ and $F_p; F_*$ are planetary; stellar radius and flux respectively. Both the fluxes can be modeled using radiative transfer calculations with the considerations of scattering processes as well as ionic, atomic and molecular opacities shown in (Chandrasekhar 1960; Liou 2002; Annamaneni Peraiah 2002). For typical Hot-Jupiter planet system the emission spectra in infrared region gives a contrast ratio of about 10^{-3} as shown in fig 1.2 (Seager 2010a), (Madhusudhan and Seager 2009).

It is customary to model the secondary eclipse flux ratio which best-fits with the observed data and retrieve day-side atmospheric temperature-pressure profile and chemical composition (Swain, Vasisht, and Tinetti 2008). The atmospheric dynamics of the Hot-Jupiter planets are also studied in a great detail (Showman, Menou, and Cho 2007). A pedagogical view to study the atmospheric circulation in terms of the emission spectra has been shown in Hansen 2008. At the same time the modeling of the temperature-pressure profiles of highly irradiated exoplanets is given analytically (Guillot 2010) as well as numerically (Parmentier, Guillot, et al. 2015; Parmentier and Guillot 2014). Once we obtain the atmospheric temperature-pressure profiles as well as chemical compositions, then we can solve the radiative transfer equation to generate the atmospheric spectra as shown in literature (see Sengupta, Chakrabarty, and Tinetti 2020, Paul Mollière et al. 2015, Batalha et al. 2019, Waldmann et al. 2015, Kempton et al. 2017).

While modeling the Hot-Jupiter atmosphere we particularly use the temperature-pressure profiles obtained using the formalism given in Parmentier, Guillot, et al. 2015 and chemical composition using the formalism in Kempton et al. 2017. Then to solve the line by line radiative transfer equation, we use the discrete space theory method (Grant and Hunt 1968, Peraiah and Grant 1973, Sengupta and Marley 2009, Sengupta, Chakrabarty, and Tinetti 2020). We discussed more about it in sec 1.5 and in sec 3.3.3 .

For modeling the exoplanetary atmosphere, the analytic solutions of the diffuse reflection problem developed by Chandrasekhar 1960 is widely used (e.g. Nikku Madhusudhan and Burrows 2012). However in case of highly irradiated Hot-Jupiter atmosphere the basic conditions are very different than those in which Chandrasekhar's solutions were provided. In such a scenario the modifications of the radiative transfer equation (Bellman et al. 1967; Domanus and Cogley 1974) and its solutions are important to obtain a more complete interpretation of the Hot-Jupiter atmosphere. Mainly, the importance of scattering and emission ef-

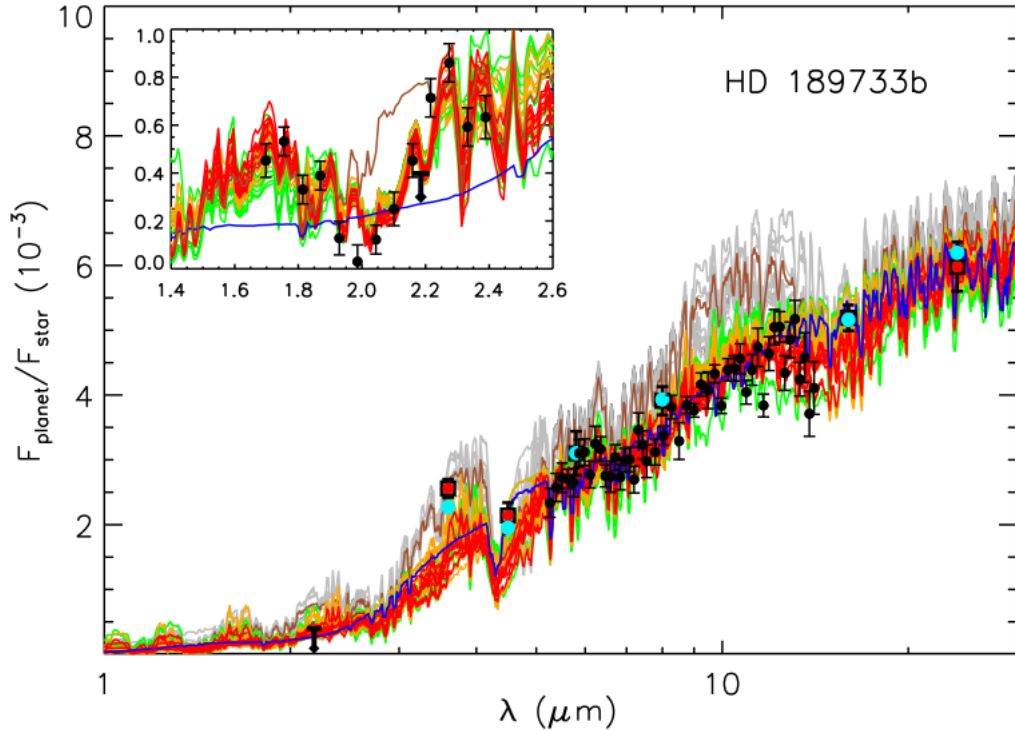


Figure 1.2: This is the secondary eclipse emission flux ratio of the Hot-Jupiter HD189733b. It shows the best fit radiative transfer model plotted against the observed data (in blue). The wavelength range is clearly in μm and the flux ratio is at magnitude 10^{-3} . This figure is taken from Madhusudhan and Seager 2009.

fect in Hot-Jupiter atmosphere has been discussed independently in Sengupta, Chakrabarty, and Tinetti 2020 and Chakrabarty and Sengupta 2020. But the consideration of their simultaneous effect has not been done so far. Hence, we set our goal of the thesis as follows.

1.5 Goal of the Thesis:

Here we discuss the goal of the work presented in this thesis.

- The main goal of this thesis is to study and characterize the exoplanetary atmosphere. For that we take the theoretical approach to model the atmosphere of hot-jupiter planets.
- We want to find a relationship between the atmospheric heat redistribution and the observed secondary eclipse spectra of this particular type of planets. For that we target to parameterize the heat redistribution factor and simulate the synthetic spectra by numerical codes and solve the fiducial equation of radiative transfer.

- Then we target to generalize the diffuse reflection problem used to model the planetary atmosphere. For this purpose we include the scattering and emission effect simultaneously in the radiative transfer modeling which is expected to be more appropriate while characterizing the hot-Jupiter atmosphere.
- We show some modifications on the present theory. Also we discuss the limitations, approximations and future aspects.

1.6 Plan of the Thesis:

Here we discuss the chapter wise planning of this thesis.

1. In chapter 2 we discuss the basics of theory of radiative transfer which is used while modeling of the exoplanetary atmosphere. We start from the basic definitions used in different literature and the transfer equation appropriate for studying the astrophysical problems. Then we introduce different conditions and approximations used in this project and discuss their applicability in the present context. After that we concentrate on the atmospheric diffuse reflection problem introduced by Chandrasekhar (1960) and the invariance principle method which is used to solve this problem. In later chapter we discuss this problem and its solution with some modification and generalization.
2. In the 3rd chapter we discuss our ongoing work on simulating the synthetic secondary eclipse emission spectra for hot-Jupiter planets. Our main motive is to study the variation of the day-side emission spectra of hot-Jupiters with the amount of day to night atmospheric heat redistribution. For that at first we derive the analytical values of redistribution parameter f and then model the temperature-pressure profile as well as emission spectra for hot-Jupiter type planets. We used line by line radiative transfer code based on discrete space theory to generate the synthetic spectra. The numerical results and interpretations are similar with the previous literature results as discussed in the chapter. This work is under preparation.
3. In Chapter 4 we introduce the Effect of Thermal emission in the problem of semi-infinite diffuse reflection introduced by Chandrasekhar and solve it by the Principle of Invariance method. Our motive is to study how the atmospheric thermal emission modifies Chandrasekhar's final results as discussed in chapter 2. For that we derived the transfer equation appropriate for scattering, transmission and emission. Then by invariance principle we derive the general equation of scattering function. At this point we showed the specific

form of scattering function for four different types of scattering (e.g. Isotropic scattering, Rayleigh scattering etc.). Then we explicitly show the contribution of thermal emission on the final radiation emitted from the semi-infinite atmosphere. Finally we compare our results with literature results and it shows a perfect match of our results with Chandrasekhar at the low thermal emission limit. This part of the work is published in Sengupta, Soumya, ApJ, 911, 126 (S. Sengupta [2021](#)).

4. In the concluding chapter 5 we summarize the work presented in this thesis as well as the caveats and way to improvement. We also mention some of the future aspects of this current work.

Resource Summary:

In this chapter we present the brief introduction and overview about the exoplanets from literature. Then we discuss our target followed by the goal and plan of the thesis. The resources we used here are as follows,

1. Exoplanetary Atmosphere by Sara Seager (2010)
2. Exoplanets by Sara Seager (2010)
3. Radiative Transfer by S. Chandrasekhar (1960)
4. A Review Article by Tinetti et al. 2013

Chapter 2

Radiative Transfer Theory

2.1 Introduction

The study of analytical transfer theory of radiation is a very important and well established branch of physics. In mid 20th century, while developing the analytical formulation of this theory, Chandrasekhar introduced the well known atmospheric diffuse reflection problem. Almost at the same time Ambartsumian introduced his well known invariance principle (Ambartsumian 1943; Ambartsumian 1944). For diffuse reflection case these principles are reformulated by Chandrasekhar 1960. S. Chandrasekhar 1947 analytically solved the semi-infinite atmosphere problem and it reduced in terms of the well known Chandrasekhar's Scattering function (S) and H-function. The same treatment has been done for different scattering phase functions (Horak 1950; Horak and S. Chandrasekhar 1961; Abhyankar and Fymat 1970). For a full review on analytical radiative transfer problem, see G. B. Rybicki 1996.

2.2 Basic definitions

2.2.1 Specific Intensity I :

In vacuum when an element of energy dE_ν transfer through an elemental area $d\vec{A}$ along a direction \vec{ds} in time dt within the solid angular range $\omega, \omega + d\omega$ and the photon frequency range $\nu, \nu + d\nu$, then the amount of energy hold the following

proportionalities,

$$\begin{aligned}
 dE_\nu &\propto |\vec{dA}| \\
 &\propto dt \\
 &\propto d\nu \\
 &\propto d\omega \\
 &\propto \hat{a} \cdot \hat{s}
 \end{aligned}$$

where, \hat{a} and \hat{s} are the unit vectors along the directions \vec{dA} and \vec{ds} respectively which creates an angle ν between them. We can write them down in the form of an equation as follows,

$$\begin{aligned}
 dE_\nu &= I_\nu \cos \nu d\omega d\nu dt dA \\
 \therefore \frac{dE_\nu}{\cos \nu d\omega d\nu dt dA} &= I_\nu
 \end{aligned} \tag{2.1}$$

The proportionality constant I_ν is known as the *Specific intensity of radiation*.

2.2.2 Absorption co-efficient:

Now in Free Space the specific intensity or the intensity of radiation I , remains constant over a distance covered by the ray (G. Rybicki 1979; G. B. Rybicki 1996). Hence in free space the derivative of the intensity with distance will be,

$$\frac{dI_\nu}{ds} = 0$$

However, the intensity I will vary with distance ds only when there is a radiation and matter interaction. If a radiation pencil I_ν enters in a medium contained with some amount of matter instead of free space and exit as radiation $I_\nu + dI_\nu$ from it, then

$$\begin{aligned}
 dI_\nu &\propto I_\nu && \text{Incident radiation} \\
 &\propto \rho && \text{Medium density} \\
 &\propto ds && \text{Covered distance}
 \end{aligned}$$

When this is the case, the formal equation can be written in terms of the *mass absorption co-efficient* κ_ν as proportionality constant,

$$dI_\nu = -\kappa_\nu \rho I_\nu ds \tag{2.2}$$

Due to κ_ν , there is a loss of radiation along the direction of \vec{ds} which explains the negative sign in eqn.(2.2). Now the energy lose can contribute in terms of

radiation along other directions which is commonly specified as scattering or it will transform into any other form of energy (thermal energy for example) in the medium. Let's mention these two distinct cases as: *True Absorption* and *Scattering*. For true absorption case eqn.(2.2) is correct, whereas for true scattering this equation needs some modifications due to the directional property of the scattering medium. Hence for scattering case, κ_ν plays the role of mass scattering co-efficient and the variation of intensity can be expressed as,

$$dI_\nu = -\kappa_\nu p(\cos \Theta) \frac{d\omega'}{4\pi} \rho ds \quad (2.3)$$

Here Θ is the angle between incident and scattering radiation and $p(\cos \Theta)$ is the scattering phase function. $p(\cos \Theta)$ can be defined as the probability of scattering of radiation from the incident solid angle direction to any direction $d\omega'$ (Note that $d\omega'$ does not exclude $d\omega$). Due to the probabilistic nature of $p(\cos \Theta)$, the normalization condition satisfied this function can be written as follows,

$$\frac{1}{4\pi} \int p(\cos \Theta) d\omega' = 1 \quad (2.4)$$

We will discuss more about phase function in a later section.

2.2.3 Emission co-efficient:

In case of radiation-matter interaction, there will be some contribution from the medium itself to the outgoing radiation dI_ν which obviously enhance the radiation dI_ν . This again contribute in terms of emission and scattering from the medium. Now the contribution from the medium may or may not depend on the incident radiation and hence it is better to discuss the dependency case by case. In general, the contribution which is coming from the medium is expressed by the terms of the relation of proportionality as,

$$\begin{aligned} dI_\nu &\propto \rho \\ &\propto ds \end{aligned}$$

Thus the *mass emission co-efficient* can be defined as,

$$\begin{aligned} dI_\nu &= \epsilon_\nu \rho ds \\ \frac{dI_\nu}{\rho ds} &= \epsilon_\nu \end{aligned} \quad (2.5)$$

In case of scattering the contribution on ϵ_ν take the form as,

$$\epsilon_\nu^{(s)}(\nu, \phi) = \kappa_\nu \frac{1}{4\pi} \int_0^\pi \int_0^{2\pi} I_\nu(\nu', \phi') p(\nu, \phi; \nu', \phi') d\phi' \sin \nu' d\nu' \quad (2.6)$$

Here the radiation falling along the direction (v', ϕ') will contribute along (v, ϕ) after scattering due to the scattering phase function $p(v, \phi; v', \phi')$. The solid angle of radiation is expressed as, $d\omega' = \frac{\sin v' dv' d\phi'}{4\pi}$.

The other case is the *Local Thermodynamic equilibrium* (see section 2.5) in the medium where the radiation passes through. If the medium temperature is T then the emission co-efficient can be written as,

$$\epsilon_v^{(LTE)} = \kappa_v B_v(T) \quad (2.7)$$

2.2.4 The Source Function

In the radiative transfer theory the contribution to the radiation due to matter-radiation interaction can be denoted by a function called as the *Source Function*. The definition of source function is,

$$\xi_v = \frac{\epsilon_v}{\kappa_v} \quad (2.8)$$

where ϵ_v and κ_v are the emission co-efficient and absorption co-efficients respectively.

Hence for a scattering atmosphere,

$$\xi_v = \frac{1}{4\pi} \int_0^\pi \int_0^{2\pi} I_v(v', \phi') p(v, \phi; v', \phi') d\phi' \sin v' dv' \quad (2.9)$$

On the other hand for an atmosphere in Local thermodynamic Equilibrium,

$$\xi_v = B_v(T) \quad (2.10)$$

2.2.5 Optical Depth

When there is no source function in the medium, then the incident radiation will decay exponentially (e.g. $I(z) = I(z')e^{-\tau(z, z')}$) due to the radiation-matter interaction while covering a distance from z' to z . The logarithm of the ratio of the initial radiation $I(z')$ to the final radiation $I(z)$ is known as the optical depth for that particular path of that particular medium.

On the other way, if a distance covered by the beam is dz (say) and the matter radiation interaction is $\kappa_v \rho$ then the optical depth expression can be represented as,

$$d\tau_v = -\kappa_v \rho dz \quad (2.11)$$

2.3 General equation of transfer

From the above discussion it is clear that, when a radiation beam transfers through a medium then the variation dI_ν can be written explicitly as,

$$dI_\nu(s, \theta, \phi) = -\kappa_\nu(s)\rho I_\nu(s, \theta, \phi)ds + \epsilon_\nu(s, \theta, \phi)\rho ds$$

Hence the differential form of the radiative transfer equation will be,

$$\boxed{\frac{dI_\nu(s, \theta, \phi)}{-\kappa_\nu\rho ds} = I_\nu(s, \theta, \phi) - \xi_\nu(s, \theta, \phi)} \quad (2.12)$$

From now on we will drop the notation ν and consider the equation for a particular frequency ν in the remaining discussion.

2.4 The Plane Parallel Approximation

Here we introduce the plane-parallel approximation in radiative transfer equation. The atmospheric layers are approximated with negligible curvature and each of them are parallel to other. Whatever direction the light beam goes, it considers the projection of the beam along the area vector of the atmospheric layers which is fixed for all layers due to the current approximation. figure 2.1.

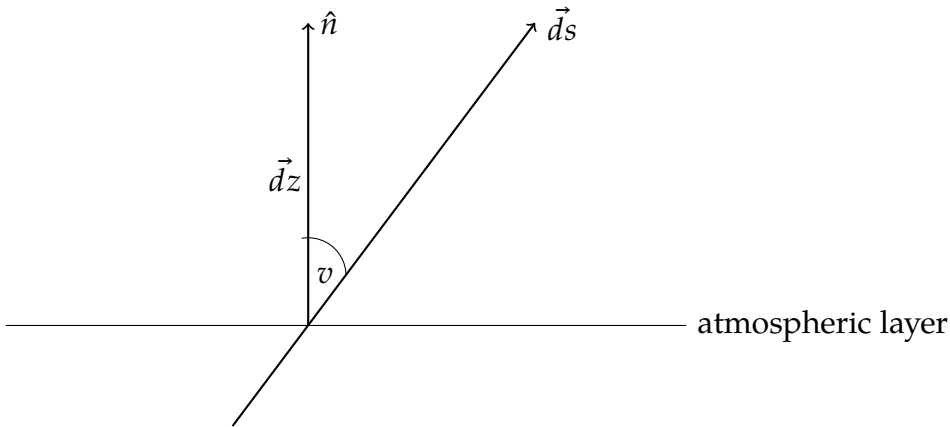


Figure 2.1: Pictorial representation of the plane parallel approximation

If the distance covered by the light is $\vec{d}s$ and the area vector is $\vec{d}z$, then they hold the following relation,

$$\vec{d}s = \frac{\vec{d}z}{\cos v} = \frac{\vec{d}z}{\mu}$$

where μ is the direction cosine of $\vec{d}s$ along $\vec{d}z$.

Hence, in one dimensional plane-parallel approximation the radiative transfer equation will take the form as,

$$\mu \frac{dI(\tau, \mu, \phi)}{d\tau} = I(\tau, \mu, \phi) - \xi(\tau, \mu, \phi) \quad (2.13)$$

2.4.1 Moments of specific intensity

Here we define different specific intensity moments using integration of specific intensity over the solid angle, which are useful in the context of modeling. Fundamentally, there are three moments of specific intensity defined as follows,

Average intensity,

$$\begin{aligned} J_\nu &= \frac{1}{4\pi} \int_0^{2\pi} \int_0^\pi I_\nu d\Omega \\ &= \frac{1}{4\pi} \int_0^{2\pi} \int_0^\pi I \sin \theta d\theta d\phi \end{aligned}$$

For an axially symmetric radiation I_ν is independent of ϕ and in that case,

$$J_\nu = \frac{1}{2} \int_{-1}^1 I_\nu d\mu \quad (2.14)$$

In the same way the other two moments can be defined as,

$$H_\nu = \frac{1}{2} \int_{-1}^1 \mu I_\nu d\mu \quad (2.15)$$

and,

$$K_\nu = \frac{1}{2} \int_{-1}^1 \mu^2 I_\nu d\mu \quad (2.16)$$

These moments are directly related with the macroscopic quantities as follows,

$$\begin{aligned} \text{Energy Density} & \quad u_\nu = \frac{4\pi}{c} J_\nu \\ \text{Net Flux} & \quad F_\nu = 4H_\nu \\ \text{Radiation Pressure} & \quad P_\nu = \frac{4\pi}{c} K_\nu \end{aligned} \quad (2.17)$$

Finally, to get the total moment we need to integrate the in frequency space as follows,

$$(J, H, K) = \int_0^\infty (J_\nu, H_\nu, K_\nu) d\nu$$

In astrophysical context the net flux can be connected with with the effective temperature T_e of considered atmospheric layer as follows,

$$\pi F = \pi \int_0^{\infty} F_{\nu} d\nu = \sigma_B T_e^4 \quad (2.18)$$

where $\sigma_B = 5.75 \times 10^{-5} \text{ergsec}^{-1} \text{cm}^{-2} \text{degree}^{-4}$ is the Stefan-Boltzmann constant.

While considering the Planck emission B_{ν} , there holds a similar relation for the integrated function over the frequency ν as follows,

$$B(T) = \int_0^{\infty} B_{\nu}(T) d\nu = \frac{\sigma_B}{\pi} T_e^4 \quad (2.19)$$

where T_e is customarily known as the *Effective Temperature* (Chandrasekhar 1960).

The Eddington Approximation:

One important approximation we use in our work is the famous Eddington's Approximation. This approximation gives a simple relation between the moments of specific intensity, specifically between J_{ν} and K_{ν} . Eddington considered that the radiation I_{ν} can be approximated as a linear function of μ expanded upto first order. Thus, in a parametric form it can be represented as (G. Rybicki 1979),

$$I_{\nu}(\mu) = a_{\nu} + b_{\nu}\mu \quad (2.20)$$

where a and b are the parameter of the equation.

Using the expression of I_{ν} we can get the form of the moments equations as $J_{\nu} = a_{\nu}$ and $K_{\nu} = \frac{a_{\nu}}{3}$. Hence we can write,

$$K_{\nu} = \frac{J_{\nu}}{3} \quad (2.21)$$

We will show later how to use this relation in exoplanetary atmosphere modeling.

2.5 The Local Thermodynamic Equilibrium Condition

The Thermodynamic equilibrium condition is applied to an isolated system, which behaves like a blackbody and can be fully characterized by the kinetic temperature of the system. But the *Local Thermodynamic Equilibrium* (LTE) is a local approximation of that more general equilibrium conditions. In this case the whole system is divided into very small isolated parts and the thermodynamic equilibrium conditions are valid in each of the parts separately (For extensive discussion on it see Seager 2010a, Chandrasekhar 1960).

While modeling of a planetary atmosphere this LTE Condition is very much useful as it provides a simplification of the analytical solution as well as the solution for the numerical approach of the transfer equation. The atmospheric layer in LTE condition will have an extinction co-efficient

$$\epsilon_\nu = \kappa_\nu B_\nu(T) = \kappa_\nu \frac{2h\nu^3}{c^2} \frac{1}{\exp(h\nu/KT) - 1} \quad (2.22)$$

It is worthnoting that the LTE conditions are applicable only if the photon mean free path is small compared to the thermal, physical and chemical gradients of the corresponding atmospheric layers. Hence for planetary atmosphere case the LTE conditions are valid in lower atmospheric region where density and optical depth are high enough. In such a scenario the source function will explicitly depend only on the temperature of the corresponding atmospheric layer (see section 2.2.4).

2.6 The condition of Radiative Equilibrium

The other important approximation which is useful in the modeling of planetary atmosphere is the *Radiative Equilibrium Condition*. All of our work is done under the radiative equilibrium condition only.

The assumption in this case is, in each atmospheric layers there is no source or sink of energy and the energy will transport by the radiation mechanism only. This assumption ensures that the total flux will remain constant, i.e.

$$F = \int_0^\infty F_\nu d\nu = \int_0^\infty 4H_\nu d\nu = 2 \int_0^\infty \int_{-1}^1 \mu I_\nu(z, \mu) d\mu d\nu = \text{constant}$$

Then the flux variation over height will be,

$$\frac{dF}{dz} = 0$$

This condition can be stated in other terms as,

$$\frac{dF}{dz} = 2 \int_0^\infty [-\rho(\kappa_\nu J_\nu - \kappa_\nu B_\nu)] d\nu = 0$$

Thus the constancy of the net integrated flux can be realized as,

$$\boxed{\int_0^\infty \kappa_\nu J_\nu d\nu = \int_0^\infty \kappa_\nu B_\nu d\nu} \quad (2.23)$$

2.7 The Hydrostatic Equilibrium Condition

For an atmospheric layer, if the vertical pressure gradient on that layer is balanced by the gravity then that atmospheric layer is known to be in hydrostatic equilibrium. The mathematical expression for this equilibrium condition is,

$$\frac{dP}{dz} = -\rho g \quad (2.24)$$

Hence for an atmosphere with hydrostatic equilibrium the optical depth can be expressed as,

$$d\tau = -\kappa\rho dz = -\kappa\frac{dP}{g} \quad (2.25)$$

This particular expression is used to model the atmospheric temperature-pressure profile.

2.8 The Transfer equation with scattering

Till now we have discussed the fundamental concepts and methods of radiative transfer equation. Now we focus on the application of these concepts and discuss specifically the scattering case.

The radiative transfer equation in case of plane- parallel approximation is,

$$\mu\frac{dI(\tau, \nu, \mu, \phi)}{d\tau_\nu} = I(\tau, \nu, \mu, \phi) - \xi(\tau, \nu, \mu, \phi) \quad (2.26)$$

Here, $I(\tau, \nu, \mu, \phi)$ represents the specific intensity at frequency ν along μ and ϕ is the azimuthal angle. Here, $d\tau_\nu$ is the *optical thickness* defined as,

$$d\tau_\nu(z) = -\kappa_\nu(z)dz \quad (2.27)$$

where, z is the atmospheric height. $\kappa(\tau, \nu)$ and $\xi(\tau, \nu)$ are the volumetric absorption co-efficient and source function respectively at the frequency ν along the direction μ , from the atmospheric layer with optical depth τ . A semi-infinite atmosphere is bounded on one side at $\tau = 0$ and extends upto ∞ on the other direction.

Now if πF is the amount of flux incident on a plane-parallel atmospheric layer along the direction $(-\mu_0, \phi_0)$, then $\pi F e^{-\frac{\tau}{\mu_0}}$ is the *reduced incident radiation* that penetrates upto the optical depth τ without experiencing any scattering (fig. 2.2). The diffused radiation scattered at optical depth τ will be expressed in terms of the incident radiation & phase function $p(\mu, \phi; \mu', \phi')$, which is the angular distribution of photons before and after scattering (see section 2.9).

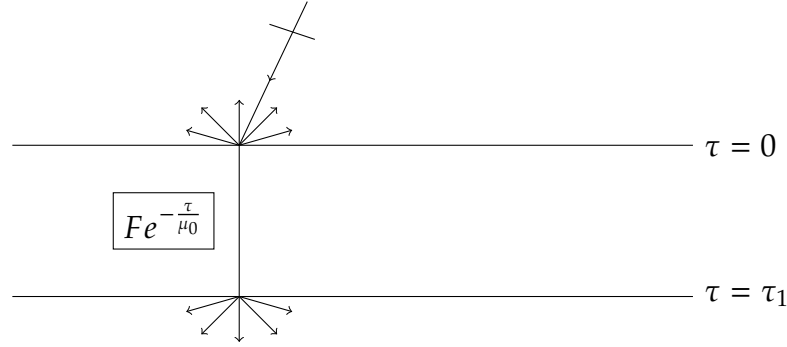


Figure 2.2: This figure shows the total effect due to diffuse scattering from incident direction $(-\mu_0, \phi_0)$ to scattered direction (μ', ϕ') for a *semi-infinite atmosphere*. The downward is the negative direction whereas the upward is the positive direction (from Chandrasekhar 1960).

We mention that the radiation field $I(\tau, \nu, \mu, \phi)$ at optical depth τ is the sum of the diffuse radiation $I_D(\tau, \nu, \mu, \phi)$ and an attenuated field along the direction of incident radiation. It can be expressed mathematically using Dirac-delta function (δ) as,

$$\begin{aligned} I(\tau, \nu, +\mu, \phi) &= I_D(\tau, \nu, +\mu, \phi) & (0 < \mu \leq 1) \\ I(\tau, \nu, -\mu, \phi) &= I_D(\tau, \nu, -\mu, \phi) + \pi F \delta(\mu - \mu_0) \delta(\phi - \phi_0) & (0 < \mu \leq 1) \end{aligned} \quad (2.28)$$

The boundary conditions for the diffuse reflection radiation is,

$$\begin{aligned} I_D(0, -\mu, \phi) &= 0 & (0 < \mu \leq 1) \\ I_D(\infty, -\mu, \phi) &\rightarrow 0 \end{aligned} \quad (2.29)$$

Hereinafter we will drop the suffix 'D' and $I(\tau, \mu, \phi)$ will denote the diffused radiation only.

When there is only scattering in the atmosphere then,

$$\begin{aligned} \xi(\tau, \mu, \phi) &= \frac{1}{4\pi} \int_{-1}^1 \int_0^{2\pi} p(\mu, \phi; \mu', \phi') I(\tau, \mu', \phi') d\phi' d\mu' \\ &+ \frac{1}{4} F e^{-\tau/\mu_0} p(\mu, \phi; -\mu_0, \phi_0) \end{aligned} \quad (2.30)$$

Thus the radiative transfer equation appropriate for diffuse radiation and transmission can be expressed as,

$$\begin{aligned} \mu \frac{dI(\tau, \nu, \mu, \phi)}{d\tau_\nu} &= I(\tau, \nu, \mu, \phi) - \frac{1}{4\pi} \int_{-1}^1 \int_0^{2\pi} p(\mu, \phi; \mu', \phi') I(\tau, \mu', \phi') d\phi' d\mu' \\ &- \frac{1}{4} F e^{-\tau/\mu_0} p(\mu, \phi; -\mu_0, \phi_0) \end{aligned} \quad (2.31)$$

Here $p(\mu, \phi; \mu', \phi')$ is known as the scattering phase function which we will discuss in the following section.

2.9 Scattering phase functions:

From the discussion in the previous section it is evident that the radiative transfer equation explicitly depends on the phase function $p(\mu, \phi; \mu', \phi')$. In this section we will define the phase function and different types of it.

In case of Plane - Parallel Approximation (see 2.4) if a light beam falls along a direction (μ, ϕ) , where ϕ is an azimuthal angle then either true absorption or scattering may happen as shown by Chandrasekhar 1960. In this chapter we are interested for the scattering phenomena only. The light can scatter to any arbitrary direction $(\mu', \phi'$ say) with a probability $p(\cos \Theta)$ — commonly known as phase function, where Θ is the angle between the incident (μ, ϕ) and scattered (μ', ϕ') direction. Mathematically $\cos \Theta$ can be represented in terms of $(\mu, \phi; \mu', \phi')$ as follows,

$$\cos \Theta = \mu\mu' + \sqrt{1 - \mu^2}\sqrt{1 - \mu'^2} \cos(\phi - \phi') \quad (2.32)$$

Hence, the scattering phase function $P(\cos \Theta)$ can be defined as the probability of scattering of an incident beam along an element of solid angle $d\omega$. The normalization condition applicable to the phase function can be expressed as,

$$\int p(\cos \Theta) \frac{d\omega'}{4\pi} = \tilde{\omega}_0 \leq 1 \quad (2.33)$$

where $\tilde{\omega}_0$ is known as the single scattering albedo. The equality sign holds for the conservative case of pure scattering.

Now the phase function, in general can be expanded for a finite number of terms N (say) as follows,

$$p(\cos \Theta) = \sum_{l=0}^N \tilde{\omega}_l P_l(\cos \Theta) \quad (2.34)$$

where $P_l(\cos \Theta)$ is the Legendre polynomial of degree l .

The phase functions can also be represented explicitly by the direction of incident (μ, ϕ) and scattered (μ', ϕ') radiation in terms of associated legendre polynomials $P_l^m(\mu)$ as follows,

$$p(\mu, \phi; \mu', \phi') = \sum_{m=0}^N (2 - \delta_{0,m}) \left[\sum_{l=m}^N \tilde{\omega}_l^m P_l^m(\mu) P_l^m(\mu') \right] \cos m(\phi - \phi') \quad (2.35)$$

where, $\tilde{\omega}_l^m = \tilde{\omega}_l \frac{(l-m)!}{(l+m)!}$ and δ is the Kronecker delta

Depending on the physical nature of scattering, the phase function can be represented in different ways as described below,

1. **Isotropic phase function:** In this case the incident light scatters isotropically to every direction. Hence the probability of scattering is the same in all direction. Mathematically it can be obtained by considering $\tilde{\omega}_l = \delta_{0,l}$. Thus the phase function can be written as,

$$p(\cos \Theta) = \tilde{\omega}_0 \leq 1 \quad (2.36)$$

2. **Asymmetric scattering:** In this case, the scattering probability is not the same along every direction. The asymmetry parameter $x \in (0, 1)$ was introduced by Chandrasekhar 1960 and thus can be expressed as,

$$p(\cos \Theta) = \tilde{\omega}_0(1 + x \cos \Theta) \quad (-1 \leq x \leq 1) \quad (2.37)$$

or in explicit form as,

$$p(\mu, \phi; \mu', \phi') = \tilde{\omega}_0[1 + x\mu\mu' + x\sqrt{(1 - \mu^2)(1 - \mu'^2)} \cos(\phi - \phi')] \quad (2.38)$$

3. **Rayleigh scattering:** Rayleigh scattering is a very important phenomena in the astrophysical context. It was first introduced by Lord Rayleigh in the context of explaining the blueness of the sky. For planetary atmospheres it is the most dominant scattering process in the absence of Mie scattering (Nikku Madhusudhan and Burrows 2012; Kattawar and Adams 1971). For substellar-mass objects (e.g. T-dwarfs), multiple Rayleigh scattering shows polarization effect (Sengupta and Marley 2009). In case of hot stars the neutral hydrogen and singly ionized helium shows Rayleigh scattering from the atmosphere (Fišák et al. 2016). The mathematical formulation can be given as (Chandrasekhar 1960),

$$p(\cos \Theta) = \frac{3}{4}(1 + \cos^2 \Theta) \quad (2.39)$$

and in explicit form as,

$$p(\mu, \phi; \mu', \phi') = \frac{3}{8}[p^{(0)}(\mu, \mu') + 4\mu\mu'\sqrt{(1 - \mu^2)(1 - \mu'^2)} \cos(\phi - \phi') + (1 - \mu^2)(1 - \mu'^2) \cos 2(\phi - \phi')] \quad (2.40)$$

where,

$$\begin{aligned} p^{(0)}(\mu, \mu') &= \frac{1}{2\pi} \int_0^{2\pi} p(\mu, \phi; \mu', \phi') d\phi' \\ &= \frac{1}{3}(3 - \mu^2)(3 - \mu'^2) + \frac{8}{3}\mu^2\mu'^2 \end{aligned}$$

4. **General third order expansion:** This is the the most general phase function we will consider in this work. The phase function is expanded in terms of Legendre polynomials upto order 2.

$$\begin{aligned} p(\cos \Theta) &= \sum_{m=0}^2 \tilde{\omega}_m P_m(\cos \Theta) \\ &= \tilde{\omega}_0 + \tilde{\omega}_1 P_1(\cos \Theta) + \tilde{\omega}_2 P_2(\cos \Theta) \end{aligned} \quad (2.41)$$

where $\tilde{\omega}_0, \tilde{\omega}_1, \tilde{\omega}_2$ are constants and P_1, P_2 are Legendre polynomials of $\cos \Theta$ given in eqn.(2.32). The analytical solutions for semi-infinite atmosphere using this phase function in case of diffuse reflection only have been obtained in Horak and S. Chandrasekhar 1961. Note that at different values of $\tilde{\omega}_0$ (*single scattering albedo*), $\tilde{\omega}_1$ and $\tilde{\omega}_2$ this phase function will reduce into the previous phase functions. If $\tilde{\omega}_1 = \tilde{\omega}_2 = 0$ then it is isotropic scattering, if $\tilde{\omega}_2 = 0, \tilde{\omega}_1 = x\tilde{\omega}_0$, then it is asymmetric scattering and for rayleigh scattering $\tilde{\omega}_0 = 1, \tilde{\omega}_1 = 0, \tilde{\omega}_2 = \frac{1}{2}$. For an extensive discussion of different phase functions produced due to the choices of different set of $\tilde{\omega}_0, \tilde{\omega}_1, \tilde{\omega}_2$ values we refer Bhatia and Abhyankar 1983. Thus, we can say this is the most general phase function till now discussed.

Now this phase function can be expanded explicitly in terms of $(\mu, \phi; \mu', \phi')$ as follows,

$$\begin{aligned} p(\mu, \phi; \mu', \phi') &= p^{(0)}(\mu, \mu') + (\tilde{\omega}_1 + 3\tilde{\omega}_2\mu\mu')\sqrt{(1-\mu^2)(1-\mu'^2)}\cos(\phi-\phi') \\ &\quad + \frac{3}{4}\tilde{\omega}_2(1-\mu^2)(1-\mu'^2)\cos 2(\phi-\phi') \end{aligned} \quad (2.42)$$

where in this case,

$$p^{(0)}(\mu, \mu') = \frac{3\tilde{\omega}_2}{4} \frac{1}{\zeta} [\zeta - \mu^2)(\zeta - \mu'^2) + \frac{4\tilde{\omega}_0}{\tilde{\omega}_2}(\mu\mu')^2] + \tilde{\omega}_1\mu\mu'$$

with $\zeta = \frac{4\tilde{\omega}_0 + \tilde{\omega}_2}{3\tilde{\omega}_2}$

2.10 The Scattering and Transmission Function:

When a light beam incident on a plane-parallel atmosphere then that light can diffusely scatter and transmit by (through) the atmosphere. Hence to treat the diffuse reflection and transmission problem, Chandrasekhar 1960 introduced two fundamental functions as the *scattering function* $\mathbf{S}(\tau_1; \mu, \phi; \mu_0, \phi_0)$ and *Transmission*

function $\mathbf{T}(\tau_1; \mu, \phi; \mu_0, \phi_0)$. The total output radiation from the atmosphere can be expressed by these two fundamental functions.

For example, if πF amount of flux incident along the direction $(-\mu_0, \phi_0)$ on a plane-parallel atmosphere (see fig. 2.2), then the diffusely reflected intensity $I(0, +\mu, \phi)$ from $\tau = 0$ and diffusely transmitted intensity $I(\tau_1, -\mu, \phi)$ from $\tau = \tau_1$ can be expressed as,

$$\begin{aligned} I(0, +\mu, \phi) &= \frac{F}{4\mu} S(\tau_1; \mu, \phi; \mu_0, \phi_0) \\ I(\tau_1, -\mu, \phi) &= \frac{F}{4\mu} T(\tau_1; \mu, \phi; \mu_0, \phi_0) \end{aligned} \quad (2.43)$$

where, $(0 \leq \mu \leq 1)$

The term $\frac{1}{\mu}$ is introduced due to the fact of securing symmetry between the pair of variables (μ, ϕ) and (μ_0, ϕ_0) required to satisfy the Helmholtz's reciprocity principle, that says,

$$\begin{aligned} S(\tau_1; \mu, \phi; \mu_0, \phi_0) &= S(\tau_1; \mu_0, \phi_0; \mu, \phi) \\ T(\tau_1; \mu, \phi; \mu_0, \phi_0) &= T(\tau_1; \mu_0, \phi_0; \mu, \phi) \end{aligned} \quad (2.44)$$

In other words the reciprocity principle can be stated as (Chandrasekhar 1960), *While the incidence and emergence directions of light interchange, the Scattering and Transmission functions remain unaltered.* This principle actually depends on the fact that light beam follows the same path if the direction is reversed.

2.11 Different types of plane-parallel atmosphere:

For the specification of a plane-parallel atmosphere, it is customary to define the atmospheric properties in terms of the optical depth τ of the atmosphere. Depending on τ two fundamentally different atmospheres can be defined as follows (Chandrasekhar 1960),

1. **Semi-infinite Atmosphere:** When an atmosphere extends from optical depth $\tau = 0$ to $\tau \rightarrow \infty$, then that is named as Semi-infinite atmosphere.
2. **Finite Atmosphere:** On the other hand, if an atmosphere extends from optical depth $\tau = 0$ to $\tau = \tau_1$ (where τ_1 is finite), then it is recognized as finite atmosphere.

In this project we will constrain ourself for these two types of atmosphere only.

2.12 The principle of Invariance:

The *Invariance principle* was first formulated by Ambartsumian 1943 in case of semi-infinite atmosphere and Ambartsumian 1944 for finite atmosphere. But these laws were used at their full efficiency for the first time by Chandrasekhar 1960. In the following sections we will discuss this principle for the two cases separately.

2.12.1 Semi-infinite Atmosphere:

In case of diffuse reflection in semi-infinite atmosphere, the invariance principle was formulated by Chandrasekhar 1960 for emergent radiation and for diffuse reflection. The statements are as follows,

- *The emergent radiation from a semi-infinite plane-parallel atmosphere remains invariant when we add (subtract) some layers with arbitrary optical thickness to (from) the considered atmosphere.*
- *The Law which governs the diffuse reflection process in case of a plane-parallel semi-infinite atmosphere remains invariant while we add (subtract) some layers with arbitrary optical thickness to (from) the considered atmosphere.*

These laws are very useful in the context of determining the scattering function of semi-infinite atmosphere. Infact it assures the translational invariance of the scattering function $S(\mu, \phi; \mu', \phi')$ over the whole semi-infinite atmosphere. Now we will derive the mathematical form of the invariance principle in case of semi-infinite diffuse reflection problem.

For semi-infinite atmosphere it is natural to be interested only in the diffuse reflection. Hence, in the same case described in sec 2.10 the only interesting part here is the reflected intensity $I(0, \mu, \phi)$ which can be expressed as,

$$I(0, +\mu, \phi) = \frac{F}{4\mu} S(\mu, \phi; \mu_0, \phi_0) \quad (2.45)$$

When there is radiation, clearly there are three parts of it,

1. The reduced incident flux $F e^{-\tau/\mu_0}$
2. The inward directed flux $I(\tau, -\mu, \phi)$
3. The outward directed flux $I(\tau, +\mu, \phi)$

Now the atmosphere below the optical depth τ , will give the reflection of the incident flux which is reduced due to traversing up to that optical depth and the

flux which is directed inward according to the same law of diffuse reflection. The final outward flux must be equal to the total reflected flux. Hence the mathematical form of the invariance principle for semi-infinite atmosphere can be written as follows,

$$I(\tau, +\mu, \phi) = \frac{F}{4\mu} e^{-\frac{\tau}{\mu_0}} S(\mu, \phi; \mu_0, \phi_0) + \frac{1}{4\pi\mu} \int_0^1 \int_0^{4\pi} I(\tau, -\mu', \phi') S(\mu, \phi; \mu', \phi') d\mu' d\phi' \quad (2.46)$$

2.12.2 Finite Atmosphere case:

The semi-infinite atmosphere is a special case of the more general finite atmosphere case. Thus, the principle for finite atmosphere case should be reduced to the semi-infinite one in the condition of $\tau_1 \rightarrow \infty$. For finite atmosphere the direction of radiation can be divided into two parts as follows,

- The outward flux $I(\tau, +\mu, \phi)$, directed from τ towards $\tau \rightarrow 0$.
- The inward flux $I(\tau, -\mu, \phi)$, directed from τ towards $\tau = \tau_1$.

In both the cases the direction cosine will vary in the range of $(0 \leq \mu \leq 1)$

Hence, to estimate the radiation field at any layer of optical depth τ (where, $0 < \tau < \tau_1$) we need to estimate the following quantities as mentioned by Annamaneni Peraiah 2002,

1. The outward intensity $I(\tau, +\mu, \phi)$ from τ
2. The inward intensity $I(\tau, -\mu, \phi)$ from τ
3. The diffusely reflected flux $\frac{F}{4\mu} S(\tau_1; \mu, \phi; \mu_0, \phi_0)$ by the whole medium extended from $\tau = 0 \rightarrow \tau_1$.
4. The diffusely transmitted flux $\frac{F}{4\mu} T(\tau_1; \mu, \phi; \mu_0, \phi_0)$ by the whole medium extended from $\tau = 0 \rightarrow \tau_1$

To estimate these quantities, the following statements of invariance principle can be formulated (Annamaneni Peraiah 2002),

- $I(\tau, +\mu, \phi)$, the outward intensity will be combined by the reflection of the reduced incident flux $\pi F e^{-\tau/\mu_0}$ & inward directed diffused radiation $I(\tau, -\mu', \phi')$ from the medium of optical thickness $(\tau_1 - \tau)$.

Mathematical form,

$$I(\tau, +\mu, \phi) = \frac{F}{4\mu} e^{-\tau/\mu_0} S(\tau_1 - \tau; \mu, \phi; \mu_0, \phi_0) + \frac{1}{4\pi\mu} \int_0^{2\pi} \int_0^1 I(\tau, -\mu', \phi') S(\tau_1 - \tau; \mu, \phi; \mu', \phi') d\mu' d\phi' \quad (2.47)$$

- The intensity $I(\tau, -\mu, \phi)$ will be a combined by the transmission of incident flux F and reflection of outward directed flux $I(\tau, +\mu', \phi')$ incident below τ by the medium of optical thickness τ .

Mathematical form,

$$I(\tau, -\mu, \phi) = \frac{F}{4\mu} T(\tau; \mu, \phi; \mu_0, \phi_0) + \frac{1}{4\pi\mu} \int_0^{2\pi} \int_0^1 I(\tau, +\mu', \phi) S(\tau; \mu, \phi; \mu', \phi') d\mu' d\phi' \quad (2.48)$$

- The total diffuse reflection of the entire atmosphere will be a result of the reflection of the incident flux F , direct and diffusion transmission of outward directed radiation, which is $I(\tau, +\mu, \phi)$, incident below of the optical thickness τ .

Mathematical form,

$$\frac{F}{4\mu} S(\tau_1; \mu, \phi; \mu_0, \phi_0) = \frac{F}{4\mu} S(\tau; \mu, \phi; \mu_0, \phi_0) + e^{-\tau/\mu} I(\tau, +\mu, \phi) + \frac{1}{4\pi\mu} \int_0^{2\pi} \int_0^1 I(\tau, +\mu', \phi') T(\tau; \mu, \phi; \mu', \phi') d\mu' d\phi' \quad (2.49)$$

- The total diffuse transmission by the entire atmosphere will be combined by the diffusely transmitted reduced incident flux $\pi F e^{-\tau/\mu_0}$ as well as direct and diffuse transmission of the inward directed flux $I(\tau, -\mu', \phi')$ incident below τ through the optical thickness $\tau_1 - \tau$.

The mathematical form will be,

$$\frac{F}{4\mu} T(\tau_1; \mu, \phi; \mu_0, \phi_0) = \frac{F}{4\mu} e^{-\tau/\mu_0} T(\tau_1 - \tau; \mu, \phi; \mu_0, \phi_0) + e^{-(\tau_1 - \tau)/\mu} I(\tau, -\mu, \phi) + \frac{1}{4\pi\mu} \int_0^{2\pi} \int_0^1 I(\tau, -\mu', \phi') T(\tau_1 - \tau; \mu, \phi; \mu', \phi') d\mu' d\phi' \quad (2.50)$$

2.13 Integral form of Scattering function in semi-infinite atmosphere:

It is clear that the scattering function is very crucial while modeling the semi-infinite atmosphere. In fact the final reflected radiation from such an atmosphere can be estimated in terms of scattering function only. Hence, we will derive the integral form of scattering function in this present section.

Taking differentiation of the equation (2.46) and set the condition of optical depth $\tau = 0$ we will get,

$$\begin{aligned} \frac{dI(\tau, +\mu, \phi)}{d\tau} \Big|_{\tau=0} &= -\frac{F}{4\mu\mu_0} S(\mu, \phi; \mu_0, \phi_0) \\ &+ \frac{1}{4\pi\mu} \int_0^1 \int_0^{2\pi} S(\mu, \phi; \mu', \phi') \left[\frac{dI(\tau, -\mu', \phi')}{d\tau} \right]_{\tau=0} d\mu' d\phi' \end{aligned} \quad (2.51)$$

Putting $\tau = 0$ in eqn.(2.26) we will get the following equation,

$$\left[\frac{dI_\lambda(\tau, +\mu, \phi)}{d\tau} \right]_{\tau=0} = \frac{1}{\mu} [I_\lambda(0, +\mu, \phi) - \xi_\lambda(0, +\mu, \phi)] \quad (2.52)$$

$$\left[\frac{dI_\lambda(\tau, -\mu, \phi)}{d\tau} \right]_{\tau=0} = \frac{1}{\mu} \xi_\lambda(0, -\mu, \phi) \quad (2.53)$$

To get the integral equation of the scattering function we follows the same formalism given in Chandrasekhar 1960 for boundary condition

$$I(0, -\mu, \phi) = 0; 0 < \mu \leq 1 \quad (2.54)$$

That means, no radiation will go in $(-\mu, \phi)$ direction at $\tau = 0$. Now, putting eqn.(2.52) and (2.53) in (2.51) we will get,

$$\begin{aligned} \frac{1}{\mu} [I_\lambda(0, +\mu, \phi) - \xi_\lambda(0, +\mu, \phi)] &= -\frac{F}{4\mu\mu_0} S(\mu, \phi; \mu_0, \phi_0) \\ &+ \frac{1}{4\pi\mu} \int_0^1 \int_0^{2\pi} S(\mu, \phi; \mu', \phi') \frac{1}{\mu'} \xi_\lambda(0, -\mu', \phi') d\mu' d\phi' \\ \therefore \frac{F}{4} \left(\frac{1}{\mu} + \frac{1}{\mu_0} \right) S(\mu, \phi; \mu_0, \phi_0) &= \xi(0, +\mu, \phi) \\ &+ \frac{1}{4\pi} \int_0^1 \int_0^{2\pi} S(\mu, \phi; \mu', \phi') \xi(0, -\mu', \phi') \frac{d\mu'}{\mu'} d\phi' \end{aligned} \quad (2.55)$$

Now at $\tau = 0$, the source function ξ (eqn.(2.30)) with the boundary condition (2.54) will take the form as,

$$\begin{aligned} \xi_{\lambda}(0, \mu', \phi') &= \frac{F}{16\pi} \int_0^1 \int_0^{2\pi} p(\mu', \phi'; \mu'', \phi'') S(\mu_0, \phi_0; \mu'', \phi'') d\phi'' \frac{d\mu''}{\mu''} \\ &+ \frac{F}{4} p(\mu', \phi'; -\mu_0, \phi_0) \end{aligned} \quad (2.56)$$

While putting this expression in eqn.(2.55) we obtain,

$$\begin{aligned} & \left(\frac{1}{\mu_0} + \frac{1}{\mu} \right) S(\mu, \phi, \mu_0, \phi_0) \\ &= p(\mu, \phi; -\mu_0, \phi_0) + \frac{1}{4\pi} \int_0^1 \int_0^{2\pi} S(\mu, \phi; \mu', \phi') p(-\mu', \phi'; -\mu_0, \phi_0) \frac{d\mu'}{\mu'} d\phi' \\ &+ \frac{1}{4\pi} \left[\int_0^1 \int_0^{2\pi} p(\mu, \phi; \mu'', \phi'') S(\mu_0, \phi_0; \mu'', \phi'') d\phi'' \frac{d\mu''}{\mu''} \right. \\ &+ \left. \frac{1}{4\pi} \int_0^1 \int_0^{2\pi} \int_0^1 \int_0^{2\pi} S(\mu, \phi; \mu', \phi') p(-\mu', \phi'; \mu'', \phi'') S(\mu_0, \phi_0; \mu'', \phi'') \right. \\ & \left. d\phi'' \frac{d\mu''}{\mu''} \frac{d\mu'}{\mu'} d\phi' \right] \end{aligned} \quad (2.57)$$

Eqn. (2.57) represents the required integral equation of scattering function in general case for a scattering only atmosphere.

2.14 Explicit form of the scattering integral equation for different phase functions

The integral equation derived in the last section is the general form of its own and it may take specific form depending on the phase functions explicitly. We have discussed a good deal about the phase functions in section 2.9. Here we will show how the general form of scattering integral equation 2.57 changes with different kind of scattering phase functions.

2.14.1 Isotropic Phase Function:

For isotropic scattering case, the phase function is given in eqn.(2.36). Hence the scattering function will also be axially symmetric and thus eqn.(2.57) will take the form as,

$$\left(\frac{1}{\mu_0} + \frac{1}{\mu} \right) S(\mu; \mu_0) = \tilde{\omega}_0 \left[1 + \frac{1}{2} \int_0^1 S(\mu; \mu') \frac{d\mu'}{\mu'} \right] \left[1 + \frac{1}{2} \int_0^1 S(\mu_0; \mu'') \frac{d\mu''}{\mu''} \right] \quad (2.58)$$

Due to the symmetric property of scattering function with respect to μ and μ' , the bracketed terms in the right hand side should be a function which depends only on the values of either μ or μ_0 . This function is known as Chandrasekhar's H-function defined as (Chandrasekhar 1960),

$$H(\mu) = 1 + \frac{1}{2} \int_0^1 S(\mu; \mu') \frac{d\mu'}{\mu'} \quad (2.59)$$

Hence the scattering function, given in Eqn. (2.58) can be expressed as,

$$\left(\frac{1}{\mu_0} + \frac{1}{\mu}\right)S(\mu; \mu_0) = \tilde{\omega}_0 H(\mu)H(\mu_0) \quad (2.60)$$

Thus the non-linear integral equation of $H(\mu)$ can be obtained by putting this expression back into equation (2.59) as,

$$H(\mu) = 1 + \frac{\tilde{\omega}_0}{2} \mu H(\mu) \int_0^1 \frac{H(\mu')}{\mu + \mu'} d\mu' \quad (2.61)$$

Now the diffusely scattered radiation expression can be given by eqn.(2.45) as,

$$I(0, \mu, \mu_0) = \tilde{\omega}_0 H(\mu)H(\mu_0) \quad (2.62)$$

It is worthnoting that for conservative scattering case, the required expressions can be obtained just by putting $\tilde{\omega}_0 = 1$.

2.14.2 Asymmetric scattering:

This type of phase function generally occurs for planetary illumination case introducing the asymmetry as shown by Chandrasekhar 1960. The *asymmetric scattering phase function* can be written as, $p(\cos \Theta) = \tilde{\omega}_0(1 + x \cos \Theta)$, see eqn.(2.37).

The scattering function here, will have the similar form of eqn.(2.38) (Chandrasekhar 1960),

$$S(\mu, \phi; \mu', \phi') = \tilde{\omega}_0 [S^{(0)}(\mu; \mu') + S^{(1)}(\mu; \mu') x \sqrt{(1 - \mu^2)(1 - \mu'^2)} \cos(\phi' - \phi)] \quad (2.63)$$

To solve for the scattering function we need to use the following identity,

$$\begin{aligned} \frac{1}{2\pi} \int_0^{2\pi} \cos m(\phi' - \phi_0) \cos n(\phi - \phi') d\phi' &= 0; m \neq n \\ &= \frac{1}{2} \cos m(\phi - \phi_0); m = n \neq 0 \\ &= 1; m = n = 0 \end{aligned} \quad (2.64)$$

Using eqns.(2.38),(2.57) and (2.64) we will deduce the form of $S(\mu, \phi; \mu_0, \phi_0)$ and comparing with eqn.(2.63) with (μ', ϕ') replaced by (μ_0, ϕ_0) we will get the form of $S^{(0)}$ as,

$$\begin{aligned} \left(\frac{1}{\mu_0} + \frac{1}{\mu}\right)S^{(0)}(\mu; \mu_0) &= \left[1 + \frac{\tilde{\omega}_0}{2} \int_0^1 S^{(0)}(\mu'', \mu_0) \frac{d\mu''}{\mu''}\right] \left[1 + \frac{\tilde{\omega}_0}{2} \int_0^1 S^{(0)}(\mu', \mu) \frac{d\mu'}{\mu'}\right] \\ &\quad - x \left[\mu_0 - \frac{\tilde{\omega}_0}{2} \int_0^1 S^{(0)}(\mu'', \mu_0) d\mu''\right] \left[\mu - \frac{\tilde{\omega}_0}{2} \int_0^1 S^{(0)}(\mu', \mu) d\mu'\right] \end{aligned} \quad (2.65)$$

We can write eqn.(2.65) in closed form as follows,

$$\left(\frac{1}{\mu_0} + \frac{1}{\mu}\right)S_a^{(0)}(\mu; \mu_0) = \psi_a(\mu_0)\psi_a(\mu) - x\phi_a(\mu_0)\phi_a(\mu) \quad (2.66)$$

where we define¹,

$$\begin{aligned} \psi_a(\mu) &= 1 + \frac{1}{2}\tilde{\omega}_0 \int_0^1 S_a^{(0)}(\mu; \mu') \frac{d\mu'}{\mu'} \\ \phi_a(\mu) &= \mu - \frac{1}{2}\tilde{\omega}_0 \int_0^1 S_a^{(0)}(\mu; \mu') d\mu' \end{aligned} \quad (2.67)$$

Putting the expression of $S^{(0)}$ back into equation (2.67) we will get the expressions of ϕ and ψ as follows,

$$\psi_a(\mu) = 1 + \frac{\tilde{\omega}_0}{2}\mu\psi_a(\mu) \int_0^1 \psi_a(\mu') \frac{d\mu'}{\mu + \mu'} - \frac{\tilde{\omega}_0}{2}x\mu\phi_a(\mu) \int_0^1 \phi_a(\mu') \frac{d\mu'}{\mu + \mu'} \quad (2.68)$$

and

$$\phi_a(\mu) = \mu - \frac{\tilde{\omega}_0}{2}\mu\psi_a(\mu) \int_0^1 \psi_a(\mu') \frac{\mu'}{\mu + \mu'} d\mu' + \frac{\tilde{\omega}_0}{2}x\mu\phi_a(\mu) \int_0^1 \phi_a(\mu') \frac{\mu'}{\mu + \mu'} d\mu' \quad (2.69)$$

In the same way we can find the expression of $S^{(1)}(\mu, \mu_0)$ by comparing the $\cos(\phi - \phi_0)$ term,

$$\begin{aligned} \left(\frac{1}{\mu_0} + \frac{1}{\mu}\right)S^{(1)}(\mu; \mu_0) &= \left[1 + \frac{\tilde{\omega}_0}{4}x \int_0^1 S^{(1)}(\mu', \mu)(1 - \mu'^2) \frac{d\mu'}{\mu'}\right] * \left[1 + \frac{\tilde{\omega}_0}{4}x \int_0^1 S^{(1)}(\mu'', \mu_0)(1 - \mu''^2) \frac{d\mu''}{\mu''}\right] \\ &= H^{(1)}(\mu)H^{(1)}(\mu_0) \end{aligned} \quad (2.70)$$

¹Hereinafter the subscript "a" denotes the *asymmetric scattering case*.

This $H^{(1)}(\mu)$ is defined as Chandrasekhar 1960,

$$H^{(1)}(\mu) = 1 + \frac{\tilde{\omega}_0}{4} x \mu H^{(1)}(\mu) \int_0^1 \frac{H^{(1)}(\mu')}{\mu + \mu'} (1 - \mu'^2) d\mu' \quad (2.71)$$

Finally, we can put the values of $S^{(0)}$ and $S^{(1)}$ in eqn.(2.63) we will get,

$$\begin{aligned} S_a(\mu, \phi; \mu_0, \phi_0) &= \frac{\mu\mu_0}{\mu + \mu_0} \tilde{\omega}_0 [(\psi_a(\mu)\psi_a(\mu_0) - x\phi_a(\mu)\phi_a(\mu_0))] \\ &+ H^{(1)}(\mu)H^{(1)}(\mu_0)x\sqrt{(1 - \mu^2)(1 - \mu_0^2)} \cos(\phi_0 - \phi) \end{aligned} \quad (2.72)$$

Thus, the diffusely reflected intensity from thermally emitting atmosphere in asymmetric scattering can be determined using eqns. (2.72) and (2.45) as,

$$\begin{aligned} I(0, \mu; \mu_0) &= \frac{F}{4\mu} S_a(\mu, \phi; \mu_0, \phi_0) \\ &= \frac{F}{4} \frac{\mu_0}{\mu + \mu_0} \tilde{\omega}_0 [(\psi_a(\mu)\psi_a(\mu_0) - x\phi_a(\mu)\phi_a(\mu_0))] \\ &+ H^{(1)}(\mu)H^{(1)}(\mu_0)x\sqrt{(1 - \mu^2)(1 - \mu_0^2)} \cos(\phi_0 - \phi) \end{aligned} \quad (2.73)$$

2.14.3 Rayleigh scattering phase function:

This scattering phenomena is very important in the astrophysical context (see section 2.9). Thus it is important to evaluate the scattering function for Rayleigh scattering case.

We can express the scattering function which will be similar to the phase function equation (2.40) as,

$$\begin{aligned} S(\mu, \phi; \mu', \phi') &= \frac{3}{8} [S^{(0)}(\mu, \mu') \\ &+ S^{(1)}(\mu, \mu') 4\mu\mu' \sqrt{(1 - \mu^2)(1 - \mu'^2)} \cos(\phi - \phi') \\ &+ S^{(2)}(\mu, \mu') (1 - \mu^2)(1 - \mu'^2) \cos 2(\phi - \phi')] \end{aligned} \quad (2.74)$$

Following the same procedure as we have done before we can derive the expressions of $S^{(0)}(\mu, \mu_0)$, $S^{(1)}(\mu, \mu_0)$ and $S^{(2)}(\mu, \mu_0)$.

$$\begin{aligned}
& \left(\frac{1}{\mu_0} + \frac{1}{\mu}\right)S^{(0)}(\mu, \mu_0) \\
&= \frac{1}{3}\left[3 - \mu^2 + \frac{3}{16} \int_0^1 (3 - \mu'^2)S^{(0)}(\mu, \mu')\frac{d\mu'}{\mu'}\right]* \\
&* \left[3 - \mu_0^2 + \frac{3}{16} \int_0^1 (3 - \mu''^2)S^{(0)}(\mu_0, \mu'')\frac{d\mu''}{\mu''}\right] \\
&+ \frac{8}{3}\left[\mu^2 + \frac{3}{16} \int_0^1 \mu'^2 S^{(0)}(\mu, \mu')\frac{d\mu'}{\mu'}\right]* \left[\mu_0^2 + \frac{3}{16} \int_0^1 \mu''^2 S^{(0)}(\mu_0, \mu'')\frac{d\mu''}{\mu''}\right]
\end{aligned} \tag{2.75}$$

We define the following terms²,

$$\begin{aligned}
\psi_R(\mu) &= 3 - \mu^2 + \frac{3}{16} \int_0^1 (3 - \mu'^2)S_R^{(0)}(\mu, \mu')\frac{d\mu'}{\mu'} \\
\phi_R(\mu) &= \mu^2 + \frac{3}{16} \int_0^1 \mu'^2 S_R^{(0)}(\mu, \mu')\frac{d\mu'}{\mu'}
\end{aligned} \tag{2.76}$$

Now eqn.(2.75) can be expressed as,

$$\therefore \left(\frac{1}{\mu_0} + \frac{1}{\mu}\right)S_R^{(0)}(\mu, \mu_0) = \frac{1}{3}\psi_R(\mu)\psi_R(\mu_0) + \frac{8}{3}\phi_R(\mu)\phi_R(\mu_0) \tag{2.77}$$

Now putting eqn.(2.77) in eqn.(2.76) we can get the explicit forms for ϕ_R and ψ_R as follows,

$$\begin{aligned}
\psi_R(\mu) &= (3 - \mu^2) + \frac{1}{16}\mu\psi_R(\mu) \int_0^1 \frac{3 - \mu'^2}{\mu + \mu'}\psi_R(\mu')d\mu' \\
&+ \frac{1}{2}\mu\phi_R(\mu) \int_0^1 \frac{3 - \mu'^2}{\mu + \mu'}\phi_R(\mu')d\mu'
\end{aligned} \tag{2.78}$$

and

$$\begin{aligned}
\phi_R(\mu) &= \mu^2 + \frac{1}{16}\mu\psi_R(\mu) \int_0^1 \frac{\mu'^2}{\mu + \mu'}\psi_R(\mu')d\mu' \\
&+ \frac{1}{2}\mu\phi_R(\mu) \int_0^1 \frac{\mu'^2}{\mu + \mu'}\phi_R(\mu')d\mu'
\end{aligned} \tag{2.79}$$

The remaining expressions for $S^{(1)}(\mu, \mu')$ and $S^{(2)}(\mu, \mu')$ can be found by comparing the co-efficients of $\cos(\phi - \phi_0)$ and $\cos 2(\phi - \phi_0)$ respectively. We write

²Hereinafter the subscript "R" stands for Rayleigh scattering

them down here,

$$\begin{aligned} \left(\frac{1}{\mu} + \frac{1}{\mu_0}\right)S^{(1)}(\mu, \mu_0) &= \left[1 + \frac{3}{8} \int_0^1 \mu''^2(1 - \mu''^2)S^{(1)}(\mu'', \mu_0) \frac{d\mu''}{\mu''}\right] \\ &* \left[1 + \frac{3}{8} \int_0^1 \mu'^2(1 - \mu'^2)S^{(1)}(\mu, \mu') \frac{d\mu'}{\mu'}\right] \end{aligned} \quad (2.80)$$

and,

$$\begin{aligned} \left(\frac{1}{\mu} + \frac{1}{\mu_0}\right)S^{(2)}(\mu, \mu_0) &= \left[1 + \frac{3}{32} \int_0^1 (1 - \mu''^2)^2 S^{(2)}(\mu'', \mu_0) \frac{d\mu''}{\mu''}\right] \\ &* \left[1 + \frac{3}{32} \int_0^1 (1 - \mu'^2)^2 S^{(2)}(\mu, \mu') \frac{d\mu'}{\mu'}\right] \end{aligned} \quad (2.81)$$

Now, eqns. (2.80) and (2.81) can be expressed in terms of $H^{(1)}(\mu)$ and $H^{(2)}(\mu)$ as follows (Chandrasekhar 1960),

$$\begin{aligned} \left(\frac{1}{\mu} + \frac{1}{\mu_0}\right)S^{(1)}(\mu, \mu_0) &= H^{(1)}(\mu_0)H^{(1)}(\mu) \\ \left(\frac{1}{\mu} + \frac{1}{\mu_0}\right)S^{(2)}(\mu, \mu_0) &= H^{(2)}(\mu_0)H^{(2)}(\mu) \end{aligned} \quad (2.82)$$

Where $H^{(1)}(\mu)$ and $H^{(2)}(\mu)$ can be expressed as,

$$H^{(1)}(\mu) = 1 + \frac{3}{8}\mu H^{(1)}(\mu) \int_0^1 \frac{\mu'^2(1 - \mu'^2)}{\mu + \mu'} H^{(1)}(\mu') d\mu' \quad (2.83)$$

$$H^{(2)}(\mu) = 1 + \frac{3}{32}\mu H^{(2)}(\mu) \int_0^1 \frac{(1 - \mu'^2)^2}{\mu + \mu'} H^{(2)}(\mu') d\mu' \quad (2.84)$$

Now the full equation of scattering function and intensity at the layer of $\tau = 0$ for Rayleigh scattering can be expressed as follows,

$$\begin{aligned} \left(\frac{1}{\mu} + \frac{1}{\mu_0}\right)S_R(\mu, \phi; \mu_0, \phi_0) &= \frac{1}{3}\psi_R(\mu)\psi_R(\mu_0) + \frac{8}{3}\phi_R(\mu)\phi_R(\mu_0) \\ &- H^{(1)}(\mu)H^{(1)}(\mu_0)4\mu\mu_0\sqrt{(1 - \mu^2)(1 - \mu_0^2)} \cos(\phi - \phi_0) \\ &+ H^{(2)}(\mu)H^{(2)}(\mu_0)(1 - \mu^2)(1 - \mu_0^2) \cos 2(\phi - \phi_0) \end{aligned} \quad (2.85)$$

and

$$\begin{aligned}
I(0, \mu, \phi; \mu_0, \phi_0) &= \frac{F}{4\mu} S_R(\mu, \phi; \mu_0, \phi_0) \\
&= \frac{3F}{32} \frac{\mu_0}{\mu + \mu_0} \left[\frac{1}{3} \psi_R(\mu) \psi_R(\mu_0) + \frac{8}{3} \phi_R(\mu) \phi_R(\mu_0) \right. \\
&\quad - H^{(1)}(\mu) H^{(1)}(\mu_0) 4\mu\mu_0 \sqrt{(1 - \mu^2)(1 - \mu_0^2)} \cos(\phi - \phi_0) \\
&\quad \left. + H^{(2)}(\mu) H^{(2)}(\mu_0) (1 - \mu^2)(1 - \mu_0^2) \cos 2(\phi - \phi_0) \right] \tag{2.86}
\end{aligned}$$

2.14.4 Scattering function for the general phase function:

The phase function of this type and its explicit form is discussed in section 2.9. Here we will derive the scattering function for this type of phase functions.

Observing the similarity with the phase function, the scattering function can be written as,

$$\begin{aligned}
S(\mu, \phi; \mu_0, \phi_0) &= S^{(0)}(\mu, \mu_0) \\
&\quad + S^{(1)}(\mu, \mu_0) \sqrt{(1 - \mu^2)(1 - \mu_0^2)} \cos(\phi - \phi_0) \\
&\quad + S^{(2)}(\mu, \mu_0) (1 - \mu^2)(1 - \mu_0^2) \cos 2(\phi - \phi_0) \tag{2.87}
\end{aligned}$$

Here we will not go into the detailed derivation of the scattering function which is similar to the process of the other scattering function cases and can be found in Horak and S. Chandrasekhar 1961 and S. Chandrasekhar 1989. Rather we will write the results directly.

In the same way as before we can get the ³ functional forms of the scattering function term by term as follows,

$$\left(\frac{1}{\mu} + \frac{1}{\mu_0} \right) S_l^{(0)}(\mu, \mu_0) = -\tilde{\omega}_1 \eta_l(\mu) \eta_l(\mu_0) + \frac{3\tilde{\omega}_0}{\zeta} \phi_l(\mu) \phi_l(\mu_0) + \frac{3\tilde{\omega}_2}{4\zeta} \psi_l(\mu) \psi_l(\mu_0) \tag{2.88}$$

$$\begin{aligned}
\left(\frac{1}{\mu} + \frac{1}{\mu_0} \right) S_l^{(1)}(\mu, \mu_0) &= \omega_1 \theta(\mu) \theta(\mu_0) - 3\omega_2 \sigma(\mu) \sigma(\mu_0) \\
&= [\tilde{\omega}_1 (1 + l\mu)(1 + l\mu_0) - 3\tilde{\omega}_2 m^2 \mu \mu_0] H^{(1)}(\mu) H^{(1)}(\mu_0) \tag{2.89}
\end{aligned}$$

The quantities l and m used here are the same as defined in Horak and S. Chandrasekhar 1961.

³Hereinafter the subscript "1" stands for the scattering due to phase function $p(\cos \Theta) = \tilde{\omega}_0 + \tilde{\omega}_1 P_1(\cos \Theta) + \tilde{\omega}_2 P_2(\cos \Theta)$

$$\left(\frac{1}{\mu} + \frac{1}{\mu_0}\right)S_l^{(2)}(\mu, \mu_0) = \frac{3\tilde{\omega}_2}{4}H^{(2)}(\mu)H^{(2)}(\mu_0) \quad (2.90)$$

where,

$$\eta_l(\mu) = \mu - \frac{1}{2} \int_0^1 S_l^{(0)}(\mu, \mu') d\mu' \quad (2.91)$$

$$\phi_l(\mu) = \mu^2 + \frac{1}{2} \int_0^1 S_l^{(0)}(\mu, \mu') \mu' d\mu' \quad (2.92)$$

$$\psi_l(\mu) = (\zeta - \mu^2) + \frac{1}{2} \int_0^1 S_l^{(0)}(\mu, \mu') (\zeta - \mu'^2) \frac{d\mu'}{\mu'} \quad (2.93)$$

$$\theta(\mu) = 1 + \frac{1}{4} \int_0^1 S^{(1)}(\mu, \mu') (1 - \mu'^2) \frac{d\mu'}{\mu'} \quad (2.94)$$

$$\sigma(\mu) = \mu - \frac{1}{4} \int_0^1 S^{(1)}(\mu, \mu') (1 - \mu'^2) d\mu' \quad (2.95)$$

The H-functions here are defined as,

$$H^{(i)}(\mu) = 1 + \mu H^{(i)}(\mu) \int_0^1 \frac{\Psi^{(i)}(\mu')}{\mu + \mu'} H^{(i)}(\mu') d\mu' \quad i = 1, 2 \quad (2.96)$$

where,

$$\Psi^{(i)}(\mu) = a^{(i)} + b^{(i)}\mu^2 + c^{(i)}\mu^4 \quad (2.97)$$

$$a^{(1)} = \frac{\tilde{\omega}_1}{4}; \quad b^{(1)} = \frac{1}{4}[\tilde{\omega}_2(3 - \tilde{\omega}_1) - \tilde{\omega}_1]; \quad c^{(1)} = \frac{\tilde{\omega}_2}{4}(\tilde{\omega}_1 - 3) \quad (2.98)$$

$$a^{(2)} = c^{(2)} = \frac{3\tilde{\omega}_2}{16}; \quad b^{(2)} = -\frac{3\omega_2}{8} \quad (2.99)$$

Using the expression of $S^{(0)}$ in equations (2.91), (2.92) and (2.93) we will get the non-linear form of these three equations as follows,

$$\begin{aligned} \eta_l(\mu) = & \mu + \frac{\mu}{2} \tilde{\omega}_1 \eta_l(\mu) \int_0^1 \frac{\eta_l(\mu')}{\mu + \mu'} \mu' d\mu' - \frac{\mu}{2} \frac{3\tilde{\omega}_0}{\zeta} \phi_l(\mu) \int_0^1 \frac{\phi_l(\mu')}{\mu + \mu'} \mu' d\mu' \\ & - \frac{\mu}{2} \frac{3\tilde{\omega}_2}{4\zeta} \psi_l(\mu) \int_0^1 \frac{\psi_l(\mu')}{\mu + \mu'} \mu' d\mu' \end{aligned} \quad (2.100)$$

$$\begin{aligned} \phi_l(\mu) = & \mu^2 - \frac{\mu}{2} \tilde{\omega}_1 \eta_l(\mu) \int_0^1 \frac{\eta_l(\mu')}{\mu + \mu'} \mu'^2 d\mu' + \frac{\mu}{2} \frac{3\tilde{\omega}_0}{\zeta} \phi_l(\mu) \int_0^1 \frac{\phi_l(\mu')}{\mu + \mu'} \mu'^2 d\mu' \\ & + \frac{\mu}{2} \frac{3\tilde{\omega}_2}{4\zeta} \psi_l(\mu) \int_0^1 \frac{\psi_l(\mu')}{\mu + \mu'} \mu'^2 d\mu' \end{aligned} \quad (2.101)$$

$$\begin{aligned} \psi_l(\mu) = & (\zeta - \mu^2) - \frac{\mu}{2} \tilde{\omega}_1 \eta_l(\mu) \int_0^1 \frac{\eta_l(\mu')}{\mu + \mu'} (\zeta - \mu'^2) d\mu' + \frac{\mu}{2} \frac{3\tilde{\omega}_0}{\zeta} \phi_l(\mu) \int_0^1 \frac{\phi_l(\mu')}{\mu + \mu'} (\zeta - \mu'^2) d\mu' \\ & + \frac{\mu}{2} \frac{3\tilde{\omega}_2}{4\zeta} \psi_l(\mu) \int_0^1 \frac{\psi_l(\mu')}{\mu + \mu'} (\zeta - \mu'^2) d\mu' \end{aligned} \quad (2.102)$$

Now the scattering function can be written as,

$$\begin{aligned} S(\mu, \phi; \mu_0, \phi_0) = & \frac{\mu\mu_0}{\mu + \mu_0} \left[-\tilde{\omega}_1 \eta_l(\mu) \eta_l(\mu_0) + \frac{3\tilde{\omega}_0}{\zeta} \phi_l(\mu) \phi_l(\mu_0) + \frac{3\tilde{\omega}_2}{4\zeta} \psi_l(\mu) \psi_l(\mu_0) \right. \\ & + [\tilde{\omega}_1(1 + l\mu)(1 + l\mu_0) - 3\tilde{\omega}_2 m^2 \mu \mu_0] H^{(1)}(\mu) H^{(1)}(\mu_0) \sqrt{(1 - \mu^2)(1 - \mu_0^2)} \cos(\phi - \phi_0) \\ & \left. + \frac{3\tilde{\omega}_2}{4} H^{(2)}(\mu) H^{(2)}(\mu_0) (1 - \mu^2)(1 - \mu_0^2) \cos 2(\phi - \phi_0) \right] \end{aligned} \quad (2.103)$$

Finally the diffused reflected intensity can be represented as,

$$\begin{aligned} I(0, \mu; \mu_0) = & \frac{\mu_0}{\mu + \mu_0} \frac{F}{4} \left[-\tilde{\omega}_1 \eta_l(\mu) \eta_l(\mu_0) + \frac{3\tilde{\omega}_0}{\zeta} \phi_l(\mu) \phi_l(\mu_0) + \frac{3\tilde{\omega}_2}{4\zeta} \psi_l(\mu) \psi_l(\mu_0) \right. \\ & + \{ \tilde{\omega}_1(1 + l\mu)(1 + l\mu_0) - 3\tilde{\omega}_2 m^2 \mu \mu_0 \} H^{(1)}(\mu) H^{(1)}(\mu_0) \sqrt{(1 - \mu^2)(1 - \mu_0^2)} \cos(\phi - \phi_0) \\ & \left. + \frac{3\tilde{\omega}_2}{4} H^{(2)}(\mu) H^{(2)}(\mu_0) (1 - \mu^2)(1 - \mu_0^2) \cos 2(\phi - \phi_0) \right] \end{aligned} \quad (2.104)$$

With this we conclude this chapter of what has been done till now and in the next chapters we will discuss how this theory can be used to model exoplanetary atmosphere and modification of the theory wherever needed and possible.

Resource summary

1. Chandrasekhar [1960](#)
2. S. Chandrasekhar [1989](#)
3. Horak and S. Chandrasekhar [1961](#)
4. Annamaneni Peraiah [2002](#)
5. G. Rybicki [1979](#)

Chapter 3

Effect of atmospheric heat redistribution on Emission spectra of Hot-Jupiters¹

3.1 Introduction

From the first detection of Jupiter-like exoplanet, named 51-Pegasi-b (Mayor and Queloz 1995) orbiting around a sun-like star, the giant exoplanets remain the most observed and investigated exoplanets till date. For transit observations, hot-Jupiters are the first as well as the most easily detectable planets (Tsevi Mazeh et al. 2000; Knutson et al. 2007) among a large variety of exoplanets discovered. The atmospheric temperature-pressure profiles of hot-Jupiters have been modeled using the radiative equilibrium conditions both analytically (Hansen 2008; Guillot 2010), as well as numerically (Parmentier and Guillot 2014; Parmentier, Guillot, et al. 2015). Using these modelled temperature-pressure profiles and the atmospheric chemical compositions, the atmospheric spectra of such exoplanets can be obtained by solving the radiative transfer equations (Mollière et al. 2019; Sengupta and Marley 2009; Tinetti, Encrenaz, and Coustenis 2013). Ultimately, by comparing those synthetic spectra with the extracted spectra from transit observations, one can retrieve the atmospheric compositions (Tinetti, Vidal-Madjar, et al. 2007; Swain, Vasisht, and Tinetti 2008) and the temperature-pressure profiles (Nikolov et al. 2018; Madhusudhan and Seager 2009; Tinetti, Deroo, et al. 2010).

Three types of spectra that can be obtained during transit and eclipse observations, e.g., transmission, reflection and emission spectra (Tinetti, Encrenaz, and Coustenis 2013) are studied extensively (e.g. Sengupta, Chakrabarty, and Tinetti 2020, Chakrabarty and Sengupta 2020, Waldmann et al. 2015, Mollière et al. 2019, Kempton et al. 2017, Batalha et al. 2019). Among all these, only the planetary emission spectra observed during secondary eclipse observations carry the full imprint of the atmospheric temperature-pressure profile (Tinetti, Encrenaz, and Coustenis 2013), whereas reflection and transmission spectra are sensitive to the

¹This chapter contains the material from the paper submitted in New Astronomy Journal

upper atmosphere only (Sengupta, Chakrabarty, and Tinetti 2020). These spectra carry the compositional signature of the atmospheric layers in terms of absorption and scattering as well as the temperature of each atmospheric layer (S. Sengupta 2021). Due to the tidal locking of the hot-Jupiters with its host star, there is a huge difference in the atmospheric temperature at the permanent day-side and the permanent night-side of the planet. This temperature gradient as well as the small rotation period influences the horizontal flow of atmosphere, which is very much different than that of the solar system giants (Showman, Menou, and Cho 2007). Also the stellar irradiation flux has a direct effect on planetary spectra through re-emission (Chakrabarty and Sengupta 2020) and in heat redistribution through equatorial-jet circulation (Hammond, Tsai, and Pierrehumbert 2020). Hansen 2008 pedagogically showed that the planetary atmospheric heat redistribution has a direct effect on the temperature-pressure profile as well as in the emission spectra. Recently, Komacek and Showman 2019 demonstrated that due to large scale equatorial waves generated by prominent day-night temperature contrast, there is a temporal variation in the secondary eclipse depth (2% locally) and the temperature-pressure profiles. A number of studies of atmospheric heat redistribution has been done using different available mechanisms (see Seager 2010b; Heng and Showman 2015; Showman, Tan, and Parmentier 2020 and the references therein). Initially the shallow water model is used to explain the atmospheric heat redistribution in hot-Jupiters (Perez-Becker and Showman 2013). Recently, Tan and Komacek 2019 investigated the heat transfer from dayside to nightside in ultra hot jupiters by considering the General Circulation Model with an effect of molecular hydrogen dissociation in dayside and atomic hydrogen recombination in nightside. Hence each vertical atmospheric layer in the dayside atmosphere is cooled due to the heat transfer from substellar to anti-stellar side of the planet.

Although, different kind of atmospheric spectra of hot-jupiters has been studied, the effect of atmospheric heat redistribution on hot-Jupiter's atmosphere remains unresolved. Thus, to get the full realization of the atmospheric heat redistribution, one needs to study the temperature-pressure profiles as well as the emission spectra for different degree of atmospheric heat redistribution. In this paper, we present the effect of day to night side atmospheric heat redistribution of hot-jupiters. We however, do not address the possible mechanisms of heat redistribution. The effect is analyzed in terms of temperature-pressure profile and day-side emission spectrum as suggested by Hansen 2008. We use the analytical formulation of temperature-pressure profiles presented by Guillot 2010 to derive the analytical relation of redistribution parameter with the emission profiles. Using these profiles and solar abundance composition in the atmosphere, the scatter-

ing as well as the absorption co-efficients are estimated by using the Exo-Transmit (Kempton et al. 2017; Freedman, Marley, and Lodders 2008; Freedman, Lustig-Yaeger, et al. 2014; Lupu et al. 2014) software package which is available publicly (Sengupta, Chakrabarty, and Tinetti 2020). Finally, the modelled temperature-pressure profile, absorption and scattering co-efficients are used to calculate the dayside emission spectra numerically by using discrete space theory formalism described in Sengupta and Marley 2009, Sengupta, Chakrabarty, and Tinetti 2020. Thus, from the emission spectra we infer the role of heat redistribution in the atmosphere of hot-jupiters.

In section 3.2, we present the analytical derivations of the expression that describe the explicit dependence of atmospheric thermal profile as well as the dayside emission spectra on the redistribution parameter f . The method of numerical techniques while solving for the 1-D equations of radiative transfer is described as well as their solutions are validated in section 3.3. The resulting effects of redistribution parameter on the temperature-pressure profile and the dayside emission spectra are presented in section 3.4. Finally we discuss our results and conclude this work in the last section.

3.2 Theoretical Models

A hot close-in gas giant planet is tidally locked to its host star. When the starlight is irradiated on the atmosphere, then two phenomena can occur: Either the heat can be absorbed and redistributed in the atmosphere or the heat is re-radiated immediately from the atmosphere.

The analytical expression for the atmospheric temperature under radiative equilibrium can be given as (Guillot 2010),

$$T^4 = \frac{3T_{int}^4}{4} \left(\frac{2}{3} + \tau \right) + \frac{3T_{irr}^4}{4} \mu_0 \left[\frac{2}{3} + \frac{\mu_0}{\gamma} + \left(\frac{\gamma}{3\mu_0} - \frac{\mu_0}{\gamma} \right) e^{-\frac{\gamma\tau}{\mu_0}} \right] \quad (3.1)$$

where, T_{int} is the internal temperature of the planet, T_{irr} is temperature due to the flux irradiated on the planetary atmosphere along the direction cosine μ_0 , γ is the ratio between the optical and the infrared absorption co-efficients, i.e. $\kappa_{vis}/\kappa_{inf}$ and τ is the optical depth defined in terms of pressure (P), density (ρ) and constant surface gravity g as, $d\tau = \frac{dP\kappa_{th}}{g}$ (Guillot 2010).

Thus the mean intensity expression can be obtained by multiplying equation (3.1) by $\frac{\sigma}{\pi}$, where σ is the Stefan-Boltzmann constant, on either side as,

$$J = \frac{3}{4}F_{int} \left(\frac{2}{3} + \tau \right) + \frac{3}{4}F_{irr}\mu_0 \left[\frac{2}{3} + \frac{\mu_0}{\gamma} + \left(\frac{\gamma}{3\mu_0} - \frac{\mu_0}{\gamma} \right) e^{-\frac{\gamma\tau}{\mu_0}} \right] \quad (3.2)$$

where, we replaced $\sigma T_{int}^4/\pi$ and $\sigma T_{irr}^4/\pi$ by internal flux F_{int} and irradiated flux F_{irr} respectively and make use the fact that $J = \frac{\sigma T^4}{\pi}$ (Chandrasekhar 1960).

Under radiative equilibrium condition, the specific intensity at $\tau = 0$ and the mean intensity relation can be written as (Hansen 2008),

$$I(\tau = 0, \mu, \mu_0) = \int_0^\infty J(t) e^{-\frac{t}{\mu}} \frac{dt}{\mu} \quad (3.3)$$

Now solving equation (3.3) while using equation (3.2) we obtain,

$$I(0, \mu, \mu_0) = \frac{3F_{int}}{4} \left(\frac{2}{3} + \mu \right) + \frac{3F_{irr}}{4} \mu_0 \left[\frac{2}{3} + \frac{\mu_0}{\gamma} + \left(\frac{\gamma}{3\mu_0} - \frac{\mu_0}{\gamma} \right) \frac{1}{1 + \gamma\mu/\mu_0} \right] \quad (3.4)$$

This is the flux emerging out from the uppermost atmospheric layer of the planet where $\tau = 0$. For secondary eclipse observation, the total observed flux is the radiation coming from the substellar point of the planet at full phase with $\mu = \mu_0$. Taking the integral over this phase and following the notations of Hansen 2008, we can write the full emerging flux as,

$$\begin{aligned} F_{full} &= 2 \int_0^1 \mu_0 I(0, \mu_0, \mu_0) d\mu_0 \\ &= F_{int} + \frac{3F_{irr}}{2} \left[\frac{2}{9} + \frac{1}{4\gamma} + \left(\frac{\gamma}{6} - \frac{1}{4\gamma} \right) \frac{1}{1 + \gamma} \right] \end{aligned} \quad (3.5)$$

In principal, the comparison of the flux observed during secondary eclipse to the model flux F_{full} can tell us whether the energy is redistributed from substellar side to anti-stellar side of the planet, because the observed emitted flux from the substellar side in that case would be less than that expected for no-redistribution model. Thus dividing the re-radiation term i.e. the second term in the right hand side of equation (3.5) by the irradiated flux F_{irr} we get an effective redistribution factor,

$$f_{eff} = \frac{3}{2} \left[\frac{2}{9} + \frac{1}{4\gamma} + \left(\frac{\gamma}{6} - \frac{1}{4\gamma} \right) \frac{1}{1 + \gamma} \right] \quad (3.6)$$

Similarly, the irradiated flux expressed by equation (3.5) can also be written in terms of the zero albedo equilibrium flux at planetary atmosphere (i.e. F_{eq0}). To do that we consider the average temperature-pressure profile with $\mu_0 = 1/\sqrt{3}$ as shown in Guillot 2010 and can be denoted by a particular term μ_* . This is known as isotropic approximation case and has been considered by Parmentier, Guillot,

et al. 2015 using the following relations:

$$\begin{aligned}\mu_* &= \frac{1}{\sqrt{3}} \\ T_{\mu_*}^4 &= \mu_* T_{irr}^4 = \frac{1}{\sqrt{3}} T_{irr}^4 = (1 - A_B) 4f T_{eq0}^4\end{aligned}\quad (3.7)$$

where, A_B is the Bond Albedo, T_{eq0} is the zero albedo equilibrium temperature and f is atmospheric redistribution parameter. We emphasize here that f and f_{eff} are two completely different parameters. f is the redistribution parameter that tells how much day to night side horizontal atmospheric flow occurs, whereas f_{eff} is a function of γ and represents the variation of flux absorbed at different atmospheric depth. Thus, for isotropic approximation F_{irr} of equation (3.5) can be written as,

$$\begin{aligned}F_{irr} &= \frac{\sigma}{\pi} T_{irr}^4 \\ &= 4\sqrt{3}(1 - A_B)f F_{eq0}\end{aligned}\quad (3.8)$$

where $F_{eq0} = \frac{\sigma}{\pi} T_{eq0}^4$

Thus considering equation (3.6), (3.7) and (3.8) we can write equation (3.5) as,

$$F_{full} = F_{int} + 4\sqrt{3}(1 - A_B)f_{eff}f F_{eq0}\quad (3.9)$$

Equation (3.9) represents total emergent flux in case of secondary eclipse emission spectra. In this work we study the particular case for fixed internal and equilibrium temperature as well as for fixed albedo. Thus, the total flux F_{full} may vary depending on the parameters f_{eff} and f only.

The explicit form of f_{eff} , is given in Equation (3.6) and its variation with γ is shown in figure 3.1. These are equivalent to that obtained by Hansen 2008 except some different boundary conditions used. The figure shows that f_{eff} saturates both at large and small γ . Also it reveals that f_{eff} is very insensitive to γ . The values of f_{eff} saturate at $f_{eff} \rightarrow 0.7083$ for $\gamma \rightarrow 0$ and $f_{eff} \rightarrow 0.583$ for $\gamma \rightarrow \infty$ as derived using python package "sympy" (Meurer et al. 2017) available in public domain². This insensitivity of f_{eff} to γ implies that the variation in the emission spectra during the secondary eclipse is effectively due to the atmospheric heat redistribution factor f . It also suggests that the emission spectra almost remain unaffected by the atmospheric depth at which the irradiated energy penetrates. Therefore the degree of thermal redistribution in the planetary atmosphere can be determined by comparing the observed flux during the secondary eclipse with model spectra calculated by using different heat redistribution parameters.

²<https://www.sympy.org/en/index.html>

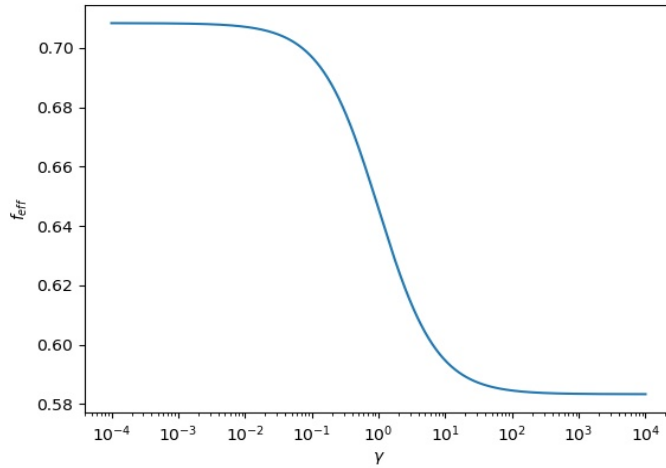


Figure 3.1: Variation of the function f_{eff} with γ , the ratio between the optical and the infrared absorption co-efficients.

3.2.1 Values of the redistribution parameter for isotropic approximation

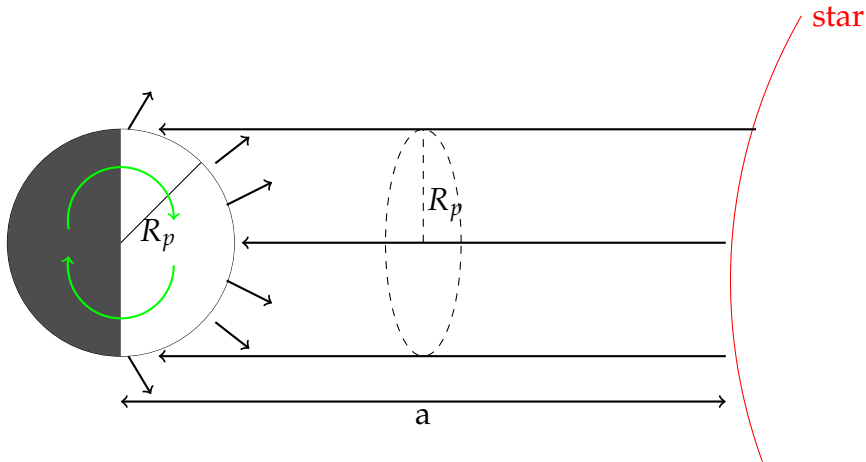


Figure 3.2: The isotropic irradiation approximation. The starlight incidents on the dayside of the planet isotropically through the area πR_p^2 . Due to atmospheric heat redistribution from dayside to nightside (shown in green arrow), the redistribution parameter is altered. The energy emitted from the dayside of a hot Jupiter decreases with the increase in the heat redistribution.

Since the close-in hot-Jupiters are usually gravitationally locked to their parent star, they have permanent day and night sides. Under such circumstance, the irradiation can be treated by isotropic approximation (Guillot 2010). In this case the irradiation flux is assumed to be incident on a circular area πR_p^2 as shown in fig. 3.2. Before the energy is re-emitted from the planet, the irradiated energy is redistributed on the planetary atmosphere in three possible ways. The redistribution parameter f can be defined as the ratio of irradiated area to the redistribution

area. In the present case, as the irradiated area is fixed at πR_p^2 , the redistribution parameter f should entirely depend on the area of redistribution by an inverse relation. The three possible cases of heat redistribution are as follows:

1. When the irradiated energy is redistributed over the whole planetary surface, then $f = \frac{\pi R_p^2}{4\pi R_p^2} = \frac{1}{4}$ as mentioned in Parmentier, Guillot, et al. 2015
2. For only dayside heat redistribution, $f = \frac{\pi R_p^2}{2\pi R_p^2} = \frac{1}{2}$
3. For no heat redistribution at all, Seager 2010a suggests $f = \frac{2}{3}$

It is worth noting that the value of f decreases with the increase in the heat redistribution from the dayside to the nightside. Thus from equation (3.9) it is evident that the re-radiated flux at the dayside increases with the decrease in the redistribution of the irradiated energy.

3.3 Numerical methodology

3.3.1 Atmospheric temperature-pressure profiles

The variation of temperature as well as pressure with atmospheric height is considered an involved and unique character of any exoplanetary atmosphere. This temperature-pressure (T-P) profiles can be affected by internal energy of the planet, irradiated flux from its host star, atmospheric redistribution, molecular mixing ratio etc. For a hot-Jupiter planet, these (T-P) profiles are well studied by Parmentier and Guillot 2014, Guillot 2010, Parmentier, Guillot, et al. 2015 in the presence of internal as well as irradiated flux on the planetary atmosphere. We use the analytical expressions prescribed by them in order to study the effect of redistribution on planetary atmosphere. The study of the variation of the gas mixing ratio on the atmospheric redistribution is however beyond the scope of the present work.

The atmospheric temperature-pressure profiles are generated using the numerical code developed by Parmentier, Guillot, et al. 2015 and available in public domain³. The numerical code is based on the analytical model given in Guillot 2010; Parmentier and Guillot 2014 and can be expressed by equation (3.1). We have ignored the convective region at the bottom of the model T-P profiles. The derived T-P profiles are used to solve the radiative transfer equations numerically in order to obtain the planetary emission spectra. Since the emission spectra probe deep of the atmosphere, therefore, unlike the transmission and reflection spectra, the

³NonGrey Code

T-P profile up to a deeper atmospheric region is required to calculate the emission flux. Hence, we consider the T-P profile for a wide range of atmospheric pressure, e.g., $10^{-6} - 10^2$ bar. Also the profiles are generated for a Jupiter like planet with surface gravity $25m/s^2$ and internal temperature 200K but equilibrium temperature of 1800K for zero albedo. The opacity is considered to be Rosseland mean opacity as given by Valencia et al. 2013. Finally all the temperature-pressure profiles are calculated in the presence of Tio and VO so that effect of thermal inversion could be incorporated. These T-P profiles are used to generate the absorption and scattering co-efficients as well as to get the solutions of the radiative transfer equations.

3.3.2 Co-efficients of absorption and scattering

In the present work we aim to study the influence of heat redistribution on the atmosphere of hot-Jupiters. Now an exoplanetary atmosphere can be characterized by its temperature-pressure profile, atmospheric chemistry and atmospheric emission. Here we investigate how the temperature-pressure profile as well as atmospheric emission varies with the atmospheric heat redistribution for a fixed atmospheric chemistry. Hence, we present models with fixed abundance, e.g., solar abundance of atoms and molecules for hot-Jupiters. The scattering as well as absorption co-efficients are calculated by the numerical software "Exo-Transmit" developed by Kempton et al. 2017⁴ along with the atomic and molecular database provided (Freedman, Marley, and Lodders 2008; Freedman, Lustig-Yaeger, et al. 2014; Lupu et al. 2014). The model description as well as validity check of "Exo-Transmit" software package with Tau-REx package Waldmann et al. 2015 is discussed in Sengupta, Chakrabarty, and Tinetti 2020. We fix the chemical composition by choosing solar abundance equation of state (EOS) data provided with the package. For this particular chemical composition, the absorption and scattering co-efficients are generated for different temperature-pressure profiles. These co-efficients are further used to calculate the single scattering albedo at each temperature-pressure point for different wavelengths. We ignore cloud or condensate opacities or any collision induced scattering.

3.3.3 Numerical method to generate the emission spectra:

In order to generate the synthetic emission spectra, we need to solve the radiative transfer equations by using the atmospheric temperature-pressure profile as well as the absorption and scattering co-efficients. The radiative transfer equations

⁴https://github.com/elizakempton/Exo_Transmit

appropriate for an atmosphere in thermodynamic equilibrium can be expressed as,

$$\mu \frac{dI(\mu, \nu, \tau)}{d\tau} = I(\mu, \nu, \tau) - \xi(\mu, \tau, \nu) \quad (3.10)$$

where, $\xi(\mu, \tau, \nu)$ is the source function. We consider local thermodynamic equilibrium at each atmospheric layer and thus the source function can be written as $\xi(\mu, \tau, \nu) = B(\nu, T) = \frac{2h\nu^3}{c^2}(e^{h\nu/kT} - 1)^{-1}$ (Chandrasekhar 1960; Seager 2010a). Thus, each atmospheric layer contributes to the specific intensity I in terms of their blackbody temperature. To solve this equations numerically we use the formalism of the theory of discrete space as developed by Peraiah and Grant 1973, Sengupta and Marley 2009. The numerical method, runtime and efficiency of the code is provided in Sengupta, Chakrabarty, and Tinetti 2020.

3.3.4 Validation of our model

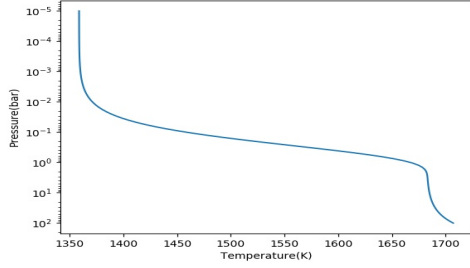
In order to validate our numerical derivations, we compare the emission spectra with the synthetic spectra generated by the numerical package developed by Mollière et al. 2019 and available in the public domain⁵. This software package is itself benchmarked with the petitCODE (Paul Mollière et al. 2015). The comparisons of the two different model spectra are given in figure 3.3c and figure 3.3d. In our model calculations we consider a planetary atmosphere with abundance 9.72×10^{-1} , 2.3×10^{-2} , 6.3×10^{-4} and 2.9×10^{-5} for the elements He, H₂, CH₄, NH₃ respectively, with surface gravity $25m/s^{-2}$. The temperature-pressure profiles with and without thermal inversion are presented in figure 3.3a and figure 3.3b respectively. We note that, in figure 3.3e and 3.3f the relative error between these two model spectra are very small implying good agreement. The small mismatch in the emission spectra presented in figure 3.3c and figure 3.3d is due to the fact that we solved the radiative transfer equations using line by line method whereas Mollière et al. 2019 solve the same using correlated-k approximation.

Next our modeled emission spectra have been compared with the observed planet-star flux ratio for the hot-Jupiters HAT-P-32b (Nikolov et al. 2018) and HAT-P-7b (Mansfield et al. 2018). The planet-star flux ratio is calculated as a function of wavelength λ from the relationship (Tinetti, Encrenaz, and Coustenis 2013),

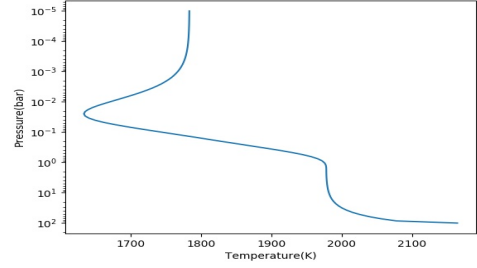
$$\eta(\lambda) = \frac{F_p(\lambda) R_p^2}{F_s(\lambda) R_s^2} \quad (3.11)$$

Here, R_p and R_s are the planetary and stellar radius respectively. F_p is the same as F_{full} in equation (3.9). Thus the emission spectra is dependent on the redis-

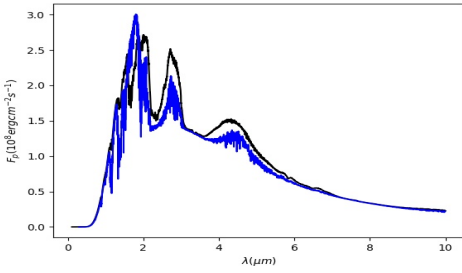
⁵<https://gitlab.com/mauricemolli/petitRADTRANS>



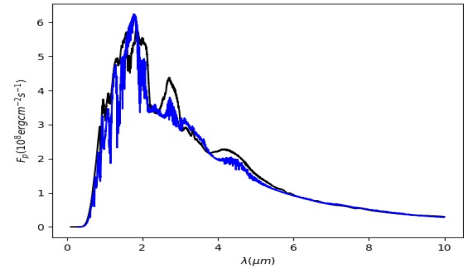
(a) Without inversion



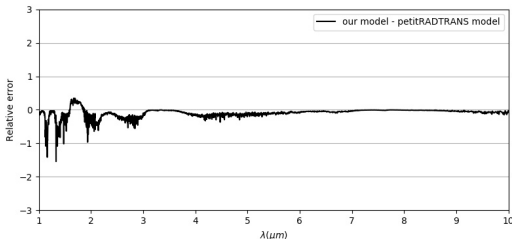
(b) With inversion



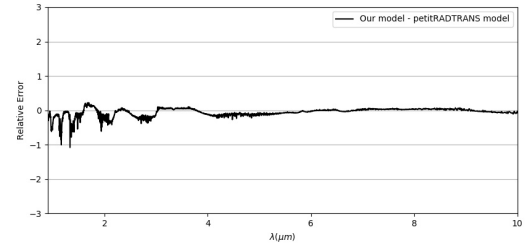
(c) Emission spectra



(d) Emission Spectra

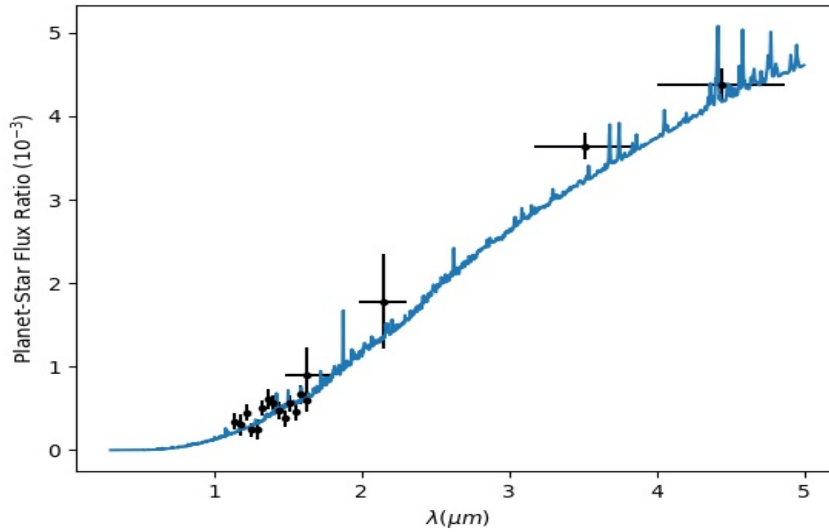


(e) Relative error

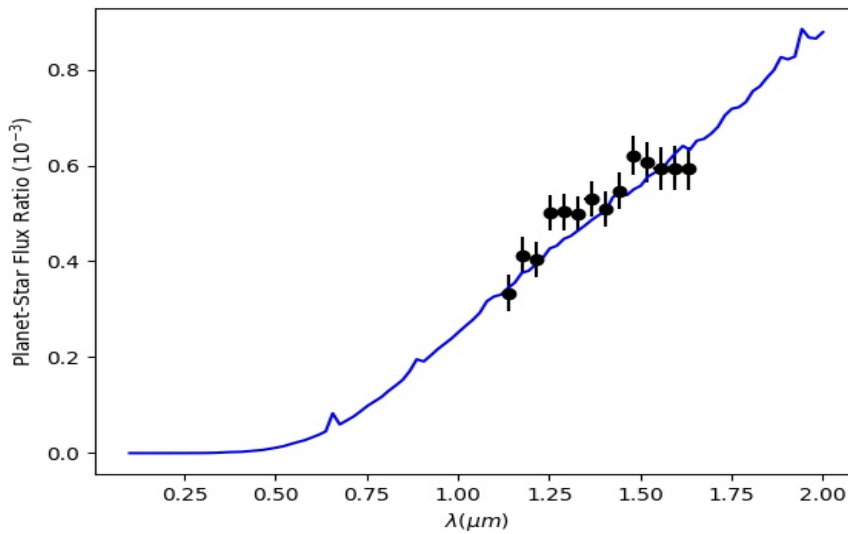


(f) Relative error

Figure 3.3: Comparison of our model emission spectra (blue curve) with the model spectra calculated by using petitRADTRANS code (black curve) (Mollière et al. 2019) without thermal inversion ($T_{int} = 200K$ and $T_{eq} = 1500K$; left panel) and with thermal inversion ($T_{int} = 200K$ and $T_{eq} = 1800K$; right panel). In uppermost panel the temperature-pressure profiles are presented. In the middle panel (3.3c and 3.3d) the emission spectra are compared. The relative error of these two models are presented in 3.3e and 3.3f.



(a) HAT-P-32b Flux Ratio at Secondary Eclipse



(b) HAT-P-7b Flux Ratio at Secondary Eclipse

Figure 3.4: Comparison of our modeled planet-to-star flux ratio (in blue) with the observed HST/WFC3 spectrum (in black). In the upper panel 3.4a the planet-to-star flux ratio for HAT-P-32b is presented by considering an isothermal atmosphere with $T_p = 1995\text{K}$. The observed data for HAT-P-32b is taken from Nikolov et al. 2018. In the lower panel 3.4b, the planet-to-star flux ratio for HAT-P-7b is presented by considering an isothermal planetary atmosphere with $T_p = 2692\text{K}$. The observed data for HAT-P-7b is presented by Mansfield et al. 2018. In both the cases, solar composition is adopted.

tribution parameter f . While calculating the emission spectra by using equation (3.11), we have used the stellar flux F_s of PHEONIX models (Husser et al. 2013). For HAT-P-32b, the planetary surface gravity is taken to be $g = 6.6 \text{ m/s}^2$ (Hartman et al. 2011), and an isothermal atmosphere with $T_p = 1995 \text{ K}$ (Nikolov et al. 2018) is considered. R_p/R_{star} is fixed at $= 0.1506$. The result is presented in figure 3.4a. For the case of HAT-P-7b, an isothermal atmosphere with $T_p = 2692 \text{ K}$ (Mansfield et al. 2018) is considered with the surface gravity $g = 20 \text{ m/s}^2$ (Stassun, Collins, and Gaudi 2017) and $\frac{R_p}{R_{star}} = 0.07809$ (Wong et al. 2016). The observed data for the planet-star flux ratio in this case was obtained using HST/WFC3 camera within the wavelength range $1.1\text{-}1.7 \mu\text{m}$ (Mansfield et al. 2018). Figure 3.4b presents the model spectrum along with the observed data. For both cases, our modeled emission spectra fits reasonably well with the observed data within the errorbars.

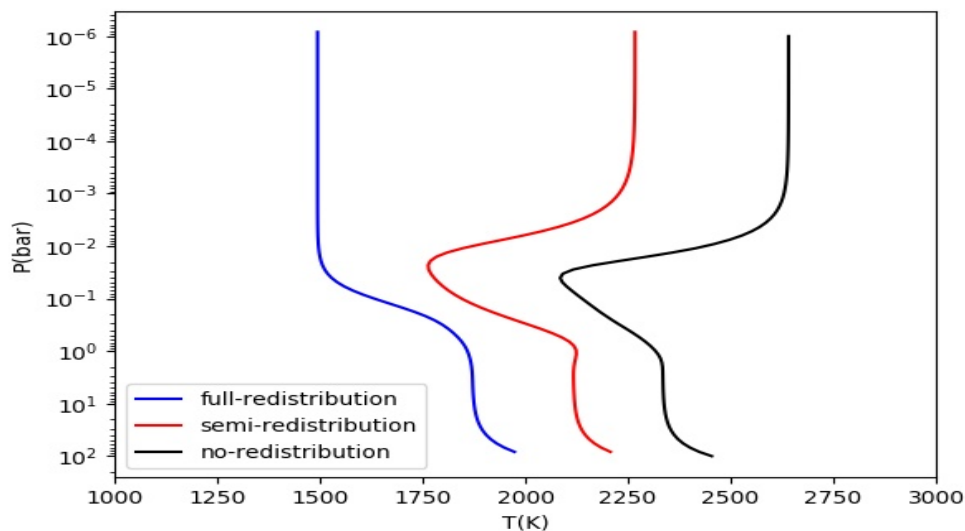
3.4 Results

3.4.1 Effect of redistribution parameter on T-P profiles and on emission spectra

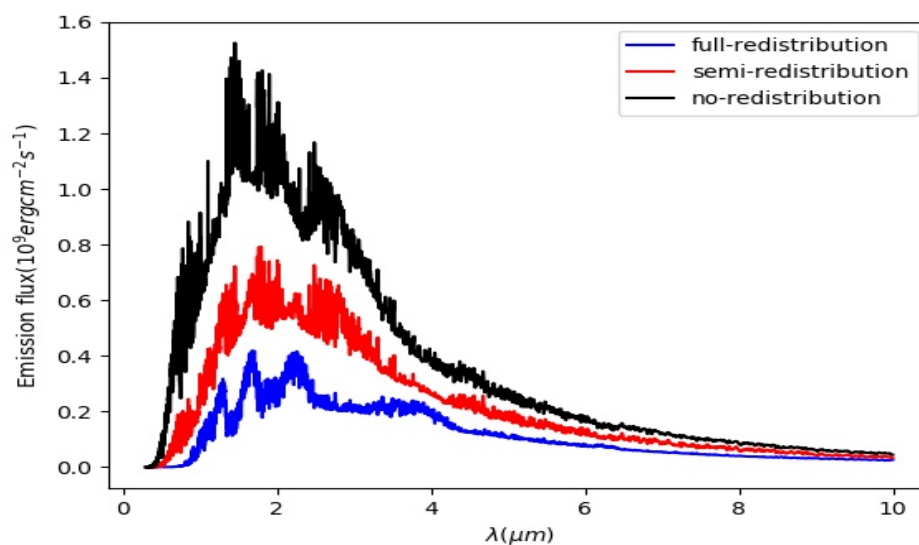
We investigate the effect of atmospheric heat redistribution on the T-P profiles as well as on the emission spectra during the secondary eclipse of hot-Jupiters by using the procedure described in section 3.3. Without loss of generality, we fixed the internal temperature $T_{int} = 200 \text{ K}$ and the equilibrium temperature for zero albedo $T_{eq0} = 1800 \text{ K}$, surface gravity $g = 25 \text{ m/s}^2$. We use Rosseland mean opacity given in Valencia et al. 2013 and included TiO and VO. The Bond albedo is fixed for different redistribution cases and its values are calculated from the fit given in Parmentier and Guillot 2014. We have not considered the convective solution as provided in Parmentier, Guillot, et al. 2015 and only the radiative solution is considered.

First we consider the three different heat redistribution cases under isotropic approximation as discussed in section 3.2.1. In figure 3.5a we present the T-P profiles under these three special conditions, e.g., full, semi and no heat redistribution. The corresponding emission flux for an atmosphere with solar abundances are presented in figure 3.5b with the same conditions as mentioned earlier. Next we consider a general case of simulation for the redistribution parameter f varying from 0.1 to 0.9 with an equal interval of 0.2. The corresponding T-P profiles are given in figure 3.6. These are calculated by using the formalism provided in Parmentier, Guillot, et al. 2015.

According to equation (3.9) the total flux emitted from the substellar point of the planet at full phase is directly proportional to the heat redistribution parame-



(a) Temperature-pressure profile



(b) Emission spectra

Figure 3.5: Effect of heat redistribution on the T-P profiles and on the planetary emission spectra. The upper panel shows the T-P profiles for the different values of redistribution parameter $f = 0.25$ (full-redistribution), $f = 0.5$ (semi-redistribution) and $f = 2/3$ (no-redistribution). In the lower panel, the emission spectra during the secondary eclipse is presented with different atmospheric redistribution.

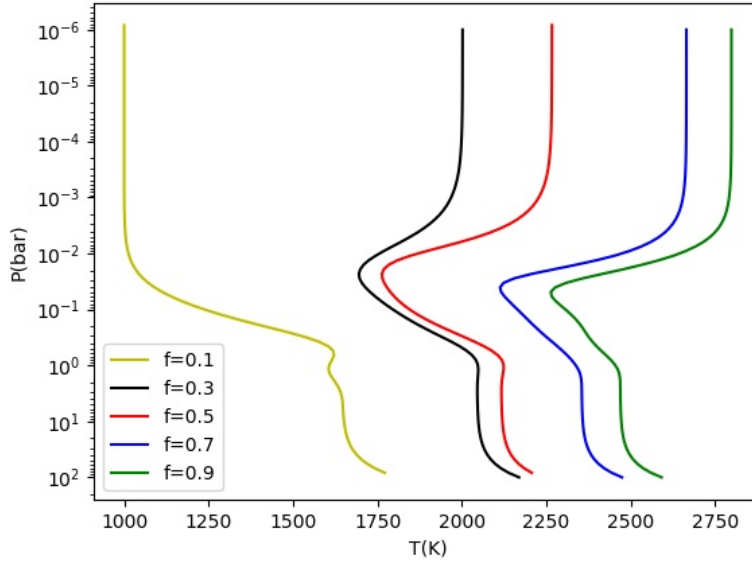


Figure 3.6: T-P profiles for different values of the heat-redistribution parameter f . Here the planetary parameters adopted are (i) equilibrium temperature $T_{eq} = 1800K$ (ii) internal temperature $T_{int} = 200K$ and surface gravity $g = 25 \text{ ms}^{-2}$. Solar composition with TiO is assumed

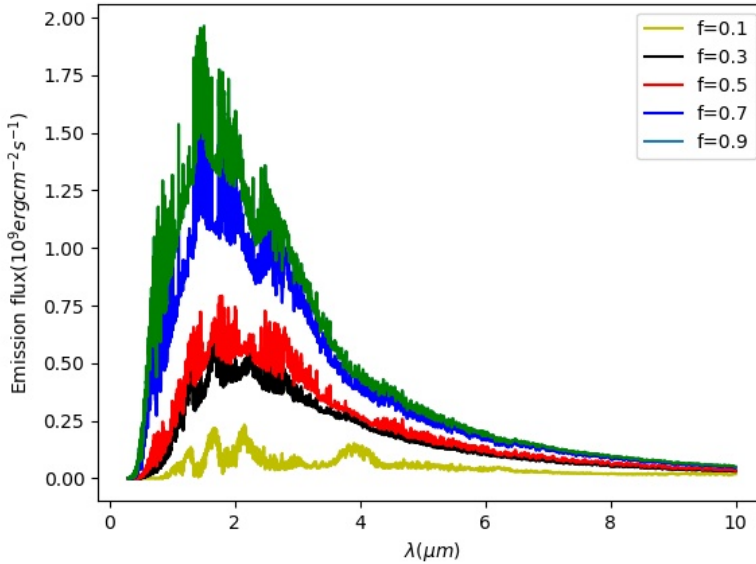


Figure 3.7: Planetary emission spectra for different values of atmospheric heat redistribution parameter f .

ter f . With the change in the T-P profiles, the emission spectra alter with different values of the heat redistribution parameter f . This variation is studied by obtaining the solutions of the radiative transfer equations numerically for an atmosphere

with solar abundances and presented in figure 3.7.

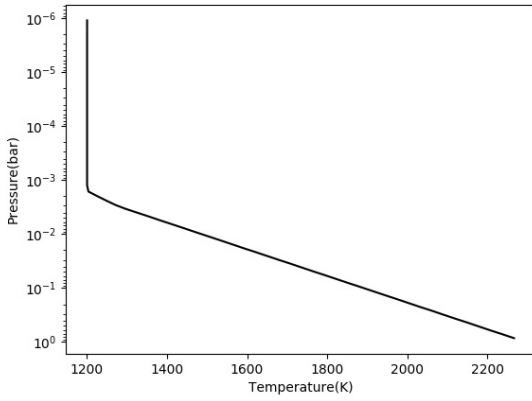
3.4.2 Case study: Emission Spectra of exoplanet XO-1b:

Finally we model the emission spectra of the hot-Jupiter XO-1b with atmospheric heat redistribution. Using IRAC of Spitzer Telescope, (Machalek et al. 2008) for the first time observed this planet during secondary eclipse. Subsequently, Tinetti, Deroo, et al. 2010 obtained the NIR transmission spectra of XO-1b by probing the terminator region. They (Tinetti, Deroo, et al. 2010) considered the planet mass $M_p = 0.9 \pm 0.07 M_J$, planet-star radius ratio $R_p/R_{star} = 0.1326 \pm 0.0004$, star-planet distance $a = 0.04928 \pm 0.00089$ AU, effective temperature of the host star $T_{eff} = 5750K$ and planetary equilibrium temperature $T_{eq} = 1200K$. From transmission spectra analysis, they estimated the best fitted atmospheric abundances to be $H_2O \approx 4.5 \times 10^{-4}$, $CH_4 \approx 10^{-5}$, $CO_2 \approx 4.5 \times 10^{-4}$ and $CO \approx 10^{-2}$. However, while retrieving the T-P profile, they found a degeneracy that T-P profiles for both thermal inversion and non-inversion could explain the transmission spectra accurately (see figure 3 of Tinetti, Deroo, et al. 2010). Since the transmission spectra is not very sensitive to the atmospheric T-P profile (Sengupta, Chakrabarty, and Tinetti 2020), the dayside emission spectra may serve as a potential tool to remove this degeneracy. Tinetti, Deroo, et al. 2010 calculated the emission spectra of the planet by assuming total atmospheric heat redistribution i.e., by keeping the chemical composition and T-P profile the same in the terminator region as well as in the dayside of the planet. We adopt the same condition here and calculated the dayside emission spectra by solving line by line radiative transfer equations using the discrete space theory formalism.

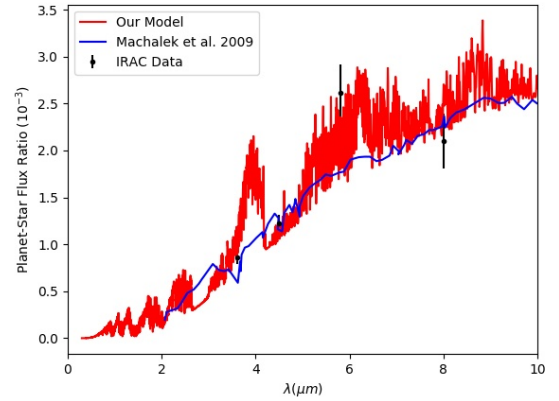
We have calculated the EOS by using the atmospheric mixing ratios as described above and used them in the Exo-Transmit package to estimate the absorption and scattering co-efficients. In the next step, we solve the radiative transfer equations using the T-P profile presented in figure 3.8a and calculate the emission spectrum for XO-1b. Finally, by using PHOENIX model spectrum (Husser et al. 2013) of the star with effective temperature 5750K, we calculated the planet-to-star flux ratio. In figure 3.8b we present our model emission spectrum along with the observed data of IRAC and the model spectrum presented by Machalek et al. 2008.

3.5 Discussions & Conclusion

We demonstrate the effect of atmospheric heat redistribution on the thermal properties of hot-Jupiter's e.g., on the temperature distribution at different height of the



(a) T-P profile



(b) Flux Ratio at Secondary Eclipse

Figure 3.8: Left Panel: The T-P profile of hot-Jupiter XO-1b with no thermal inversion appropriate for the night side atmospheric composition derived by Tinetti, Deroo, et al. 2010. Right Panel: A comparison of our model emission spectrum corresponding to this T-P profile (see left panel) and the atmospheric composition derived in Tinetti, Deroo, et al. 2010, the observed IRAC emission flux and the model emission spectrum presented by Machalek et al. 2008.

atmosphere and the dayside emission spectra. For the simplest case of isotropic approximation of the incident flux, the heat redistribution parameter f can have three different values depending on the degree of heat redistribution. The value of the redistribution parameter f decreases as the amount of heat redistribution increases. When heat redistribution is less, the temperature of the dayside atmosphere is higher because less amount of heat is transferred from sub-stellar side to anti-stellar side. Fig. 3.5a shows that when the heat redistribution reduces, the entire T-P profile shifts towards a higher temperature. For a full redistribution ($f = 1/4$), the vertical temperature profile does not show any thermal inversion whereas for semi-redistribution ($f = 1/2$) and no redistribution ($f = 2/3$), the T-P profile shows significant thermal inversion in the upper atmospheric region. Similarly, figure 3.5b shows that the emission flux is maximum when there is no heat redistribution and minimum when the heat is fully redistributed. This is because of the fact that the less the heat redistributed, the less amount of heat is transferred from dayside to nightside and hence greater amount of radiation emerges out from the dayside. For a fixed atmospheric composition, the features of the emission spectra remains unaltered.

For isotropic approximation, only three cases of heat redistribution may take place. But for more realistic situation, the amount of heat redistribution parametrized by the redistribution parameter f can take any values within the range $0 \leq f \leq 1$. So in the next part of our work we have performed the whole simulation for the redistribution parameter values of 0.1, 0.3, 0.5, 0.7 and 0.9. The corresponding

T-P profiles as well as the emission profiles are shown in fig. 3.6 and 3.7 respectively. While comparing figures 3.5a and 3.6, we notice that the T-P profiles start showing thermal inversion when $f > 0.25$. The temperature increases significantly with the increase in the value of f i.e., with the decrease in heat redistribution. Consequently, the emission flux increases with the increase in the redistribution parameter f i.e., with the decrease in heat redistribution as shown in figure 3.7. This behaviour of the emission flux is obvious from equation (3.9). Since, the planet-to-star flux ratio increases with the increase in the value of f , i.e. with the decrease in the heat redistribution, a model fit of the observed dayside emission spectra may provide good idea on the amount of heat redistribution in the planetary atmosphere.

Finally, we apply our analysis to the exoplanet XO-1b. The transmission spectra of this planet was observed by Tinetti, Deroo, et al. 2010 at the terminator region and the T-P profile is retrieved thereby as shown in figure 3.8a. The absence of thermal inversion in the retrieved T-P profile implies almost full atmospheric heat redistribution. We compare the observed planet-to-star flux ratio with our model spectrum by using the same T-P profile. Figure 3.8b shows that our modeled planet-to-star flux ratio matches with the observed data better than that of Machalek et al. 2008. Thus it can be inferred that almost full heat redistribution takes place in the atmosphere of XO-1b.

In this work we studied the effect of heat redistribution from sub-stellar side to anti-stellar side on the T-P profile and on the planetary emission spectra of hot gas giant planets. However, according to the chemical equilibrium, the mixing ratios of various atomic and molecular species may differ from the dayside to nightside of the atmosphere due to the difference in temperature owing to insignificant heat redistribution. For instance, Tan and Komacek 2019 considered abundance of atomic hydrogen in the dayside of the atmosphere and molecular hydrogen in the nightside of a hydrogen rich hot gas giant planet to describe the mechanism of heat redistribution. Therefore, such compositional difference may be important to understand the amount of heat redistribution from the observed emission spectra.

In this study, we have considered the LTE condition while solving the radiative transfer equation (3.10) and thus the source term ξ becomes the Planck emission which is only a function of the temperature of the layer (Chandrasekhar 1960). But the emitted radiation from one layer would be further scattered by the other atmospheric layers as well. However Goldstein 1960 showed that infrared reflectivity is an important phenomena in case of Rayleigh scattering of planetary atmosphere. Thus, the scattering term should be included along with the thermal emission in the transfer equation as shown in Bellman et al. 1967 and S. Sengupta 2021 while modeling the emission spectra.

The effect of atmospheric heat redistribution on the emission curve during secondary eclipse is not detectable by present day observation facilities (e.g. Spitzer). However, Komacek and Showman 2019 argued that the secondary eclipse depth variability $\leq 2\%$ can be detected using the future telescopes like JWST, ARIEL. Hence, it is expected that the detections of variation of secondary eclipse emission spectra due to atmospheric redistribution can be possible using these telescopes in near future.

Chapter 4

Effects of thermal emission on Chandrasekhar's semi-infinite diffuse reflection problem¹

4.1 Introduction

The analytic solutions of radiative transfer given by Chandrasekhar 1960 has a large range of direct applications, starting from planetary atmosphere modelling (Nikku Madhusudhan and Burrows 2012), to ion induced secondary electron emission (Dubus, Devooght, and Dehaes 1986). However, the solutions of semi-infinite atmosphere problem (S. Chandrasekhar 1947) is obtained specifically for a diffusely reflecting atmosphere without atmospheric emission. Although the emission effect has been studied for planetary atmosphere problem (Bellman et al. 1967; Grant and Hunt 1968; Domanus and Cogley 1974) the semi-infinite atmosphere problem with emission effect remains unsolved.

In plane-parallel radiative transfer equation, the total radiation added by each atmospheric layer to the transfer equation is known as the *Source function*. The diffused reflection as well as emission from each layer, both affect the Source function (Domanus and Cogley 1974). Recently, using diffused reflection and transmission model, Sengupta, Chakrabarty, and Tinetti 2020 demonstrated the crucial effect of scattering on transmitted flux for hot-jupiter atmospheres, while Chakrabarty and Sengupta 2020 showed the significant effect of thermal re-emission process in upper atmosphere for the same. Thus for a complete solution of semi-infinite diffuse reflection problem, the inclusion of scattering as well as emission is important.

To include the emission effect in semi-infinite atmosphere problem we consider the simplest case of homogeneous atmosphere whose layers are in *Local Thermodynamic Equilibrium*. In this case each atmospheric layer emits a planck emission $B(T_\tau)$ depending only on the layer temperature T_τ (Seager 2010a). Thus the model

¹This chapter present the work published in Sengupta, Soumya, ApJ, 911, 126

not only reveals the scattering properties of the layer but also carries the temperature information. Again the resultant radiation $I(0, \mu; \mu_0)$ is enriched by the inclusion of thermal emission over the scattering only case. Moreover the model presented here is more generalized and accurate than the scattering only reflection model.

In section 4.2 we present the derivation of radiative transfer equation appropriate for diffuse reflection in presence of thermal emission using invariance principle method. We derive the integral equation of scattering function in case of thermally emitting semi-infinite atmosphere in section 4.3. Section 4.4 will show the explicit form of the integral equation for different cases of *Isotropic scattering*, *Asymmetric scattering*, *Rayleigh scattering* and the general scattering phase function with $p(\cos \Theta) = \tilde{\omega}_0 + \tilde{\omega}_1 P_1(\cos \Theta) + \tilde{\omega}_2 P_2(\cos \Theta)$. The comparison of end results in semi-infinite atmosphere problem in presence of thermal emission (our work) and in absence of it (Chandrasekhar 1960) is given in section 4.5. Section 4.6 is devoted on explaining how thermal emission actually effects the analytic end results. Finally, we interpret our results and suggest future work in the last section.

4.2 Derivation of Diffusion Transfer equation in presence of Thermal Emission

The radiative transfer equation in case of plane parallel approximation is given by eqn. (2.26), and the subsequent discussion has been done in that chapter. The derivation of analytic solutions for the semi-infinite diffuse reflection problem of a *scattering only atmosphere* has been shown there following S. Chandrasekhar 1947. Here we will introduce the atmospheric emission along with the scattering. Thus for an atmosphere with both emission as well as scattering, the atmospheric extinction can be characterized in terms of volumetric *absorption co-efficient* κ , *scattering co-efficient* σ and *extinction co-efficient* χ which follows the relation given by, Domanus and Cogley 1974 and Sengupta, Chakrabarty, and Tinetti 2020

$$\chi(\tau, \nu) = \kappa(\tau, \nu) + \sigma(\tau, \nu) \quad (4.1)$$

So, eqn.(2.27) will change as,

$$d\tau_\nu = -\chi(z, \nu)dz \quad (4.2)$$

In general the contribution of atmospheric emission can be considered in terms of $\beta(\tau, \nu, \mu, \phi)$, which represents the angular distribution of the energy emitted from the atmospheric layer at optical depth τ and at frequency ν . While consid-

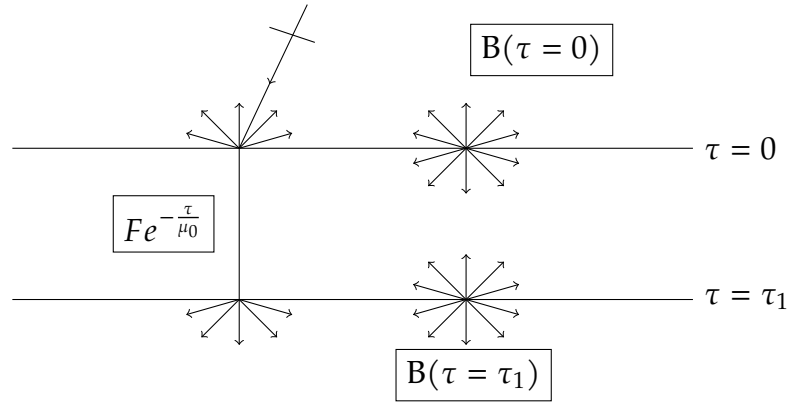


Figure 4.1: This figure shows the total effect due to diffuse scattering as well as thermal emission for a *semi-infinite atmosphere*. The thermal emission B is Isotropic in nature and emitted from the particular atmospheric layer where the optical depth is τ (from S. Sengupta 2021).

ering this, the source function can be written as,

$$\begin{aligned} \xi(\tau, \mu, \phi) = & \beta(\tau, \mu, \phi) + \frac{1}{4\pi} \int_{-1}^1 \int_0^{2\pi} p(\mu, \phi; \mu', \phi') I(\tau, \mu', \phi') d\phi' d\mu' \\ & + \frac{1}{4} F e^{-\tau/\mu_0} p(\mu, \phi; -\mu_0, \phi_0) \end{aligned} \quad (4.3)$$

From this equation onwards we will consider all expressions at a single frequency unless otherwise mentioned and thus drop ν .

The emission, $\beta(\tau, \mu, \phi)$ can be caused by internal energy source distribution (Bellman et al. 1967), the thermal re-emission process (Chakrabarty and Sengupta 2020) or the temperature dependent planck emission (Malkevich 1963). However, for an atmosphere satisfying homogeneity and Local Thermodynamic Equilibrium conditions, $\beta(\tau, \mu, \phi)$ can be written in terms of planck function (Seager 2010a) as, $\beta(\tau, \mu, \phi) = \frac{\kappa}{\chi} B(T_\tau)$. Here T_τ is the temperature of an atmospheric layer with optical depth τ . Now in the low scattering limit $\kappa \gg \sigma$, eqn.(4.1) will be reduced into $\chi \approx \kappa$. In this limit, the atmospheric emission β will be equivalent to the planck function B (See fig. 4.1) . So eqn.(4.3) will then have the following form,

$$\begin{aligned} \xi(\tau, \mu, \phi) = & B(T_\tau) + \frac{1}{4\pi} \int_{-1}^1 \int_0^{2\pi} p(\mu, \phi; \mu', \phi') I(\tau, \mu', \phi') d\phi' d\mu' \\ & + \frac{1}{4} F e^{-\tau/\mu_0} p(\mu, \phi; -\mu_0, \phi_0) \end{aligned} \quad (4.4)$$

So the radiative transfer equation for *an atmosphere with both emission as well as*

diffuse reflection can be written as,

$$\begin{aligned} \mu \frac{dI(\tau, \mu, \phi)}{d\tau} = & I(\tau, \mu, \phi) - B(T_\tau) - \frac{1}{4\pi} \int_{-1}^1 \int_0^{2\pi} p(\mu, \phi; \mu', \phi') I(\tau, \mu', \phi') d\mu' d\phi' \\ & - \frac{1}{4} F e^{-\tau/\mu_0} p(\mu, \phi; -\mu_0, \phi_0) \end{aligned} \quad (4.5)$$

This equation represents *the general form of radiative transfer appropriate for diffuse reflection and transmission, where both scattering as well as atmospheric emission takes place.*

4.3 General Integral equation of scattering Function

Here we use the same definition of scattering function as given in section 2.10 in case of semi-infinite atmosphere. Now it is apparent from eqn.(2.45) that the diffused intensity is directly proportional to the incident flux F . Chandrasekhar 1960 showed that, this is indeed the case while considering *only the atmospheric scattering and no emission*. Thus for an atmosphere without emission, the diffused intensity vanishes when there is no flux incident on the surface (i.e. $F=0$). But this is not the case for a thermally emitting atmosphere. We will show later in this section (eqn.(4.7)) as well as in section 4.6 that the scattering function S for a thermally emitting atmosphere always contains an additive term in the form of $\frac{B(T)}{F}$. Thus, eqn(2.45) gives a non-vanishing intensity of radiation even in the absence of incident flux (i.e. $F=0$) due to the thermal emission of the atmosphere. Therefore we mention that although eqn.(2.45) shows apparent proportionality of the emitting radiation to the incident flux, in case of thermally emitting atmosphere the scattering function itself takes care of the fact that the thermal emission contribution remains independent of the incident flux.

We now calculate the general functional form of $S(\mu, \phi; \mu_0, \phi_0)$ in case of diffuse scattering and thermal emission process using *invariance principle method* (see section 2.12) as formulated in Chandrasekhar 1960 and applied in S. Chandrasekhar 1947 and Horak and S. Chandrasekhar 1961. Only for diffuse reflection case the integral equation for scattering function is given in section 2.13. Here we will show how the inclusion of thermal emission affects the results derived in chapter 2.

Now the principle of invariance in semi-infinite atmosphere is applicable only if the atmosphere shows the translational invariance. For such case the atmospheric emission β will be independent of optical depth τ . For thermal emission this case can be realized by considering an isothermal atmosphere. Then the planck emission can be written as $B(T)$, where $T_{\tau_0} = T_{\tau_1} = \dots = T$. Thus, for an isothermal

atmosphere, at $\tau = 0$, the source function in eqn.(4.4) can be written using the boundary condition (2.54) as,

$$\begin{aligned} \xi(0, \mu, \phi) = & B(T) + \frac{F}{16\pi} \int_0^1 \int_0^{2\pi} p(\mu, \phi; \mu'', \phi'') S(\mu'', \phi''; \mu_0, \phi_0) \frac{d\mu''}{\mu''} d\phi'' \\ & + \frac{1}{4} F p(\mu, \phi; -\mu_0, \phi_0) \end{aligned} \quad (4.6)$$

It is worthnoting that the only difference between the source functions given in (2.56) and (4.6) is that in case of thermal emission there is only a $B(T)$ term added. Now by the procceding the same way as before we will get the integral form of scattering function as,

$$\begin{aligned} & \left(\frac{1}{\mu_0} + \frac{1}{\mu}\right) S(\mu, \phi, \mu_0, \phi_0) \\ & = 4U(T) \left[1 + \frac{1}{4\pi} \int_0^1 \int_0^{2\pi} S(\mu, \phi; \mu', \phi') \frac{d\mu'}{\mu'} d\phi' \right] \\ & + [p(\mu, \phi; -\mu_0, \phi_0) + \frac{1}{4\pi} \int_0^1 \int_0^{2\pi} S(\mu, \phi; \mu', \phi') p(-\mu', \phi'; -\mu_0, \phi_0) \frac{d\mu'}{\mu'} d\phi'] \\ & + \frac{1}{4\pi} \left[\int_0^1 \int_0^{2\pi} p(\mu, \phi; \mu'', \phi'') S(\mu'', \phi''; \mu_0, \phi_0) d\phi'' \frac{d\mu''}{\mu''} \right. \\ & \left. + \frac{1}{4\pi} \int_0^1 \int_0^{2\pi} \int_0^1 \int_0^{2\pi} S(\mu, \phi; \mu', \phi') p(-\mu', \phi'; \mu'', \phi'') S(\mu'', \phi''; \mu_0, \phi_0) d\phi'' \frac{d\mu''}{\mu''} \frac{d\mu'}{\mu'} d\phi' \right] \end{aligned} \quad (4.7)$$

where we define $U(T) = \frac{B(T)}{F}$. This is the general form of scattering function in presence of thermal emission, which is somewhat different from the equation derived in S. Chandrasekhar 1947 and presented in section 2.13

4.4 Explicit form of the scattering integral equation with different phase functions

From section 4.3 it is evident that the general expression of scattering function has an explicit dependency on the phase function. The properties and different types of phase functions has been discussed in section 2.9. Here we will show the explicit form of scattering function for different type of phase functions.

4.4.1 Isotropic scattering:

The isotropic scattering phase function and its influence on the integral form of scattering function in case of scattering only atmosphere is discussed in section 2.14.1. An atmosphere with both scattering as well as absorption is discussed in Sen Gupta, Chakrabarty, and Tinetti 2020 and thus the single scattering albedo $\tilde{\omega}_0$ can be defined as,

$$\tilde{\omega}_0 = \frac{\sigma}{\chi} \quad (4.8)$$

followed from Domanus and Cogley 1974.

The calculations are the same as given in 2.14.1 with the only modification as the addition of thermal emission to the calculations. Hence the source function S for isotropic phase function can be written using eqn.(4.7) as,

$$\begin{aligned} & \left(\frac{1}{\mu_0} + \frac{1}{\mu}\right)S(\mu; \mu_0) \\ &= 4U(T)\left[1 + \frac{1}{2} \int_0^1 S(\mu; \mu') \frac{d\mu'}{\mu'}\right] + \tilde{\omega}_0 \left[1 + \frac{1}{2} \int_0^1 S(\mu; \mu') \frac{d\mu'}{\mu'}\right] \left[1 + \frac{1}{2} \int_0^1 S(\mu_0; \mu'') \frac{d\mu''}{\mu''}\right] \end{aligned} \quad (4.9)$$

Those bracketed terms in right hand side must be the values of either μ or μ_0 of the *same function*. Let's define the function as,

$$M(\mu) = 1 + \frac{1}{2} \int_0^1 S(\mu; \mu') \frac{d\mu'}{\mu'} \quad (4.10)$$

Thus, eqn.(4.9) will reduce in terms of M -function,

$$\left(\frac{1}{\mu_0} + \frac{1}{\mu}\right)S(\mu; \mu_0) = 4U(T)M(\mu) + \tilde{\omega}_0 M(\mu)M(\mu_0) \quad (4.11)$$

The non-linear expression of M -function can be derived by putting the expression of $S(\mu, \mu')$ (eqn.(4.11)) back in eqn.(4.10) as,

$$\therefore M(\mu) = 1 + 2U(T)M(\mu)\mu \log\left(1 + \frac{1}{\mu}\right) + \frac{\tilde{\omega}_0}{2}\mu M(\mu) \int_0^1 \frac{M(\mu')}{\mu + \mu'} d\mu' \quad (4.12)$$

Here we mention that the conservative case ($\tilde{\omega}_0 = 1$) will not need any special treatment. Just by replacing $\tilde{\omega}_0 = 1$ in eqns.(4.11) and (4.12) we will get the exact forms for conservative case.

Finally, we determine diffusely reflected specific intensity from a thermally emitting atmosphere $I(0, \mu, \mu_0)$ using eqn.(2.45) for *isotropic scattering* in terms of

M-function as follows,

$$\begin{aligned} I(0, \mu, \mu_0) &= \frac{F}{4\mu} \frac{\mu\mu_0}{\mu + \mu_0} [4U(T) + \tilde{\omega}_0 M(\mu_0)] M(\mu) \\ &= \frac{\mu_0}{\mu + \mu_0} B(T) M(\mu) + \frac{F}{4} \frac{\mu_0}{\mu + \mu_0} \tilde{\omega}_0 M(\mu_0) M(\mu) \end{aligned} \quad (4.13)$$

4.4.2 Asymmetric scattering:

The phase function of asymmetric scattering and its influence on the form of scattering function is explicitly shown in section 2.14.2. Here we will show the effect of thermal emission $B(T)$ on the results derived in 2.14.2.

Using eqns.(2.38),(4.7) and (2.64) we will deduce the form of $S(\mu, \phi; \mu_0, \phi_0)$ and comparing with eqn.(2.63) with (μ', ϕ') replaced by (μ_0, ϕ_0) we will get the form of $S^{(0)}$ as,

$$\begin{aligned} \left(\frac{1}{\mu_0} + \frac{1}{\mu}\right) S^{(0)}(\mu; \mu_0) &= \frac{4U(T)}{\tilde{\omega}_0} \left[1 + \frac{\tilde{\omega}_0}{2} \int_0^1 S^{(0)}(\mu; \mu') \frac{d\mu'}{\mu'}\right] \\ &\quad + \left[1 + \frac{\tilde{\omega}_0}{2} \int_0^1 S^{(0)}(\mu'', \mu_0) \frac{d\mu''}{\mu''}\right] \left[1 + \frac{\tilde{\omega}_0}{2} \int_0^1 S^{(0)}(\mu', \mu) \frac{d\mu'}{\mu'}\right] \\ &\quad - x \left[\mu_0 - \frac{\tilde{\omega}_0}{2} \int_0^1 S^{(0)}(\mu'', \mu_0) d\mu''\right] \left[\mu - \frac{\tilde{\omega}_0}{2} \int_0^1 S^{(0)}(\mu', \mu) d\mu'\right] \end{aligned} \quad (4.14)$$

We can write eqn.(4.14) in closed form as follows,

$$\left(\frac{1}{\mu_0} + \frac{1}{\mu}\right) S_a^{(0)}(\mu; \mu_0) = \frac{4U(T)}{\tilde{\omega}_0} \psi_a(\mu) + \psi_a(\mu_0) \psi_a(\mu) - x \phi_a(\mu_0) \phi_a(\mu) \quad (4.15)$$

where we define,

$$\begin{aligned} \psi_a(\mu) &= 1 + \frac{1}{2} \tilde{\omega}_0 \int_0^1 S_a^{(0)}(\mu; \mu') \frac{d\mu'}{\mu'} \\ \phi_a(\mu) &= \mu - \frac{1}{2} \tilde{\omega}_0 \int_0^1 S_a^{(0)}(\mu; \mu') d\mu' \end{aligned} \quad (4.16)$$

Putting the expression of $S^{(0)}$ back into equation (4.16) we will get the expressions of ϕ and ψ as follows,

$$\begin{aligned} \psi_a(\mu) &= 1 + 2U(T) \psi_a(\mu) \mu \log\left(1 + \frac{1}{\mu}\right) + \frac{\tilde{\omega}_0}{2} \mu \psi_a(\mu) \int_0^1 \psi_a(\mu') \frac{d\mu'}{\mu + \mu'} \\ &\quad - \frac{\tilde{\omega}_0}{2} x \mu \phi_a(\mu) \int_0^1 \phi_a(\mu') \frac{d\mu'}{\mu + \mu'} \end{aligned} \quad (4.17)$$

and

$$\begin{aligned} \phi_a(\mu) = & \mu - 2U(T)\psi_a(\mu)\mu \log\left(1 + \frac{1}{\mu}\right) - \frac{\tilde{\omega}_0}{2}\mu\psi_a(\mu) \int_0^1 \psi_a(\mu') \frac{\mu'}{\mu + \mu'} d\mu' \\ & + \frac{\tilde{\omega}_0}{2}x\mu\phi_a(\mu) \int_0^1 \phi_a(\mu') \frac{\mu'}{\mu + \mu'} d\mu' \end{aligned} \quad (4.18)$$

The expressions of $S^{(1)}$ and $H^{(1)}$ remains the same as given in eqns. (2.70) and (2.71) respectively. Thus, we can put the values of $S^{(0)}$ and $S^{(1)}$ in eqn.(2.63) and get,

$$\begin{aligned} S_a(\mu, \phi; \mu_0, \phi_0) &= \frac{\mu\mu_0}{\mu + \mu_0}4U(T)\psi_a(\mu) + \frac{\mu\mu_0}{\mu + \mu_0}\tilde{\omega}_0[(\psi_a(\mu)\psi_a(\mu_0) - x\phi_a(\mu)\phi_a(\mu_0))] \\ &+ H^{(1)}(\mu)H^{(1)}(\mu_0)x\sqrt{(1 - \mu^2)(1 - \mu_0^2)\cos(\phi_0 - \phi)} \end{aligned} \quad (4.19)$$

Thus, the diffusely reflected intensity from thermally emitting atmosphere in asymmetric scattering can be determined using eqns. (4.19) and (2.45) as,

$$\begin{aligned} I(0, \mu; \mu_0) &= \frac{F}{4\mu}S_a(\mu, \phi; \mu_0, \phi_0) \\ &= B(T)\frac{\mu_0}{\mu + \mu_0}\psi_a(\mu) + \frac{F}{4}\frac{\mu_0}{\mu + \mu_0}\tilde{\omega}_0[(\psi_a(\mu)\psi_a(\mu_0) - x\phi_a(\mu)\phi_a(\mu_0))] \\ &+ H^{(1)}(\mu)H^{(1)}(\mu_0)x\sqrt{(1 - \mu^2)(1 - \mu_0^2)\cos(\phi_0 - \phi)} \end{aligned} \quad (4.20)$$

4.4.3 Rayleigh scattering:

The phase function and the general form of rayleigh scattering has been described in section 2.14.3. We follow the same procedure here as well and get,

$$\begin{aligned} &\left(\frac{1}{\mu_0} + \frac{1}{\mu}\right)S^{(0)}(\mu, \mu_0) \\ &= \frac{8}{3}4U(T)\left[1 + \frac{1}{2}\int_0^1 S^{(0)}(\mu; \mu')\frac{d\mu'}{\mu'}\right] \\ &+ \frac{1}{3}\left[3 - \mu^2 + \frac{3}{16}\int_0^1 (3 - \mu'^2)S^{(0)}(\mu, \mu')\frac{d\mu'}{\mu'}\right] * \left[3 - \mu_0^2 + \frac{3}{16}\int_0^1 (3 - \mu''^2)S^{(0)}(\mu_0, \mu'')\frac{d\mu''}{\mu''}\right] \\ &+ \frac{8}{3}\left[\mu^2 + \frac{3}{16}\int_0^1 \mu'^2 S^{(0)}(\mu, \mu')\frac{d\mu'}{\mu'}\right] * \left[\mu_0^2 + \frac{3}{16}\int_0^1 \mu''^2 S^{(0)}(\mu_0, \mu'')\frac{d\mu''}{\mu''}\right] \end{aligned} \quad (4.21)$$

We define the following terms as in the previous way as shown in section 2.14.3 with an additional term γ_R ,

$$\begin{aligned}\psi_R(\mu) &= 3 - \mu^2 + \frac{3}{16} \int_0^1 (3 - \mu'^2) S_R^{(0)}(\mu, \mu') \frac{d\mu'}{\mu'} \\ \phi_R(\mu) &= \mu^2 + \frac{3}{16} \int_0^1 \mu'^2 S_R^{(0)}(\mu, \mu') \frac{d\mu'}{\mu'} \\ \gamma_R(\mu) &= 1 + \frac{3}{16} \int_0^1 S_R^{(0)}(\mu, \mu') \frac{d\mu'}{\mu'}\end{aligned}\quad (4.22)$$

Now eqn.(4.21) can be expressed as,

$$\therefore \left(\frac{1}{\mu_0} + \frac{1}{\mu}\right) S_R^{(0)}(\mu, \mu_0) = \frac{32}{3} U(T) \gamma_R(\mu) + \frac{1}{3} \psi_R(\mu) \psi_R(\mu_0) + \frac{8}{3} \phi_R(\mu) \phi_R(\mu_0) \quad (4.23)$$

Now putting eqn.(4.23) in eqn.(4.22) we can get the explicit forms for ϕ_R, ψ_R and γ_R as follows,

$$\begin{aligned}\gamma_R(\mu) &= 1 + 2U(T) \gamma_R(\mu) \mu \log\left(1 + \frac{1}{\mu}\right) + \frac{1}{16} \psi_R(\mu) \mu \int_0^1 \frac{d\mu'}{\mu + \mu'} \psi_R(\mu') \\ &\quad + \frac{1}{2} \phi_R(\mu) \mu \int_0^1 \frac{d\mu'}{\mu + \mu'} \phi_R(\mu')\end{aligned}\quad (4.24)$$

and

$$\begin{aligned}\psi_R(\mu) &= (3 - \mu^2) \left[1 + 2U(T) \gamma_R(\mu) \mu \log\left(1 + \frac{1}{\mu}\right)\right] + \frac{3}{4} U(T) \gamma_R(\mu) \mu \left[\mu - \frac{1}{2}\right] \\ &\quad + \frac{1}{16} \mu \psi_R(\mu) \int_0^1 \frac{3 - \mu'^2}{\mu + \mu'} \psi_R(\mu') d\mu' + \frac{1}{2} \mu \phi_R(\mu) \int_0^1 \frac{3 - \mu'^2}{\mu + \mu'} \phi_R(\mu') d\mu'\end{aligned}\quad (4.25)$$

finally

$$\begin{aligned}\phi_R(\mu) &= \mu^2 \left[1 + 2U(T) \gamma_R(\mu) \mu \log\left(1 + \frac{1}{\mu}\right)\right] + \frac{3}{4} U(T) \mu \gamma_R(\mu) \left[\frac{1}{2} - \mu\right] \\ &\quad + \frac{1}{16} \mu \psi_R(\mu) \int_0^1 \frac{\mu'^2}{\mu + \mu'} \psi_R(\mu') d\mu' + \frac{1}{2} \mu \phi_R(\mu) \int_0^1 \frac{\mu'^2}{\mu + \mu'} \phi_R(\mu') d\mu'\end{aligned}\quad (4.26)$$

The remaining expressions for $S^{(1)}(\mu, \mu')$ and $S^{(2)}(\mu, \mu')$ can be found by comparing the co-efficients of $\cos(\phi - \phi_0)$ and $\cos 2(\phi - \phi_0)$ respectively and those expressions are given in eqns.(2.80) , (2.81) , (2.82) where they are expressed in terms of $H^{(1)}$ and $H^{(2)}$ holding the same expression as given in eqns.(2.83) and (2.84)

Now the full equation of scattering function and intensity at the layer of $\tau = 0$ for Rayleigh scattering in presence of thermal emission can be expressed as follows,

$$\begin{aligned} \left(\frac{1}{\mu} + \frac{1}{\mu_0}\right)S_R(\mu, \phi; \mu_0, \phi_0) &= \frac{3}{8}\left[\frac{32}{3}U(T)\gamma_R(\mu) + \frac{1}{3}\psi_R(\mu)\psi_R(\mu_0) + \frac{8}{3}\phi_R(\mu)\phi_R(\mu_0)\right. \\ &\quad - H^{(1)}(\mu)H^{(1)}(\mu_0)4\mu\mu_0\sqrt{(1-\mu^2)(1-\mu_0^2)}\cos(\phi-\phi_0) \\ &\quad \left.+ H^{(2)}(\mu)H^{(2)}(\mu_0)(1-\mu^2)(1-\mu_0^2)\cos 2(\phi-\phi_0)\right] \end{aligned} \quad (4.27)$$

and

$$\begin{aligned} I(0, \mu; \mu_0) &= \frac{\mu_0}{\mu + \mu_0}B(T)\gamma_R(\mu) \\ &\quad + \frac{3F}{32}\frac{\mu_0}{\mu + \mu_0}\left[\frac{1}{3}\psi_R(\mu)\psi_R(\mu_0) + \frac{8}{3}\phi_R(\mu)\phi_R(\mu_0)\right. \\ &\quad - H^{(1)}(\mu)H^{(1)}(\mu_0)4\mu\mu_0\sqrt{(1-\mu^2)(1-\mu_0^2)}\cos(\phi-\phi_0) \\ &\quad \left.+ H^{(2)}(\mu)H^{(2)}(\mu_0)(1-\mu^2)(1-\mu_0^2)\cos 2(\phi-\phi_0)\right] \end{aligned} \quad (4.28)$$

4.4.4 Scattering function for the general phase function:

The explicit form of the phase function, scattering function and the derivations for this kind of phase function are provided in section 2.14.4

It has been shown in section 4.4.2 and 4.4.3 that $S^{(1)}(\mu, \mu_0)$ or $S^{(2)}(\mu, \mu_0)$ are not effected by thermal emission $B(T_\tau)$ and only $S^{(0)}(\mu, \mu')$ is effected. Thus, here we show the calculations $S^{(0)}(\mu, \mu')$ only and write the expressions of $S^{(1)}(\mu, \mu')$, $S^{(2)}(\mu, \mu')$ as given in Horak and S. Chandrasekhar 1961.

The same procedure is followed as shown in section 2.14.4 in presence of thermal emission and hence we get the following result.

$$\left(\frac{1}{\mu} + \frac{1}{\mu_0}\right)S_l^{(0)}(\mu, \mu_0) = 4U(T)\gamma_l(\mu) - \tilde{\omega}_1\eta_l(\mu)\eta_l(\mu_0) + \frac{3\tilde{\omega}_0}{\zeta}\phi_l(\mu)\phi_l(\mu_0) + \frac{3\tilde{\omega}_2}{4\zeta}\psi_l(\mu)\psi_l(\mu_0) \quad (4.29)$$

where,

$$\gamma_l(\mu) = 1 + \frac{1}{2}\int_0^1 S_l^{(0)}(\mu, \mu')\frac{d\mu'}{\mu'} \quad (4.30)$$

$$\eta_l(\mu) = \mu - \frac{1}{2}\int_0^1 S_l^{(0)}(\mu, \mu')d\mu' \quad (4.31)$$

$$\phi_l(\mu) = \mu^2 + \frac{1}{2} \int_0^1 S_l^{(0)}(\mu, \mu') \mu' d\mu' \quad (4.32)$$

$$\psi_l(\mu) = (\zeta - \mu^2) + \frac{1}{2} \int_0^1 S_l^{(0)}(\mu, \mu') (\zeta - \mu'^2) \frac{d\mu'}{\mu'} \quad (4.33)$$

To write the explicit expressions of γ_l , η_l , ϕ_l and ψ_l we put the expression (4.29) in equations (4.30)-(4.33) and get the following expressions,

$$\begin{aligned} \gamma_l(\mu) = & 1 + 2U(T)\mu\gamma_l(\mu) \log\left(1 + \frac{1}{\mu}\right) - \frac{\mu}{2} \tilde{\omega}_1 \eta_l(\mu) \int_0^1 \frac{\eta_l(\mu')}{\mu + \mu'} d\mu' + \frac{\mu}{2} \frac{3\tilde{\omega}_0}{\zeta} \phi_l(\mu) \int_0^1 \frac{\phi_l(\mu')}{\mu + \mu'} \\ & + \frac{\mu}{2} \frac{3\tilde{\omega}_2}{4\zeta} \psi_l(\mu) \int_0^1 \frac{\psi_l(\mu')}{\mu + \mu'} d\mu' \end{aligned} \quad (4.34)$$

$$\begin{aligned} \eta_l(\mu) = & \mu - 2U(T)\gamma_l(\mu)\mu\left[1 - \mu \log\left(1 + \frac{1}{\mu}\right)\right] + \frac{\mu}{2} \tilde{\omega}_1 \eta_l(\mu) \int_0^1 \frac{\eta_l(\mu')}{\mu + \mu'} \mu' d\mu' \\ & - \frac{\mu}{2} \frac{3\tilde{\omega}_0}{\zeta} \phi_l(\mu) \int_0^1 \frac{\phi_l(\mu')}{\mu + \mu'} \mu' d\mu' - \frac{\mu}{2} \frac{3\tilde{\omega}_2}{4\zeta} \psi_l(\mu) \int_0^1 \frac{\psi_l(\mu')}{\mu + \mu'} \mu' d\mu' \end{aligned} \quad (4.35)$$

$$\begin{aligned} \phi_l(\mu) = & \mu^2 + 2U(T)\gamma_l(\mu)\mu\left[\frac{1}{2} - \mu + \mu^2 \log\left(1 + \frac{1}{\mu}\right)\right] - \frac{\mu}{2} \tilde{\omega}_1 \eta_l(\mu) \int_0^1 \frac{\eta_l(\mu')}{\mu + \mu'} \mu'^2 d\mu' \\ & + \frac{\mu}{2} \frac{3\tilde{\omega}_0}{\zeta} \phi_l(\mu) \int_0^1 \frac{\phi_l(\mu')}{\mu + \mu'} \mu'^2 d\mu' + \frac{\mu}{2} \frac{3\tilde{\omega}_2}{4\zeta} \psi_l(\mu) \int_0^1 \frac{\psi_l(\mu')}{\mu + \mu'} \mu'^2 d\mu' \end{aligned} \quad (4.36)$$

$$\begin{aligned} \psi_l(\mu) = & (\zeta - \mu^2) + 2U(T)\mu\gamma_l(\mu)\left[(\zeta - \mu^2) \log\left(1 + \frac{1}{\mu}\right) + \mu - \frac{1}{2}\right] \\ & - \frac{\mu}{2} \tilde{\omega}_1 \eta_l(\mu) \int_0^1 \frac{\eta_l(\mu')}{\mu + \mu'} (\zeta - \mu'^2) d\mu' + \frac{\mu}{2} \frac{3\tilde{\omega}_0}{\zeta} \phi_l(\mu) \int_0^1 \frac{\phi_l(\mu')}{\mu + \mu'} (\zeta - \mu'^2) d\mu' \\ & + \frac{\mu}{2} \frac{3\tilde{\omega}_2}{4\zeta} \psi_l(\mu) \int_0^1 \frac{\psi_l(\mu')}{\mu + \mu'} (\zeta - \mu'^2) d\mu' \end{aligned} \quad (4.37)$$

Finally the expressions of $S^{(1)}(\mu, \mu_0)$, $S^{(2)}(\mu, \mu_0)$ remains the same and are given

in eqns. (2.89), (2.90). Hence the total scattering function will be,

$$\begin{aligned}
S_I(\mu, \phi; \mu_0, \phi_0) &= \frac{\mu\mu_0}{\mu + \mu_0} \left\{ 4U(T)\gamma_I(\mu) - \tilde{\omega}_1\eta_I(\mu)\eta_I(\mu_0) + \frac{3\tilde{\omega}_0}{\zeta}\phi_I(\mu)\phi_I(\mu_0) + \frac{3\tilde{\omega}_2}{4\zeta}\psi_I(\mu)\psi_I(\mu_0) \right\} \\
&+ [\tilde{\omega}_1(1+l\mu)(1+l\mu_0) - 3\tilde{\omega}_2m^2\mu\mu_0]H^{(1)}(\mu)H^{(1)}(\mu_0)\sqrt{(1-\mu^2)(1-\mu_0^2)}\cos(\phi-\phi_0) \\
&+ \frac{3\tilde{\omega}_2}{4}H^{(2)}(\mu)H^{(2)}(\mu_0)(1-\mu^2)(1-\mu_0^2)\cos 2(\phi-\phi_0) \}
\end{aligned} \tag{4.38}$$

Now the final intensity $I(0, \mu; \mu_0)$ here can be expressed as,

$$\begin{aligned}
I(0, \mu; \mu_0) &= \frac{\mu_0}{\mu + \mu_0} B(T)\gamma_I(\mu) \\
&+ \frac{\mu_0}{\mu + \mu_0} \frac{F}{4} \left[-\tilde{\omega}_1\eta_I(\mu)\eta_I(\mu_0) + \frac{3\tilde{\omega}_0}{\zeta}\phi_I(\mu)\phi_I(\mu_0) + \frac{3\tilde{\omega}_2}{4\zeta}\psi_I(\mu)\psi_I(\mu_0) \right. \\
&+ \{ \tilde{\omega}_1(1+l\mu)(1+l\mu_0) - 3\tilde{\omega}_2m^2\mu\mu_0 \} H^{(1)}(\mu)H^{(1)}(\mu_0)\sqrt{(1-\mu^2)(1-\mu_0^2)}\cos(\phi-\phi_0) \\
&+ \left. \frac{3\tilde{\omega}_2}{4}H^{(2)}(\mu)H^{(2)}(\mu_0)(1-\mu^2)(1-\mu_0^2)\cos 2(\phi-\phi_0) \right]
\end{aligned} \tag{4.39}$$

4.5 Comparison of our general model with Chandrasekhar's diffusion scattering model

We introduced thermal emission effect in Chandrasekhar's semi-infinite diffused reflection problem. One can expect that all of our present results will reduce into those of Chandrasekhar's results for negligible thermal emission. Here we consider the case $B(T) \ll F$ which can also be considered as $U(T) \rightarrow 0$ to reduce our results in the limit of scattering only atmosphere and compare with previous results as given in Chandrasekhar 1960, Horak 1950 and Horak and S. Chandrasekhar 1961

1. The Transfer equation (4.5) will be:

$$\begin{aligned}
\mu \frac{dI(\tau, \mu, \phi)}{d\tau} &= I(\tau, \mu, \phi) - \frac{1}{4\pi} \int_{-1}^1 \int_0^{2\pi} p(\mu, \phi; \mu', \phi') I(\tau, \mu', \phi') d\mu' d\phi' \\
&\quad - \frac{1}{4} F e^{-\tau/\mu_0} p(\mu, \phi; -\mu_0, \phi_0)
\end{aligned} \tag{4.40}$$

Same as, eqn.(2.31) and eqn. (126) Chandrasekhar 1960, pg. 22

2. The integral equation (4.7) for Scattering function S will be:

$$\begin{aligned}
\left(\frac{1}{\mu_0} + \frac{1}{\mu}\right)S(\mu, \phi, \mu_0, \phi_0) &= p(\mu, \phi; -\mu_0, \phi_0) \\
&+ \frac{1}{4\pi} \int_0^1 \int_0^{2\pi} S(\mu, \phi; \mu', \phi') p(-\mu', \phi'; -\mu_0, \phi_0) \frac{d\mu'}{\mu'} d\phi' \\
&+ \frac{1}{4\pi} \int_0^1 \int_0^{2\pi} p(\mu, \phi; \mu'', \phi'') S(\mu'', \phi''; \mu_0, \phi_0) d\phi'' \frac{d\mu''}{\mu''} \\
&+ \frac{1}{16\pi^2} \int_0^1 \int_0^{2\pi} \int_0^1 \int_0^{2\pi} S(\mu, \phi; \mu', \phi') p(-\mu', \phi'; \mu'', \phi'') S(\mu'', \phi''; \mu_0, \phi_0) d\phi'' \frac{d\mu''}{\mu''} d\phi' \frac{d\mu'}{\mu'}
\end{aligned} \tag{4.41}$$

Same as, eqn.(2.57) and eqn. (28) in Chandrasekhar 1960, pg. 94

3. The equations for isotropic scattering,

(a) The equation (4.11) of scattering function for isotropic case will be:

$$\left(\frac{1}{\mu_0} + \frac{1}{\mu}\right)S(\mu; \mu_0) = \tilde{\omega}_0 M(\mu) M(\mu_0) \tag{4.42}$$

(b) M -function defined in eqn.(4.12) will be:

$$\therefore M(\mu) = 1 + \frac{\tilde{\omega}_0}{2} \mu M(\mu) \int_0^1 \frac{M(\mu')}{\mu + \mu'} d\mu' \tag{4.43}$$

(c) The intensity equation (4.13) will be:

$$I(0, \mu, \mu_0) = \frac{F}{4} \frac{\mu_0}{\mu + \mu_0} \tilde{\omega}_0 M(\mu_0) M(\mu) \tag{4.44}$$

This reduced form of M -function is equivalent to Chandrasekhar's H -function given in Chandrasekhar 1960, pg. 90, eqn.(42). The scattering function and intensity expressions are also equivalent to that given in Chandrasekhar 1960 and Horak 1950 only the M -functions replaced by H -function.

4. The equations for the asymmetric scattering phase function, $\tilde{\omega}_0(1 + x \cos \theta)$:

(a) The scattering function of zeroth order $S_a^{(0)}$ defined in equation (4.15) will be:

$$\left(\frac{1}{\mu_0} + \frac{1}{\mu}\right)S_a^{(0)}(\mu; \mu_0) = \psi_a(\mu_0)\psi_a(\mu) - x\phi_a(\mu_0)\phi_a(\mu) \tag{4.45}$$

(b) The $\psi_a(\mu)$ function defined in equation (4.17) will be:

$$\psi_a(\mu) = 1 + \frac{\tilde{\omega}_0}{2} \mu \psi_a(\mu) \int_0^1 \psi_a(\mu') \frac{d\mu'}{\mu + \mu'} - \frac{\tilde{\omega}_0}{2} x \mu \phi_a(\mu) \int_0^1 \phi_a(\mu') \frac{d\mu'}{\mu + \mu'} \quad (4.46)$$

(c) The $\phi_a(\mu)$ function defined in equation (4.18) will be:

$$\phi_a(\mu) = \mu - \frac{\tilde{\omega}_0}{2} \mu \psi_a(\mu) \int_0^1 \psi_a(\mu') \frac{\mu'}{\mu + \mu'} d\mu' + \frac{\tilde{\omega}_0}{2} x \mu \phi_a(\mu) \int_0^1 \phi_a(\mu') \frac{\mu'}{\mu + \mu'} d\mu' \quad (4.47)$$

(d) The intensity equation (4.20) will be:

$$I(0, \mu; \mu_0) = \frac{F}{4} \frac{\mu_0}{\mu + \mu_0} \tilde{\omega}_0 [(\psi_a(\mu)\psi_a(\mu_0) - x\phi_a(\mu)\phi_a(\mu_0)) + H^{(1)}(\mu)H^{(1)}(\mu_0)x\sqrt{(1-\mu^2)(1-\mu_0^2)}\cos(\phi_0 - \phi)] \quad (4.48)$$

The expressions of $S^{(0)}$, ψ_a and ϕ_a are all same as given in chapter 2. The intensity is exactly same as given in eqn. (2.73).

5. Reduced equations for the Rayleigh scattering phase function, $\frac{3}{4}(1 + \cos^2 \theta)$:

(a) The scattering function of zeroth order $S_R^{(0)}$ defined in equation (4.23) will change as:

$$\therefore \left(\frac{1}{\mu_0} + \frac{1}{\mu}\right) S_R^{(0)}(\mu, \mu_0) = \frac{1}{3} \psi_R(\mu)\psi_R(\mu_0) + \frac{8}{3} \phi_R(\mu)\phi_R(\mu_0) \quad (4.49)$$

(b) The $\psi_R(\mu)$ defined in equation (4.25) will change as:

$$\psi_R(\mu) = (3 - \mu^2) + \frac{1}{16} \mu \psi_R(\mu) \int_0^1 \frac{3 - \mu'^2}{\mu + \mu'} \psi_R(\mu') d\mu' + \frac{1}{2} \mu \phi_R(\mu) \int_0^1 \frac{3 - \mu'^2}{\mu + \mu'} \phi_R(\mu') d\mu' \quad (4.50)$$

(c) The functional form of $\phi_R(\mu)$ defined in equation (4.26) will be,

$$\phi_R(\mu) = \mu^2 + \frac{1}{16} \mu \psi_R(\mu) \int_0^1 \frac{\mu'^2}{\mu + \mu'} \psi_R(\mu') d\mu' + \frac{1}{2} \mu \phi_R(\mu) \int_0^1 \frac{\mu'^2}{\mu + \mu'} \phi_R(\mu') d\mu' \quad (4.51)$$

(d) The intensity equation (4.28) will be modified as:

$$\begin{aligned}
I(0, \mu; \mu_0) = & \frac{3F}{32} \frac{\mu_0}{\mu + \mu_0} \left[\frac{1}{3} \psi_R(\mu) \psi_R(\mu_0) + \frac{8}{3} \phi_R(\mu) \phi_R(\mu_0) \right. \\
& - H^{(1)}(\mu) H^{(1)}(\mu_0) 4\mu\mu_0 \sqrt{(1 - \mu^2)(1 - \mu_0^2)} \cos(\phi_0 - \phi) \\
& \left. + H^{(2)}(\mu) H^{(2)}(\mu_0) (1 - \mu^2)(1 - \mu_0^2) \cos 2(\phi_0 - \phi) \right] \quad (4.52)
\end{aligned}$$

The reduced expressions of $S_R^{(0)}$, ψ_R and ϕ_R for Rayleigh scattering are same with those given section 2.14.3.

6. Reduced equations for the phase function, $\tilde{\omega}_0 + \tilde{\omega}_1 P_1(\cos \Theta) + \tilde{\omega}_2 P_2(\cos \Theta)$

(a) The functional form of $S_l^{(0)}(\mu, \mu_0)$ will be,

$$\left(\frac{1}{\mu} + \frac{1}{\mu_0} \right) S_l^{(0)}(\mu, \mu_0) = -\tilde{\omega}_1 \eta_l(\mu) \eta_l(\mu_0) + \frac{3\tilde{\omega}_0}{\zeta} \phi_l(\mu) \phi_l(\mu_0) + \frac{3\tilde{\omega}_2}{4\zeta} \psi_l(\mu) \psi_l(\mu_0) \quad (4.53)$$

(b) The functional form of $\eta_l(\mu)$ will be,

$$\begin{aligned}
\eta_l(\mu) = & \mu + \frac{\mu}{2} \tilde{\omega}_1 \eta_l(\mu) \int_0^1 \frac{\eta_l(\mu')}{\mu + \mu'} \mu' d\mu' - \frac{\mu}{2} \frac{3\tilde{\omega}_0}{\zeta} \phi_l(\mu) \int_0^1 \frac{\phi_l(\mu')}{\mu + \mu'} \mu' d\mu' \\
& - \frac{\mu}{2} \frac{3\tilde{\omega}_2}{4\zeta} \psi_l(\mu) \int_0^1 \frac{\psi_l(\mu')}{\mu + \mu'} \mu' d\mu' \quad (4.54)
\end{aligned}$$

(c) The functional form of $\phi_l(\mu)$ will be,

$$\begin{aligned}
\phi_l(\mu) = & \mu^2 - \frac{\mu}{2} \tilde{\omega}_1 \eta_l(\mu) \int_0^1 \frac{\eta_l(\mu')}{\mu + \mu'} \mu'^2 d\mu' + \frac{\mu}{2} \frac{3\tilde{\omega}_0}{\zeta} \phi_l(\mu) \int_0^1 \frac{\phi_l(\mu')}{\mu + \mu'} \mu'^2 d\mu' \\
& + \frac{\mu}{2} \frac{3\tilde{\omega}_2}{4\zeta} \psi_l(\mu) \int_0^1 \frac{\psi_l(\mu')}{\mu + \mu'} \mu'^2 d\mu' \quad (4.55)
\end{aligned}$$

(d) The functional form of $\psi_l(\mu)$ will be,

$$\begin{aligned}
\psi_l(\mu) = & (\zeta - \mu^2) - \frac{\mu}{2} \tilde{\omega}_1 \eta_l(\mu) \int_0^1 \frac{\eta_l(\mu')}{\mu + \mu'} (\zeta - \mu'^2) d\mu' + \frac{\mu}{2} \frac{3\tilde{\omega}_0}{\zeta} \phi_l(\mu) \int_0^1 \frac{\phi_l(\mu')}{\mu + \mu'} (\zeta - \mu'^2) d\mu' \\
& + \frac{\mu}{2} \frac{3\tilde{\omega}_2}{4\zeta} \psi_l(\mu) \int_0^1 \frac{\psi_l(\mu')}{\mu + \mu'} (\zeta - \mu'^2) d\mu' \quad (4.56)
\end{aligned}$$

(e) The intensity $I(0, \mu; \mu_0)$ will be,

$$\begin{aligned}
I(0, \mu; \mu_0) = & \frac{\mu_0}{\mu + \mu_0} \frac{F}{4} \left[-\tilde{\omega}_1 \eta_l(\mu) \eta_l(\mu_0) + \frac{3\tilde{\omega}_0}{\zeta} \phi_l(\mu) \phi_l(\mu_0) + \frac{3\tilde{\omega}_2}{4\zeta} \psi_l(\mu) \psi_l(\mu_0) \right. \\
& + \{ \tilde{\omega}_1(1 + l\mu)(1 + l\mu_0) - 3\tilde{\omega}_2 m^2 \mu \mu_0 \} H^{(1)}(\mu) H^{(1)}(\mu_0) \sqrt{(1 - \mu^2)(1 - \mu_0^2)} \cos(\phi - \phi_0) \\
& \left. + \frac{3\tilde{\omega}_2}{4} H^{(2)}(\mu) H^{(2)}(\mu_0) (1 - \mu^2)(1 - \mu_0^2) \cos 2(\phi - \phi_0) \right]
\end{aligned} \tag{4.57}$$

The expression of $S_l^{(0)}(\mu, \mu')$ is same as given in eqn.(16) in Horak and S. Chandrasekhar 1961 and $I(0, \mu, \mu_0)$ is equivalent with the eqn. (20) of Nikku Madhusudhan and Burrows 2012. All of them are same as derived in section 2.14.4.

The equations from (4.40)-(4.57) are the expected forms of those expressions derived in this paper when we neglect the *atmospheric thermal emission* $B(T)$.

4.6 Contribution of thermal emission:

The scattering functions calculated in this work eqns.(4.11),(4.19) and (4.27) all contained the thermal emission in a general form as follows,

$$\frac{\mu \mu_0}{\mu + \mu_0} 4U(T) f(\mu) \tag{4.58}$$

Here, $f(\mu)$ is the distribution function depending on different phase functions given below,

$$\begin{aligned}
f(\mu) = & M(\mu) \quad \text{for } p = \tilde{\omega}_0 \\
& = \psi_a(\mu) \quad \text{for } p = \tilde{\omega}_0(1 + x \cos \theta) \\
& = \gamma(\mu) \quad \text{for } p = \frac{3}{4}(1 + \cos^2 \theta) \quad \text{and} \\
& p = \tilde{\omega}_0 + \tilde{\omega}_1 P_1(\cos \Theta) + \tilde{\omega}_2 P_2(\cos \Theta)
\end{aligned} \tag{4.59}$$

The same similarity can be seen in intensity $I(0, \mu; \mu_0)$ equations (4.13),(4.20) and (4.28) as,

$$\frac{\mu_0}{\mu + \mu_0} B(T) f(\mu) \tag{4.60}$$

This $f(\mu)$ holds a general integral form,

$$f(\mu) = 1 + \frac{1}{2} \int_0^1 S^{(0)}(\mu, \mu') \frac{d\mu'}{\mu'} \tag{4.61}$$

So the contribution of thermal emission to the intensity I can be written explicitly as,

$$B(T)f(\mu) = B(T) + \frac{1}{4\pi} \int_0^{2\pi} \int_0^1 B(T)S(\mu, \phi; \mu', \phi') \frac{d\mu'}{\mu'} d\phi' \quad (4.62)$$

In the same way, the contribution of thermal emission on scattering function S can be expressed as,

$$U(T)f(\mu) = U(T) + \frac{1}{4\pi} \int_0^{2\pi} \int_0^1 U(T)S(\mu, \phi; \mu', \phi') \frac{d\mu'}{\mu'} d\phi' \quad (4.63)$$

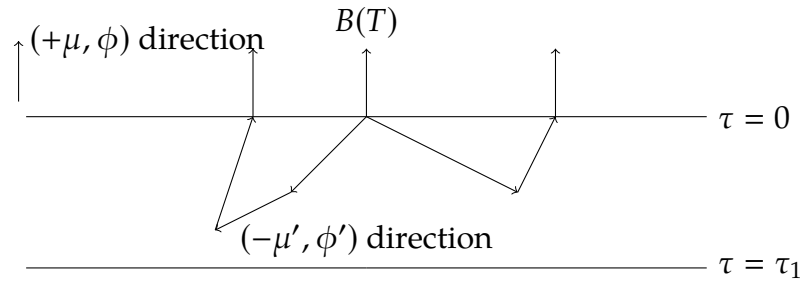


Figure 4.2: This figure shows contribution of thermal emission along the $(+\mu, \phi)$ direction by direct as well as after scattering from $(-\mu', \phi')$ direction given by equation (4.62). Ray denoted as $B(T)$ will go directly along $(+\mu, \phi)$ direction from $\tau = 0$ and other rays are initially along the directions $-\mu'$'s and then scattered a number of times to finally come along $(+\mu, \phi)$ direction.

Equation (4.62) and (4.63) shows the total effect of thermal emission on diffuse reflection radiation and scattering function respectively. The first term on right hand side gives the planck emission along the direction $(+\mu, \phi)$. This is independent of direction. The second term gives the *thermal emission reflected diffusely* along (μ, ϕ) direction. Here the scattering function $S(\mu, \phi; \mu', \phi')$ scatters the thermal emission from $(-\mu', \phi')$ direction to (μ, ϕ) direction (see fig. 4.2).

4.7 Discussion:

We derive the analytic solutions of diffuse reflection problem of semi-infinite homogeneous atmosphere introduced by Chandrasekhar 1960 in presence of thermal emission using *invariance principle method* (Ambartsumian 1943). In absence of thermal emission our treatment will reduce into only diffusely reflected case which has been previously studied by Chandrasekhar in a series of papers and tabulated in Chandrasekhar 1960, Horak 1950, S. Chandrasekhar and Breen 1947. We mention that those tabulated expressions are exactly same with the reduced form of our generalized equations as shown here in (4.40)-(4.52).

The reduction of the scattering integral equations have been done for three different phase functions other than the isotropic case. In each case the azimuth independent component of scattering function $S^{(0)}$ is affected by the thermal emission and get modified from that of Chandrasekhar. Other $S^{(i)}$ and $H^{(i)}$ terms (with $i \neq 0$) for Asymmetric scattering, Rayleigh scattering and the scattering for the phase function $\tilde{\omega}_0 + \tilde{\omega}_1 P_1(\cos \Theta) + \tilde{\omega}_2 P_2(\cos \Theta)$ remains unaffected. They are exactly the same as given in Chandrasekhar 1960, Horak and S. Chandrasekhar 1961. This is because we consider the atmospheric emission is thermal emission only. Now, as the thermal emission $B(T_\tau)$ is isotropic in nature (see fig. 4.1), so the emission contribution will always affect the isotropic (i.e. azimuth independent) terms of the scattering function and all other constituent terms remains unaffected as expected.

This comparison shows that, the emission alongwith the diffusion reflection is more general than the case of only diffusion reflection considered in Chandrasekhar 1960. We considered here three special cases (other than isotropic scattering) of $p(\mu, \phi; \mu', \phi')$, the scattering phase function, by expanding it in terms spherical harmonics. We can expand it even in more general form of Legendre polynomial introduced in Chandrasekhar 1960 as,

$$p(\cos \Theta) = \sum_{l=0}^{\infty} \tilde{\omega}_l P_l(\cos \Theta) \quad (4.64)$$

where $\tilde{\omega}_l$'s are constants. Then the corresponding *Scattering Function* will be represented as follows,

$$S = \sum_{l=0}^{\infty} \tilde{\omega}_l S^{(l)} P_l(\cos \theta) \quad (4.65)$$

From our study we can directly imply that, the effect of thermal emission $B(T_\tau)$ will contribute in $S^{(0)}$ terms only and all other terms remains unaffected for $l \neq 0$ of whatever expansion is considered. To see the emission effect in higher degree of scattering functions (i.e. $S^{(1)}, S^{(2)} \dots$ etc) one can consider the asymmetry in atmospheric emission, which is different from planck emission.

The intensity $I(0, \mu; \mu_0)$ derived in this paper always includes a thermal emission of whatever scattering phase function is considered as shown in section 4.6. Thus the blackbody emission $B(T)$ always adds some radiation to $I(0, \mu, \mu_0)$, multiplied by the function $f(\mu)$. The explicit form of $f(\mu)$ reveals that the contribution of thermal emission contains direct emission along (μ, ϕ) as well as diffusely scattered radiation from other directions to (μ, ϕ) (see fig. 4.2).

The scattering function $S^{(0)}(\mu, \mu_0)$ affected by the thermal emission in terms of $U(T)$ as shown in eqn. (4.58). As, the multiplication factor $U(T)$ is the ratio of

planck emission and incident flux πF , so it can be stated that *the effect of thermal emission on scattering function is inversely proportional to the incident flux πF and directly proportional to the blackbody emission from the corresponding layer*. Thus, when the irradiation flux πF increases but the planck emission remains fixed then the relative effect of thermal emission on scattering function is suppressed.

Chandrasekhar's semi-infinite atmosphere model is used for a large number of cases. For example King 1963 solved the green house effect of semi-infinite atmosphere, Dubus, Devooght, and Dehaes 1986 used the model to evaluate ion induced secondary electron emission whereas Nikku Madhusudhan and Burrows 2012 analytically model exoplanetary albedo, phase curve and polarization of reflected light using the direct results derived in Chandrasekhar 1960. We have shown that the specific intensity and scattering functions are underestimated while not considering the thermal emission. Thus to get accurate estimations the inclusion of thermal emission is important while using the diffuse reflection model of semi-infinite atmosphere.

The inclusion of atmospheric emission in terms of planck function to semi-infinite atmosphere problem is the first step towards the generalization of Chandrasekhar's treatment. Though there are some limitations to this model. For instance, in case of exoplanetary atmosphere the assumption of Local thermodynamic equilibrium is not valid at upper atmospheric region (Seager 2010a). Thus, the atmospheric emission will show a departure from pure blackbody emission and should be modified by other emission effects. One can treat this problem for atmospheric re-emission case (Chakrabarty and Sengupta 2020), by replacing $\beta(\tau, \mu, \phi) = (1 - \tilde{\omega}_0)B(T_\tau)$ in eqn.(4.3) and all the results follows accordingly.

Again, we considered the low scattering limit ($\kappa \gg \sigma$) in this work for which β entirely boils down into the planck function $B(T)$. To remove this restriction, the thermal emission $B(T)$ can be replaced by, $\frac{\kappa}{\chi}B(T)$ which modifies the results.

Also we assume that the atmospheric emission is planck emission only, which is isotropic in nature. This is oversimplification of the practical problem. The anisotropic effect of atmospheric emission can be included by taking the fourier expansion,

$$\beta(\tau, \Omega) = \sum_{m=0}^n \beta_m(\tau, \mu; \mu_0) \cos(\phi - \phi_0)$$

as given in Bellman et al. 1967. In that case not only $S^{(0)}$ but all $S^{(i)}$ terms of the scattering function as well as the $I(0, \mu, \mu_0)$ will be modified. This can be a more practical approach to the problem and much rigorous calculations are needed.

The phase functions considered here, all have analytical forms given in Chandrasekhar 1960. But for more realistic problems of single or direct scattering with

a forward scattering effect, Henyey and Greenstein 1941 introduced a phase function,

$$p(\cos \Theta) = \frac{1 - g^2}{(1 + g^2 - 2g \cos \Theta)^{\frac{2}{3}}}$$

where, $g \in [-1, 1]$ is the asymmetry parameter. This type of phase function has been well studied for reflected spectroscopy using numerical analysis (Batalha et al. 2019). To treat this in our semi-infinite atmosphere diffuse reflection problem one should shift from analytical treatment to numerical one.

Finally, we did not include the polarization effect to our calculations. Following Chandrasekhar 1960, we can say that all of our results will be valid while including polarization effect with some replacements as follows. The intensity I will become a vector \mathbf{I} whose components are the stokes parameters. The phase function p and scattering function S will be replaced by the analogous phase matrix \mathbf{P} and scattering matrix \mathbf{S} . In that scenario, polarization effect in semi-infinite atmosphere problem with atmospheric emission can be studied.

Chapter 5

Summary and Conclusions

My research on radiative transfer gave me the most satisfaction. I worked on it for five years, and the subject, I felt, developed on its own initiative and momentum. Problems arose one by one, each more complex and difficult than the previous one, and they were solved. The whole subject attained an elegance and a beauty which I do not find to the same degree in any of my other work.

- S. Chandrasekhar

The work presented here also took five years but I can add only a minute modification to that what Chandrasekhar has accomplished. We modeled the exoplanetary atmosphere, especially the hot-Jupiters and showed how by observing the secondary eclipse emission spectra the amount of day-night heat redistribution can be estimated. Then we studied Chandrasekhar's diffuse reflection problem in the presence of atmospheric thermal emission. Hence we generalize Chandrasekhar's results so that it can be used to model hot-Jupiter atmosphere. In this chapter we will summarize the whole work presented in this thesis with some highlights followed by the limitation and future work.

5.1 Highlights:

Here we discuss the summary and highlights of each chapter sequentially.

- **Chapter 1:** It is an introductory chapter where we have discussed what are the Exoplanets, their types, detection techniques etc. Then we provide a brief discussion about the exoplanetary atmosphere, their characterization through the observed and modeled spectra followed by a literature survey which clearly defines our main target of this thesis. Then we discuss the main goal of the thesis and the plan accordingly.
- **Chapter 2:** In this chapter we discussed the fundamental concepts of Radiative transfer used in the astrophysical context in two different parts. In the

first part we established the basic transfer equation appropriate for transmission and scattering from literature survey. Then we discussed different conditions applied for atmospheric modeling such as LTE, Radiative Equilibrium, hydrostatic equilibrium etc. In the second part we discussed the invariance principle and its use in solving the atmospheric diffuse reflection problem. We conclude by showing the results derived by Chandrasekhar 1960 and their interpretations.

- **Chapter 3:** We model the hot-Jupiter's day-side atmospheric emission spectra by obtaining the solutions of the radiative transfer equation. Hot-jupiters are the gas giants and gravitationally locked to their host stars. Hence the day and night side of these planets has a huge temperature difference. This temperature difference causes a pressure gradient which generates atmospheric flow and redistribute the heat from day-side to night-side. To specify the amount of heat redistribution we defined a heat redistribution parameter f as the ratio of the stellar flux irradiated area to heat redistributed area. Thus more the redistribution less the value of f . Then we simulate the day-side emission spectra with the different values of f . For simulation we use line by line radiative transfer code developed by Sengupta and Marley 2009, and verify this with some literature results as well as some of the observed spectra.

In results we showed that the magnitude of the simulated day side emission spectra decreases significantly with more the heat redistribution from day side to night side. Hence we conclude that by observing only the day-side emission spectra (also known as secondary eclipse spectra) of hot-jupiters and comparing it with theoretically modeled spectra, the amount of heat redistribution can be estimated. Finally, we study a particular case of the hot-jupiter XO-1b with this technique and showed that the day to night heat redistribution is very high in this particular planet.

- **Chapter 4:** In this chapter we took an analytical approach to fundamentally model the hot-jupiter atmosphere. This particular planets have their own emission as well as irradiation from their host star. Hence the source function of the radiative transfer equation should consist scattering and thermal emission. We add this emission in terms of planck emission to the radiative transfer equation and show its effect on the solution of semi-infinite diffuse reflection problem introduced by Chandrasekhar 1960. We use invariance principle method to analytically derive the scattering function and the final radiation coming out from the atmospheric layer. The solutions are provided for different type of scattering phase functions such as,

1. Isotropic scattering
2. Asymmetric scattering
3. Rayleigh scattering
4. General case of scattering function expanded up to 3rd order legendre polynomial.

Our results clearly show that the final radiation emits from the atmospheric layer contain two distinct parts. First the thermal emission from the corresponding atmospheric layer, second the scattering from the same layer. We further study the isotropic scattering case in greater detail and introduced a new function **M-function** which is analogous to Chandrasekhar's well known H-function. It is worth noting that both the emission and scattering contributes in terms of M-function to the final radiation. Finally we performed a consistency check of our model in the low thermal emission limit. It shows that all of our results are consistent with the results derived in Chandrasekhar 1960. Thus we conclude that our modified model is more complete than Chandrasekhar's model and hence it can be used for those atmosphere where scattering and thermal emission occur simultaneously.

5.2 Limitations:

Here we list some caveats in our modeling.

- While studying the variation of hot-Jupiter day-side emission spectra with respect to the atmospheric heat redistribution we neglected the effect of atmospheric chemical composition, optical opacity, variation of irradiated flux from the host star on the planetary atmosphere. They can have a crucial effect on the variation of atmospheric emission spectra. Although the resulting trend of variation of the emission spectra with the redistribution factor remains unchanged.
- While including the thermal emission in Chandrasekhar's diffuse reflection problem, we consider each atmospheric layer is in local thermodynamic equilibrium and emits only blackbody radiation depending on the corresponding layer temperature. This is true only at high optical depth of the atmosphere and in the upper part of the atmosphere, the emission is much different than the blackbody emission. This will give a complicated solution compared to that provided here. However the enhancement of the final radiation will be still there.

5.3 Future Aspects:

- The modeling of atmospheric convection in gas giant atmosphere is a challenging problem in exoplanetary science. Here we consider a simple approach to understand the amount of day to night heat redistribution by establishing a relation between the heat redistribution and the observed day side secondary eclipse emission spectra from the planet. Although there are other factors like chemical composition, optical opacity, stellar activity etc, which influence the temperature-pressure profiles and the final emission spectra. We will take care of those factor to give a complete picture.
- The simultaneous atmospheric emission and scattering model presented here is the first step towards generalizing Chandrasekhar's novel approach to solve the atmospheric diffuse reflection problem by including atmospheric emission along with scattering. Here we have considered the atmospheric emission in terms of thermal emission only. In future we can further generalize the atmospheric emission by considering atmospheric re-emission, anisotropic emission etc.
- Here we introduce the M-function for isotropic scattering case only. It is obvious that the other scattering cases (e.g. asymmetric scattering, rayleigh scattering etc) can also be expressed in terms of M-function. In that case all types of scattering function and final radiation can be easily derivable once the values of M-function estimated for different values of μ . We are planning to work on that direction.
- The analytical approach taken here to solve the semi-infinite atmosphere case can also be applied in the more general and practical finite atmosphere case. The solution of the finite atmosphere problem will have direct use in exoplanetary atmosphere modeling.
- To generate the synthetic spectra using our analytical model, we need to rigorously solve the radiative transfer equation by numerical approach. In that case we can also compare the critical limit of atmospheric emission where it is important over the irradiation flux. Hence, we will simulate the synthetic spectra numerically.

The final results derived here by including thermal emission in diffuse reflection problem can be used to model the exoplanetary atmosphere especially where the atmospheric emission is comparable with that of the irradiation flux. We hope this approach will give some fruitful interpretations of the upcoming observations.

Bibliography

Book Sources

- Chandrasekhar (1960). *Radiative Transfer*. Dover Books on Intermediate and Advanced Mathematics. Dover Publications. ISBN: 9780486605906. URL: <https://books.google.co.in/books?id=CK3HDRwCT5YC>.
- Chandrasekhar, S (1989). *Radiative transfer and negative ion of hydrogen*. Chicago: University of Chicago Press. ISBN: 0226100936.
- Liou, Kuo-Nan (2002). *An introduction to atmospheric radiation*. Vol. 84. Elsevier.
- Peraiah, Annamaneni (2002). *An Introduction to Radiative Transfer: Methods and applications in astrophysics*. Cambridge University Press.
- Perryman, M. A. C. (2011). *The exoplanet handbook*. Cambridge New York: Cambridge University Press. ISBN: 9780521765596.
- Rybicki, George (1979). *Radiative processes in astrophysics*. New York: Wiley. ISBN: 9780471827597.
- Seager, Sara (2010a). *Exoplanet atmospheres : physical processes*. Princeton, N.J: Princeton University Press. ISBN: 9780691146454.
- (2010b). *Exoplanets*. Tucson Houston: University of Arizona Press In collaboration with Lunar and Planetary Institute. ISBN: 978-0-8165-2945-2.

Paper Sources

- Abhyankar, KD and AL Fymat (1970). "Imperfect Rayleigh scattering in a semi-infinite atmosphere". In: *Astronomy and Astrophysics* 4, p. 101.
- Ambartsumian, VA (1943). "CR (Doklady), Acad". In: *Sci. URSS* 38, p. 257.
- (1944). "On the problem of diffuse reflection of light". In: *J. Phys. USSR* 8.1, p. 65.
- Batalha, Natasha E et al. (2019). "Exoplanet Reflected-light Spectroscopy with PICASO". In: *The Astrophysical Journal* 878.1, p. 70.
- Bellman, Richard et al. (1967). "Chandrasekhar's planetary problem with internal sources". In: *Icarus* 7.1-3, pp. 365–371.
- Bhatia, RK and KD Abhyankar (1983). "Multiple scattering and the phase variation of equivalent widths for phase functions of type $P(\cos\theta) = \omega + \omega_1 P_1(\cos\theta) + \omega_2 P_2(\cos\theta)$ ". In: *Astrophysics and space science* 96.1, pp. 107–123.
- Chakrabarty, Aritra and Sengupta (July 2020). "Effects of Thermal Emission on the Transmission Spectra of Hot Jupiters". In: *The Astrophysical Journal* 898.1, p. 89. doi: [10.3847/1538-4357/ab9a33](https://doi.org/10.3847/1538-4357/ab9a33). URL: <https://doi.org/10.3847/1538-4357/ab9a33>.
- Chandrasekhar, S (1947). "On the Radiative Equilibrium of a Stellar Atmosphere. XIV." In: *The Astrophysical Journal* 105, p. 164.

- Chandrasekhar, S and Frances H Breen (1947). "On the Radiative Equilibrium of a Stellar Atmosphere. XIX." In: *ApJ* 106, p. 143.
- Charbonneau, David et al. (2005). "Detection of thermal emission from an extrasolar planet". In: *The Astrophysical Journal* 626.1, p. 523.
- Deming, Drake et al. (2005). "Infrared radiation from an extrasolar planet". In: *Nature* 434.7034, pp. 740–743.
- Domanus, Henry M and Allen C Cogley (1974). "A fundamental-source-function formulation of radiative transfer and the resulting fundamental reciprocity relations". In: *Journal of Quantitative Spectroscopy and Radiative Transfer* 14.8, pp. 705–722.
- Dubus, Alain, Jacques Devooght, and Jean-Claude Dehaes (1986). "A theoretical evaluation of ion induced secondary electron emission". In: *Nuclear Instruments and Methods in Physics Research Section B: Beam Interactions with Materials and Atoms* 13.1-3, pp. 623–626.
- Fišák, Jakub et al. (2016). "Rayleigh scattering in the atmospheres of hot stars". In: *Astronomy & Astrophysics* 590, A95.
- Freedman, Richard S, Jacob Lustig-Yaeger, et al. (2014). "Gaseous mean opacities for giant planet and ultracool dwarf atmospheres over a range of metallicities and temperatures". In: *The Astrophysical Journal Supplement Series* 214.2, p. 25.
- Freedman, Richard S, Mark S Marley, and Katharina Lodders (2008). "Line and mean opacities for ultracool dwarfs and extrasolar planets". In: *The Astrophysical Journal Supplement Series* 174.2, p. 504.
- Goldstein, JS (1960). "The Infrared Reflectivity of a Planetary Atmosphere." In: *The Astrophysical Journal* 132, p. 473.
- Grant, IP and GE Hunt (1968). "Solution of radiative transfer problems in planetary atmospheres". In: *Icarus* 9.1-3, pp. 526–534.
- Guillot, Tristan (2010). "On the radiative equilibrium of irradiated planetary atmospheres". In: *Astronomy & Astrophysics* 520, A27.
- Hammond, Mark, Shang-Min Tsai, and Raymond T Pierrehumbert (2020). "The Equatorial Jet Speed on Tidally Locked Planets. I. Terrestrial Planets". In: *The Astrophysical Journal* 901.1, p. 78.
- Hansen, Brad MS (2008). "On the absorption and redistribution of energy in irradiated planets". In: *The Astrophysical Journal Supplement Series* 179.2, p. 484.
- Hartman, Joel D et al. (2011). "HAT-P-32b and HAT-P-33b: Two highly inflated hot Jupiters transiting high-jitter stars". In: *The Astrophysical Journal* 742.1, p. 59.
- Heng, Kevin (2012). "The study of climate on alien worlds". In: *American Scientist* 100.4, pp. 334–341.
- Heng, Kevin and Adam P Showman (2015). "Atmospheric dynamics of hot exoplanets". In: *Annual Review of Earth and Planetary Sciences* 43, pp. 509–540.
- Henyey, Louis G and Jesse L Greenstein (1941). "Diffuse radiation in the galaxy". In: *The Astrophysical Journal* 93, pp. 70–83.
- Horak, Henry G (1950). "Diffuse Reflection by Planetary Atmospheres." In: *The Astrophysical Journal* 112, p. 445.
- Horak, Henry G and S Chandrasekhar (1961). "Diffuse Reflection by a Semi-Infinite Atmosphere." In: *The Astrophysical Journal* 134, p. 45.
- Husser, T-O et al. (2013). "A new extensive library of PHOENIX stellar atmospheres and synthetic spectra". In: *Astronomy & Astrophysics* 553, A6.
- Kattawar, George W and Charles N Adams (1971). "Flux and polarization reflected from a Rayleigh-scattering planetary atmosphere". In: *The Astrophysical Journal* 167, p. 183.

- Kempton, Eliza M-R et al. (2017). “Exo-Transmit: An open-source code for calculating transmission spectra for exoplanet atmospheres of varied composition”. In: *Publications of the Astronomical Society of the Pacific* 129.974, p. 044402.
- King, Jean IF (1963). “Greenhouse effect in a semi-infinite atmosphere”. In: *Icarus* 2, pp. 359–363.
- Knutson, Heather A et al. (2007). “A map of the day–night contrast of the extrasolar planet HD 189733b”. In: *Nature* 447.7141, pp. 183–186.
- Komacek, Thaddeus D and Adam P Showman (2019). “Temporal variability in hot Jupiter atmospheres”. In: *The Astrophysical Journal* 888.1, p. 2.
- Lupu, RE et al. (2014). “The atmospheres of earthlike planets after giant impact events”. In: *The Astrophysical Journal* 784.1, p. 27.
- Machalek, Pavel et al. (2008). “Thermal emission of exoplanet XO-1b”. In: *The Astrophysical Journal* 684.2, p. 1427.
- Madhusudhan, N and Sara Seager (2009). “A temperature and abundance retrieval method for exoplanet atmospheres”. In: *The Astrophysical Journal* 707.1, p. 24.
- Madhusudhan, Nikku and Adam Burrows (2012). “Analytic models for albedos, phase curves, and polarization of reflected light from exoplanets”. In: *The Astrophysical Journal* 747.1, p. 25.
- Malkevich, MS (1963). “Angular and spectral distribution of radiation reflected by the earth into space”. In: *Planetary and Space Science* 11.6, pp. 681–699.
- Mansfield, Megan et al. (2018). “An HST/WFC3 thermal emission spectrum of the hot Jupiter HAT-P-7b”. In: *The Astronomical Journal* 156.1, p. 10.
- Mayor, Michel and Didier Queloz (1995). “A Jupiter-mass companion to a solar-type star”. In: *Nature* 378.6555, pp. 355–359.
- Mazeh, Tsevi et al. (2000). “The spectroscopic orbit of the planetary companion transiting HD 209458”. In: *The Astrophysical Journal Letters* 532.1, p. L55.
- Meurer, Aaron et al. (2017). “SymPy: symbolic computing in Python”. In: *PeerJ Computer Science* 3, e103.
- Mollière, P et al. (2019). “petitRADTRANS-A Python radiative transfer package for exoplanet characterization and retrieval”. In: *Astronomy & Astrophysics* 627, A67.
- Mollière, Paul et al. (2015). “Model atmospheres of irradiated exoplanets: The influence of stellar parameters, metallicity, and the C/O ratio”. In: *The Astrophysical Journal* 813.1, p. 47.
- Nikolov, N et al. (2018). “Hubble PanCET: an isothermal day-side atmosphere for the bloated gas-giant HAT-P-32Ab”. In: *Monthly Notices of the Royal Astronomical Society* 474.2, pp. 1705–1717.
- Parmentier, Vivien and Tristan Guillot (2014). “A non-grey analytical model for irradiated atmospheres I. Derivation”. In: *Astronomy & Astrophysics* 562, A133.
- Parmentier, Vivien, Tristan Guillot, et al. (2015). “A non-grey analytical model for irradiated atmospheres II. Analytical vs. numerical solutions”. In: *Astronomy & Astrophysics* 574, A35.
- Peraiah, A and IP Grant (1973). “Numerical solution of the radiative transfer equation in spherical shells”. In: *IMA Journal of Applied Mathematics* 12.1, pp. 75–90.
- Perez-Becker, Daniel and Adam P Showman (2013). “Atmospheric heat redistribution on hot Jupiters”. In: *The Astrophysical Journal* 776.2, p. 134.
- Rybicki, George B (1996). “Radiative transfer”. In: *Journal of Astrophysics and Astronomy* 17.3-4, pp. 95–112.
- Sengupta, Aritra Chakrabarty, and Giovanna Tinetti (2020). “Optical transmission spectra of hot Jupiters: effects of scattering”. In: *The Astrophysical Journal* 889.2, p. 181.
- Sengupta and Mark S Marley (2009). “Multiple scattering polarization of substellar-mass objects: T dwarfs”. In: *The Astrophysical Journal* 707.1, p. 716.
- Sengupta, Soumya (2021). “Effects of thermal emission on Chandrasekhar’s semi-infinite diffuse reflection problem”. In: *The Astrophysical Journal* 911.2, p. 126.

- Showman, Adam P, Kristen Menou, and James YK Cho (2007). "Atmospheric circulation of hot Jupiters: a review of current understanding". In: *arXiv preprint arXiv:0710.2930*.
- Showman, Adam P, Xianyu Tan, and Vivien Parmentier (2020). "Atmospheric Dynamics of Hot Giant Planets and Brown Dwarfs". In: *Space Science Reviews* 216.8, pp. 1–83.
- Stassun, Keivan G, Karen A Collins, and B Scott Gaudi (2017). "Accurate empirical radii and masses of planets and their host stars with Gaia parallaxes". In: *The Astronomical Journal* 153.3, p. 136.
- Struve, Otto (1952). "Proposal for a project of high-precision stellar radial velocity work". In: *The Observatory* 72, pp. 199–200.
- Swain, Mark R, Gautam Vasisht, and Giovanna Tinetti (2008). "The presence of methane in the atmosphere of an extrasolar planet". In: *Nature* 452.7185, pp. 329–331.
- Tan, Xianyu and Thaddeus D Komacek (2019). "The atmospheric circulation of ultra-hot Jupiters". In: *The Astrophysical Journal* 886.1, p. 26.
- Tinetti, Giovanna, P Deroo, et al. (2010). "Probing the terminator region atmosphere of the hot-Jupiter XO-1b with transmission spectroscopy". In: *The Astrophysical Journal Letters* 712.2, p. L139.
- Tinetti, Giovanna, Thérèse Encrenaz, and Athena Coustenis (2013). "Spectroscopy of planetary atmospheres in our Galaxy". In: *The Astronomy and Astrophysics Review* 21.1, pp. 1–65.
- Tinetti, Giovanna, Alfred Vidal-Madjar, et al. (2007). "Water vapour in the atmosphere of a transiting extrasolar planet". In: *Nature* 448.7150, pp. 169–171.
- Valencia, Diana et al. (2013). "Bulk composition of GJ 1214b and other sub-Neptune exoplanets". In: *The Astrophysical Journal* 775.1, p. 10.
- Waldmann, Ingo P et al. (2015). "Tau-REx I: A next generation retrieval code for exoplanetary atmospheres". In: *The Astrophysical Journal* 802.2, p. 107.
- Wong, Ian et al. (2016). "3.6 and 4.5 μm Spitzer phase curves of the highly irradiated hot Jupiters WASP-19b and HAT-P-7b". In: *The Astrophysical Journal* 823.2, p. 122.